JUSTUS-LIEBIG-UNIVERSITÄT GIESSEN

Justus-Liebig-Universität Gießen
Fachbereich 08: Biologie und Chemie
Institut für Anorganische und Analytische Chemie

Influence of the First and Second Coordination Sphere on the Stability and Reactivity of Copper(I) Complexes with Dioxygen

Kumulativ-Dissertation

zur Erlangung des Doktorgrades der Naturwissenschaften

- Dr. rer. nat. -

Vorgelegt von

Alexander Granichny

Aus Gießen

Februar 2025

Selbständigkeitserklärung

„Ich erkläre: Ich habe die vorgelegte Dissertation selbstständig und ohne unerlaubte fremde Hilfe und nur mit den Hilfen angefertigt, die ich in der Dissertation angegeben habe. Alle Textstellen, die wörtlich oder sinngemäß aus veröffentlichten Schriften entnommen sind, und alle Angaben, die auf mündlichen Auskünften beruhen, sind als solche kenntlich gemacht. Ich stimme einer evtl. Überprüfung meiner Dissertation durch eine Antiplagiat-Software zu. Bei den von mir durchgeführten und in der Dissertation erwähnten Untersuchungen habe ich die Grundsätze guter wissenschaftlicher Praxis, wie sie in der „Satzung der Justus-Liebig-Universität Gießen zur Sicherung guter wissenschaftlicher Praxis“ niedergelegt sind, eingehalten.

Datum	Unterschrift

Erstgutachter: Prof. Dr. Siegfried Schindler

Zweitgutachter: Prof. Dr. Richard Göttlich

Danksagung

Zu Beginn möchte ich meinen herzlichen Dank an Prof. Dr. Siegfried Schindler richten, der mir die Möglichkeit gab, Teil seiner Arbeitsgruppe zu sein, und mich während meiner Promotion stets unterstützt hat. Ebenso gilt mein besonderer Dank Prof. Dr. Richard Göttlich für die Übernahme des Zweitgutachtens.

Ein weiterer Dank gebührt Prof. Dr. Masahito Kodera (Kyotanabe, Kyoto, Japan), der mir die Gelegenheit ermöglichte, zwei Monate in seiner Arbeitsgruppe forschen zu dürfen. In diesem Zusammenhang möchte ich mich auch bei Kyosuke Fujikawa und Zelda Fery danken, die mich während meines Aufenthalts in Japan stets unterstützt haben.

Meinen Dank gilt zudem meinen aktuellen und ehemaligen Kolleginnen und Kollegen Chiara Campi, Kevin Keller, Christian Noß, Dr. Alexander Petrillo, Dr. Azar Rezaei, Dr. Florian Ritz, Dr. Thomas Rotärmel, Stefan Schaub, Lars Schneider, Dr. Pascal Specht, Dr. Fabian Stöhr, Luisa Träger, die durch den gemeinsamen Austausch zu einer lebendigen und inspirierenden Arbeitsatmosphäre beigetragen haben.

Bedanken möchte ich mich auch bei Anna Leah Scholl für die tatkräftige Unterstützung für Teile dieser Forschungsarbeit sowie bei Mats Georg für die stets hilfreichen und anregenden Diskussionen.

Mein Dank gilt auch Jonathan Becker und Christian Würtele für ihre Einführung in die Kristallstrukturanalyse sowie den Mitarbeiterinnen und Mitarbeiter der organisch-chemischen Analytik, der Glasbläserei und Chemikalien- und Materialausgabe, ohne die diese Arbeit nicht möglich gewesen wäre.

Nicht zuletzt möchte ich meinen Kommilitoninnen und Kommilitonen Paul Debes, Lorena Glatthaar, Florian Rink, Julian Roth und Lysander Wagner für die gemeinsame Zeit danken.

Abschließend gilt mein tiefster Dank meinen Freundinnen und Freunden sowie meiner Familie, die mich während des Studiums und der Promotion in jeder Hinsicht unterstützt haben.

"*Das Leben ist wie ein Fahrrad.*
Man muss sich vorwärts bewegen, um das Gleichgewicht nicht zu verlieren."

Albert Einstein (1879 – 1955)

Table of Contents

Abstract

Selective oxidation reactions are of crucial importance to the chemical industry. However, many current methods are not sustainable, often relying on expensive noble metal catalysts, toxic oxidants, and harsh reaction conditions. In contrast, nature demonstrates the possibility of conducting these reactions using copper proteins and dioxygen as the oxidant under mild conditions. Inspired by the functionality of copper proteins, this work focuses on the synthesis of bioinspired copper model complexes and investigates the influence of the first and second coordination sphere on the stability and reactivity with dioxygen.

Chapter 3.1 presents the first section of this research, focusing on the stabilization of labile copper(I) complexes through the integration of olefinic side arms into the ligand and examining their influence on the copper(I) complexes ability to activate dioxygen. It was demonstrated that olefinic side arms can stabilize copper(I) complexes that are prone to disproportionation, while maintaining the ability to activate dioxygen without altering the nature of the "oxygen adduct complex". However, this effect significantly depends on the position and length of the olefinic side arm. This work shows that introducing olefinic side arms into ligands represents a non-invasive strategy to explore the oxygen activation of labile copper(I) complexes in the future.

Chapter 3.2 explains the second section of this research, dealing with the role of the second coordination sphere in the dioxygen activation of the copper(I) complex with *N*-(2-Ethoxyethanol)-bis(2-picolyl)amine as the ligand. The mechanism behind the dioxygen activation was elucidated by investigating copper(I) complexes with a series of related ligands and comparing their reactivity towards dioxygen. The explored mechanism begins with the formation of an η^1-superoxido species, which rapidly reacts to form a transient hydrogen bond stabilized *trans*-μ-1,2-peroxido species, that undergoes an isomerization reaction to form a bis(μ-oxido) species. This work provides new insights into the interactions between the second coordination sphere and the activated dioxygen, highlighting the potential of hydroxyl groups in forming such interactions, which lay the groundwork for the design of future ligands and selective oxidation reactions.

Zusammenfassung

Selektive Oxidationsreaktionen sind von entscheidender Bedeutung für die chemische Industrie. Dennoch sind viele der aktuellen Verfahren nicht nachhaltig, da sie häufig auf kostspielige Edelmetallkatalysatoren, toxische Oxidationsmittel und harsche Reaktionsbedingungen angewiesen sind. Dagegen demonstriert die Natur die Möglichkeit, diese Reaktionen mittels Kupferproteinen und molekularem Sauerstoff als Oxidationsmittel unter milden Bedingungen durchzuführen. Inspiriert von der Funktionsweise dieser Kupferproteine konzentriert sich diese Arbeit auf die Synthese bioinspirierter Kupfermodellkomplexe und die Untersuchung des Einflusses der ersten und zweiten Koordinationssphäre auf die Stabilität und Reaktivität mit molekularem Sauerstoff.

Kapitel 3.1 präsentiert den ersten Abschnitt dieser Forschung, die sich mit der Stabilisierung von labilen Kupfer(I) Komplexen durch die Integration olefinischer Seitenketten befasst und deren Einfluss auf die Fähigkeit der Kupfer(I) Komplexe zur Aktivierung von molekularem Sauerstoff untersucht. Dabei wurde gezeigt, dass olefinische Seitenketten Kupfer(I) Komplexe stabilisieren kann, die zu Disproportionierungen neigen, während die Fähigkeit erhalten bleibt molekularen Sauerstoff zu aktivieren, ohne die Art des "Sauerstoff-Adduktkomplexes" zu verändern. Dieser Effekt ist jedoch maßgeblich von der Position und der Länge der olefinischen Seitenkette abhängig. Diese Arbeit zeigt, dass das Einführen olefinischer Seitenketten eine nicht invasive Strategie darstellt, um zukünftig die Sauerstoffaktivierung labiler Kupfer(I)-Komplexe zu untersuchen.

Kapitel 3.2 erläutert den zweiten Abschnitt dieser Forschung, der sich mit der Rolle der zweiten Koordinationssphäre bei der Sauerstoffaktivierung des Kupfer(I) Komplexes mit dem Liganden *N*-(2-Ethoxyethanol)-bis(2-picolyl)amin befasst. Der Mechanismus hinter der Sauerstoffaktivierung wurde aufgeklärt, indem Kupfer(I) Komplexe mit einer Reihe verwandter Liganden untersucht und deren Reaktivität gegenüber Sauerstoff verglichen wurde. Der Mechanismus beginnt mit der Bildung einer η^1-superoxido Spezies, die rasch zu einer kurzlebigen Wasserstoffbrückenbindungen stabilisierten *trans*-μ-1,2-peroxido Spezies reagiert, die über eine Isomerisierungsreaktion zu einer bis(μ-oxido) Spezies zerfällt. Diese Arbeit bietet neue Erkenntnisse hinsichtlich Wechselwirkungen zwischen der zweiten Koordinationssphäre und dem aktivierten Sauerstoff und zeigt das Potenzial von Hydroxygruppen zur Bildung solcher Interaktionen, welche die Grundlage für das Design zukünftige Liganden und selektiver Oxidationsreaktionen darstellen.

1 Introduction

1.1 Selective Oxidation Reactions

Selective oxidation reactions are crucial for transforming hydrocarbons and other raw materials into valuable synthetic building blocks and functional materials.[1] These reactions constitute roughly 20% of all processes in the chemical industry's value chain, yielding an estimated 600 million tons of chemicals annually.[1] Industrial-scale oxidation reactions often rely on noble metal catalysts, hazardous oxidants and solvents, and high-temperature and high-pressure environments, posing challenges in terms of sustainability and safety.[2] In contrast, nature employs 3d metal containing metalloproteins to catalyze a wide range of selective oxidation reactions under ambient conditions in aqueous media, utilizing dioxygen as a sustainable oxidizing agent.[3] Using dioxygen as an oxidizing agent in industrial processes is advantageous due to its sustainability, cost-efficiency, and non-toxic properties.[4] However, its stable triplet ground state ($^3O_2$) prevents reactions with singlet state organic molecules, as these reactions are spin-forbidden. To facilitate these reactions, dioxygen must be activated, either by converting it to its singlet state ($^1O_2$) *via* photochemical methods or, more commonly, through the use of a catalyst.[1,5] The Wacker-Hoechst process exemplifies an industrial application of dioxygen, wherein ethylene is oxidized to acetaldehyde using palladium(II) and copper(II) chloride as catalysts (Scheme 1).[6,7] In this process, palladium(II) chloride activates the olefinic substrate and mediates its selective oxidation, while copper(II) chloride regenerates the palladium(II) species by re-oxidizing palladium(0) back to palladium(II), thus completing the catalytic cycle.

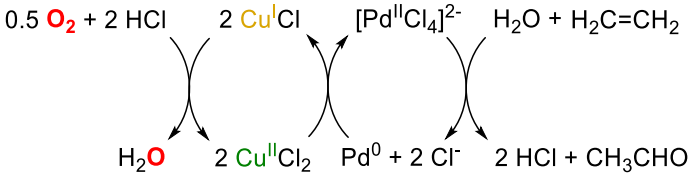

Scheme 1. Sub-steps of the Wacker-Hoechst process.[6,7]

Although the Wacker-Hoechst process effectively utilizes dioxygen, its sustainability could be improved by replacing noble metals like palladium with more abundant and environmentally benign alternatives. Furthermore, substituting palladium with other 3d metal catalysts like copper aligns with regulatory standards for pharmaceutical applications. The permitted oral concentration of palladium, platinum, iridium, rhodium, and ruthenium in pharmaceuticals is limited to 10 µg g^{-1}, whereas copper is allowed at much

higher concentrations of 300 μg g^{-1}.[8] This higher threshold reduces the need for unsustainable and costly purification processes and allows the use of metal catalysts at later stages of the synthesis, further enhancing the feasibility of such a substitution.

A selective oxidation reaction referred to as the "holy grail" of chemistry and catalysis in the twenty-first century is the direct conversion of methane into methanol (Scheme 2).[9,10] Methane, which constitutes about 70–90% of natural gas, is an abundant and readily available carbon resource.[9] Despite being the simplest hydrocarbon, selectively oxidizing methane is a significant challenge due to its highly inert C–H bonds with a bond dissociation energy (BDE) of 105 kcal mol^{-1}. Furthermore, the higher reactivity of the desired methanol (BDE: 96 kcal mol^{-1}) often leads to overoxidation.[11] Currently, large-scale conversion of methane to methanol is highly energy-intensive, relying on steam reforming along with $CuO/ZnO/Al_2O_3$ catalysis at high pressure and temperatures (Scheme 2).[12,13] Developing efficient methods for the methane to methanol conversion under mild conditions could play a transformative role in advancing a "methanol economy", a concept introduced by Nobel laureate George A. Olah.[14] In this context, methanol serves as: 1) an efficient medium for energy storage, 2) a sustainable fuel, and 3) a versatile feedstock for synthesizing hydrocarbons and their derivatives, all of which collectively help reduce climate pollution.[14] In nature, methanotrophic bacteria achieve selective oxidation of methane to methanol under ambient conditions using a class of proteins known as methane monooxygenases (MMOs). These MMOs are categorized into two types: 1) soluble cytoplasmic MMO (sMMO), featuring a diiron active site, and 2) membrane-bound particulate MMO (pMMO), which contains a copper-based active site.[15]

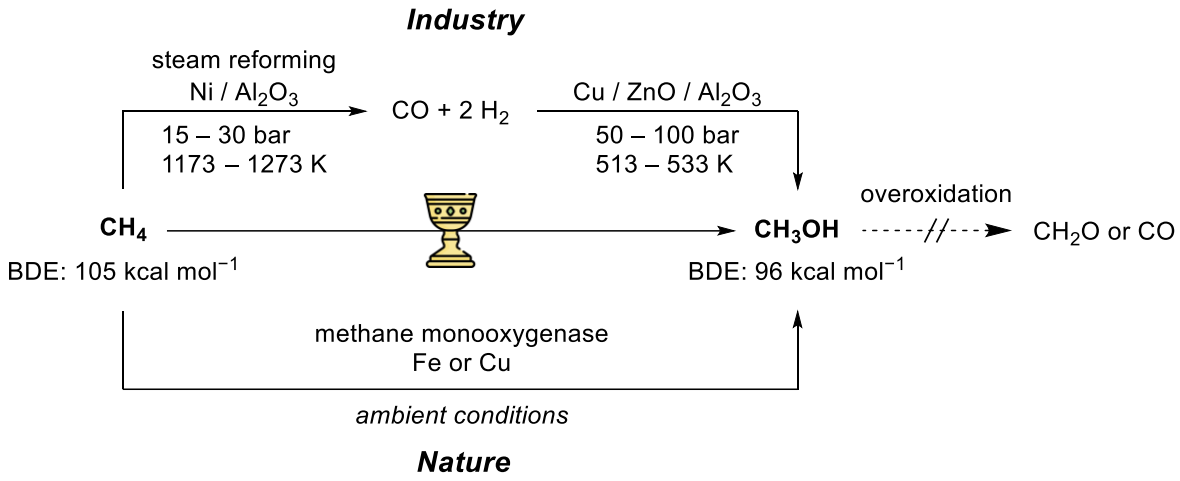

Scheme 2. Comparison of the reaction conditions for the methane to methanol conversion in industry and in nature.[13]

To gain insights into these natural processes and develop sustainable, cost-efficient catalysts for the selective oxidation of methane or other substrates under mild conditions using dioxygen, small bioinspired model complexes are synthesized, and their reactivity towards dioxygen is investigated.[16] To elucidate how small model complexes mimic the functions of metalloproteins, the following chapters focus on copper proteins and their related bioinspired copper complexes.

1.2 Copper Proteins

Copper-containing proteins are a vital class of metalloproteins that incorporate copper as the essential cofactors for their enzymatic activities. These proteins are integral to a range of biological processes (Scheme 3), including electron transfer (e.g. plastocyanin), oxygen transport and storage (e.g. hemocyanin), oxidative catalysis (e.g. cytochrome c oxidase), and detoxification of oxygen radicals (e.g. superoxide dismutase).[17] The significance of copper proteins in human physiology is evidenced by severe diseases, such as Wilson's and Menkes disease, that result from their dysfunction or deficiency, both of which involve disrupted copper metabolism.[18]

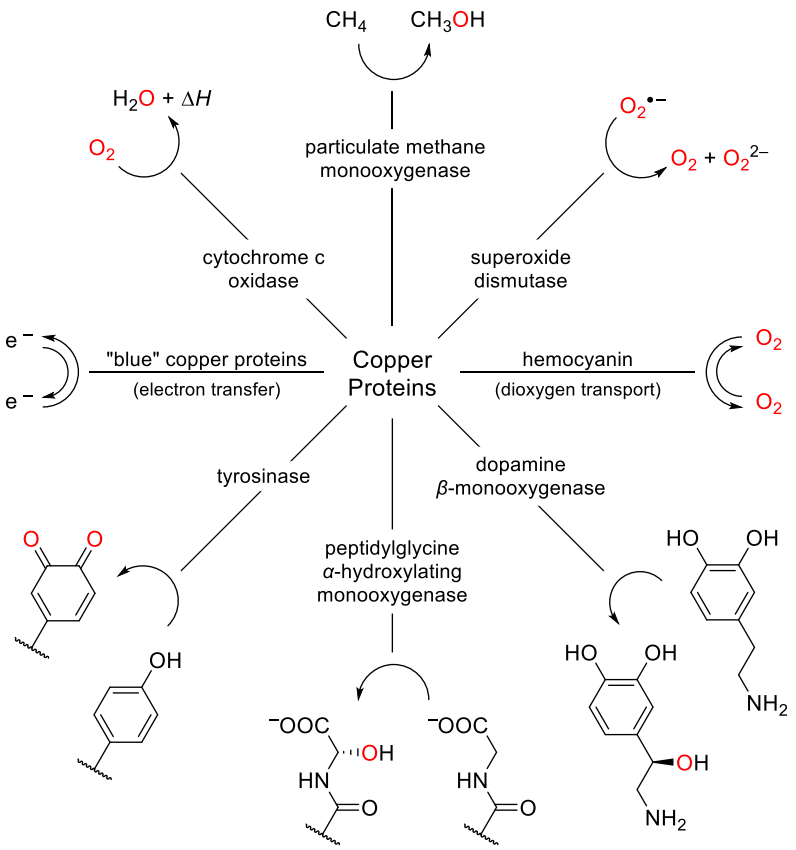

Scheme 3. Overview of important copper proteins and their biological processes.[19,20]

Numerous classes of copper proteins have been identified, and the majority are classified into type-1, type-2, or type-3 categories. This classification is based on the number of copper ions present in the active sites, the coordination geometry of these ions, and their characteristic UV-vis and Electron Spin Resonance (EPR) spectra (Scheme 4).[17,21] A detailed discussion of these classes will follow in the subsequent sections.

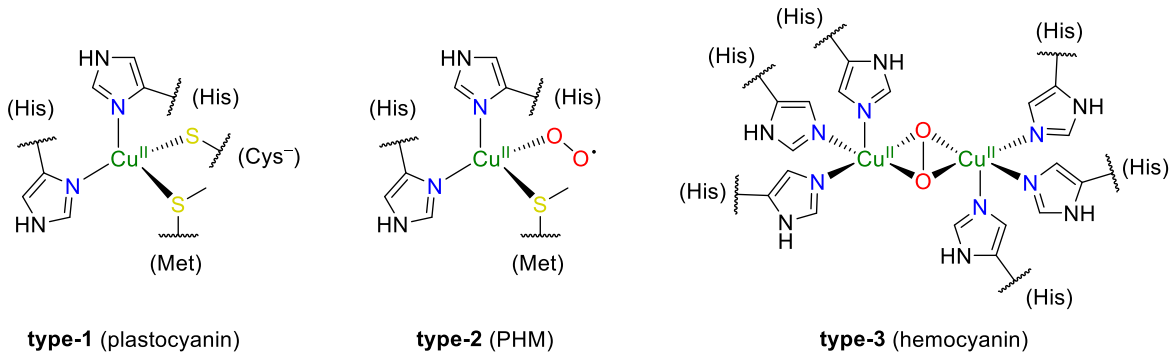

Scheme 4. Active site of type-1 (plastocyanin),[22] type-2 (peptidylglycine-α-hydroxylating-monooxygenase, PHM),[23] and type-3 (hemocyanin)[24] copper proteins in oxidized form.

1.2.1 Type-1 Copper Proteins

Type-1 copper proteins, often referred to as "blue copper proteins", are characterized by an intense deep blue color in their oxidized state. This coloration arises from an intense absorption band at around 600 nm, attributed to a ligand-to-metal charge-transfer (LMCT) from a cysteine thiolate to the copper(II) ion.[17,25] The active site of mononuclear type-1 copper proteins typically includes the coordinated thiolate cysteine, two nitrogen donor atoms from two histidine residues, and a variable axial ligand, predominantly a weakly coordinated sulfur from a methionine moiety (Scheme 4), though in occasions involve a glutamine or leucine.[17] The coordination geometry of the active site of type-1 proteins is generally depicted as distorted tetrahedral. This geometry likely represents a compromise between the tetrahedral arrangement preferred by copper(I) and the square planar coordination often adopted by copper(II) in low molecular weight copper complexes and non-blue copper proteins.[26] This distinct geometry facilitates rapid electron transfer between the two oxidation states, enabling type-1 proteins to function effectively as single electron transfer vehicles, such as plastocyanin in photosynthesis (Scheme 4).[22] Notably, the copper protein azurin is an exception to this, possessing an additional weakly bound fifth ligand, namely a carboxyl oxygen from a glycine residue, resulting in a distorted trigonal bipyramidal coordination sphere.[27]

1.2.2 Type-2 Copper Proteins

Type-2 copper proteins, commonly referred to as "normal copper proteins", exhibit EPR characteristics similar to those of typical copper(II) complexes. Unlike type-1 copper proteins, they lack the intense deep blue color due to the absence of sulfur-to-copper LMCT, instead appearing light blue in their oxidized form as a result of spin-forbidden d-d transitions. The active site of type-2 copper proteins typically consists of four nitrogen and/or oxygen donor atoms arranged in either square planar or distorted tetrahedral coordination geometry (Scheme 4).[17] In contrast to type-1 copper proteins, the coordination sites in type-2 copper proteins may be vacant or occupied by external ligands, allowing for catalytic activity. When dioxygen serves as a substrate, type-2 copper proteins can function as: (i) oxidases, reducing oxygen to water or peroxide; (ii) monooxygenases, incorporating one oxygen atom into a substrate while reducing the other to water; (iii) dioxygenases, incorporating both oxygen atoms into a substrate.[28] Additionally, their oxidase activity is not confined to dioxygen, as these proteins also catalyze the dismutation of superoxide into dioxygen and hydrogen peroxide, which is crucial for protection against oxidative stress.[29]

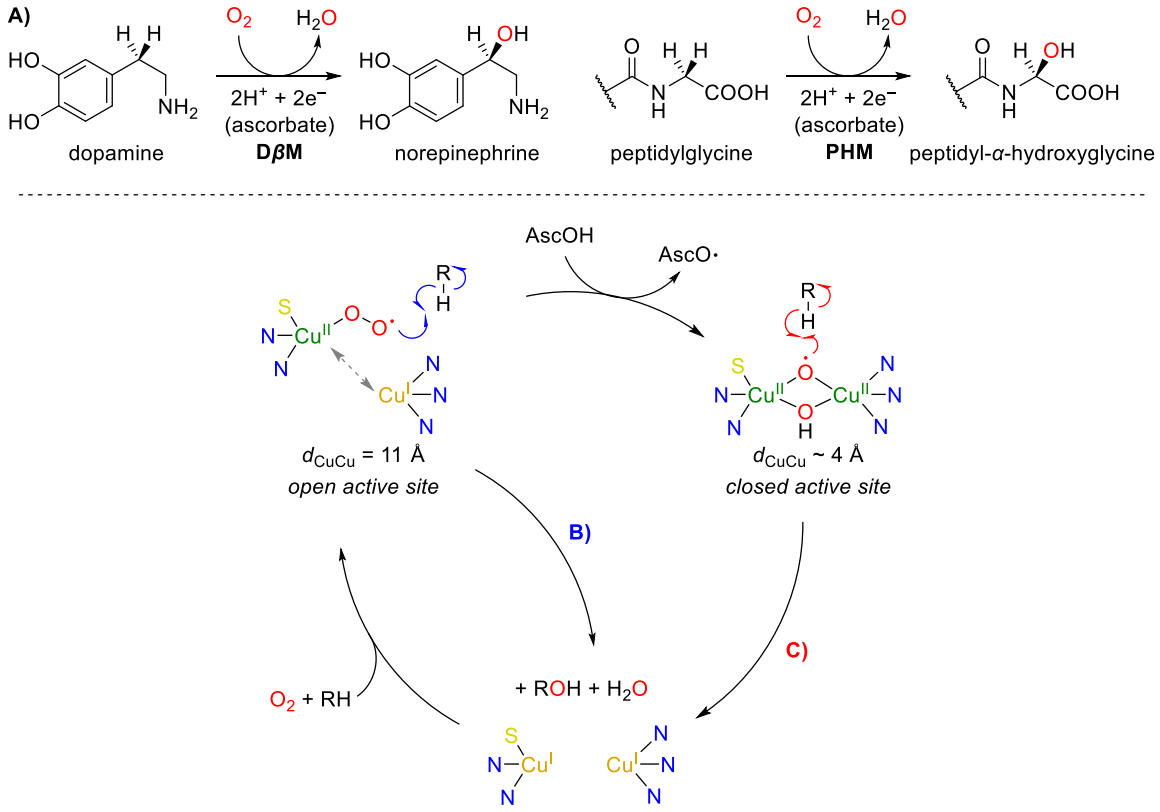

Scheme 5. Stereoselective hydroxylations (A) and revised monooxygenase mechanisms for DβM and PHM involving binuclear uncoupled (B) or coupled binuclear (C) copper sites; both incorporating hydrogen atom abstraction and reduction by sodium ascorbate.[30,31]

Type-2 oxygenases include dopamine-β-monooxygenase (DβM) and peptidylglycine-α-hydroxylating-monooxygenase (PHM, Scheme 4),[23,32] which perform stereoselective hydroxylation reactions essential for neurotransmitter regulation and hormone biosynthesis (Scheme 5A).[33] Investigations suggested that DβM and PHM have binuclear uncoupled copper sites, separated by 11 Å, with Cu_M mediating the hydroxylation process and Cu_H serving as an electronic relay (Scheme 5B).[30,33] However, recent crystal structures of human DβM reveal structural flexibility, adopting an open conformation with a 14 Å separation between the copper ions and a closed conformation where the copper sites are only 4 – 5 Å apart.[32] These findings suggest the existence of a coupled binuclear copper site within DβM and PHM, and, together with computational studies proposing a reaction mechanism, prompting a reevaluation of their classification as type-2 oxygenases (Scheme 5C).[31]

1.2.3 Type-3 Copper Proteins

Type-3 copper proteins are characterized by two antiferromagnetically coupled copper centers, each coordinated by three nitrogen donors from histidine residues, rendering them EPR-silent in their oxidized form.[21] These proteins are notable for their ability to reversibly bind dioxygen under ambient conditions, a feature that underlies their catalytic role as oxidases (e.g. catechol oxidase),[34] oxygenases (e.g. tyrosinase),[35] or dioxygen carriers (e.g. hemocyanin, Scheme 4)[24]. Hemocyanin, acts as a dioxygen carrier in various invertebrates like arthropods and mollusks,[24] and appears blue in the oxidized form, contrasting the red colored iron-based oxygen carrier hemoglobin. Other proteins of that class, such as polyphenol oxidases, include tyrosinase and catechol oxidase,[34,35] which catalyze the oxidation of *o*-diphenols to *o*-catechols (e.g. 3,4-dihydroxy-L-phenylalanine (L-DOPA) to L-dopaquinone), with tyrosinase also catalyzing the *o*-hydroxylation of monophenols to diphenols (e.g. tyrosine to L-DOPA, Scheme 6A).[36] These enzymes are crucial for melanin synthesis, affecting the browning of fruits and vegetables, as well as pigmentation in skin, hair, and eyes.[37] Numerous studies have elucidated that the catalytic mechanism of tyrosinase is initiated *via* electrophilic aromatic substitution (S_EAr) of a phenolate anion coordinated to the bis(μ-oxido) core (Scheme 6B).[21,38] Recent studies, however, propose an alternative pathway *via* radical-nucleophilic aromatic substitution ($S_{RN}1$), initiated by hydrogen bonding of the phenol followed by a proton-coupled electron transfer (PCET) to the bis(μ-oxido) core (Scheme 6C).[39,40] These insights are supported by a biomimetic model complex, which is further discussed in **Chapter 1.3.3**,[41] highlighting the importance of bioinspired model complexes in elucidating mechanistic questions.

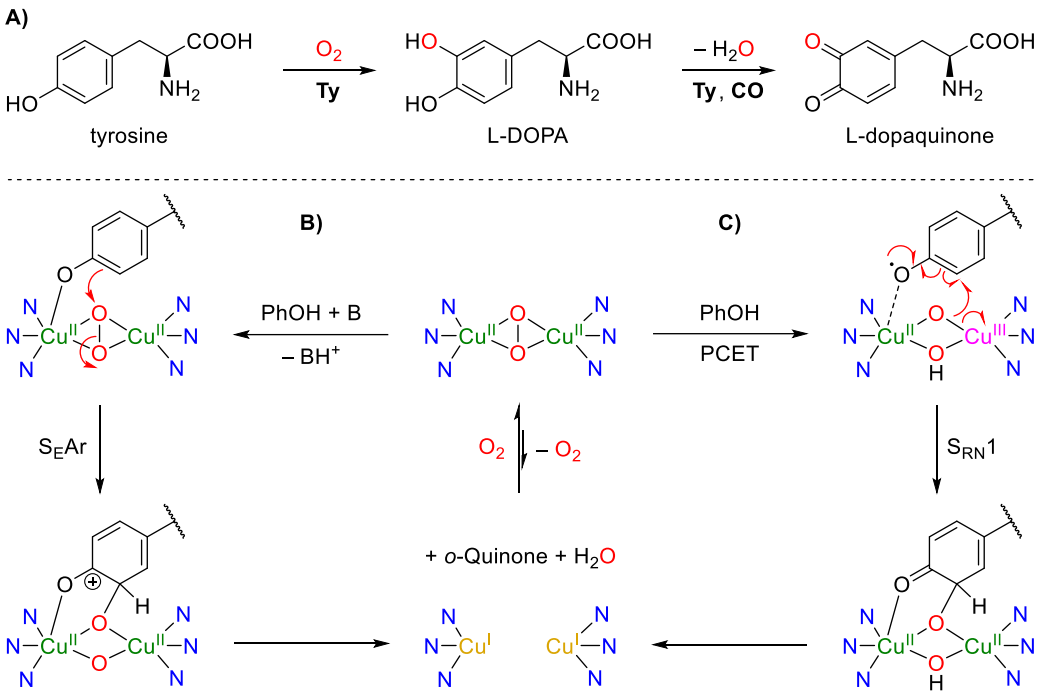

Scheme 6. (A) Reactions catalyzed by tyrosinase (Ty) and catechol oxidase (CO); Proposed mechanisms for the oxygenation of phenol to *o*-catechol by tyrosinase *via* (B) electrophilic aromatic substitution (S_EAr) or (C) radical-nucleophilic aromatic substitution ($S_{RN}1$).[30,39,40]

1.3 Bioinspired Model Complexes of Copper Proteins

Since the 1980s, bioinspired model complexes of copper proteins have been extensively studied to enhance our understanding of biochemical processes by studying their dioxygen activation capabilities.[36,42] To investigate these typically reactive and short-lived "oxygen adduct complexes", their stability needs to be enhanced under low-temperature conditions (typically below 200 K) to minimize the entropic cost of formation and suppress further reactions.[20] Despite these precautions, observing reactive species is not guaranteed, as the copper(I) complexes most commonly react with dioxygen *via* outer sphere oxidation with a 4:1 stoichiometry, without accumulating intermediates. Nevertheless, a plethora of "oxygen adduct complexes" have been identified. Some correlate with the active species of copper proteins discussed in **Chapter 1.2**, while others are not naturally occurring (Scheme 7).[20] In the inner sphere oxidation of a copper(I) complex with dioxygen, it is widely acknowledged that the initial formation of a mononuclear end-on η^1-superoxide copper(II) complex (^{E}**S**) occurs. This reactive species may further transform into a mononuclear side-on η^2-superoxide copper(II) complex (^{S}**S**) or into binuclear species such as the *trans*-μ-1,2-peroxido dicopper(II) complex (^{T}**P**), μ-η^2:η^2-peroxido dicopper(II) complex

(**^{S}P**), or bis(μ-oxido) dicopper(III) complex (**O**).[20] These sensitive equilibrium reactions and the observation of activated dioxygen species depend on several factors, which will be discussed in detail in **Chapter 1.3.3**.[20,43] Although the mononuclear and binuclear "oxygen adduct species" are isoelectric with each other, several analytical techniques have been established to determine which species is formed, which will be described in the following chapter.

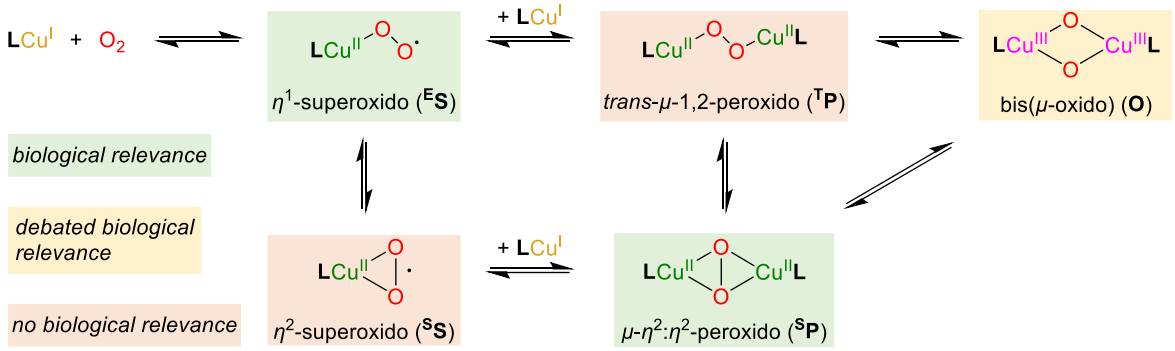

Scheme 7. Typical reaction pathways for copper(I) complexes with dioxygen and the biological relevance of the corresponding "oxygen adduct complexes".[20]

1.3.1 Characterization of Copper "Oxygen Adduct Complexes"

X-ray diffraction (XRD) is the definitive method for confirming copper "oxygen adduct complexes" and visualizing atom connectivity, but crystallization of these complexes is challenging due to their high reactivity and thermal sensitivity. Therefore, more accessible spectroscopic techniques are often employed to identify these copper "oxygen adduct complexes" and determine structural parameters. Among these, UV-vis spectroscopy is a key tool due to its simple setup coupled with its ability to characterize "oxygen adduct complexes" in solutions at low temperatures. This effectiveness is due to the highly covalent Cu–O bonds, which result in intense oxygen-to-copper charge-transfer (CT) bands characteristic for specific "oxygen adduct complexes".[20] For labile "oxygen adduct complexes" that decompose rapidly, low-temperature stopped-flow UV-vis spectroscopy is suitable as it allows for fast scan rates by rapidly mixing a solution of dioxygen-free copper(I) complex with a dioxygen-saturated solution.[44] Additionally, infrared (IR) and/or resonance Raman (rR) spectroscopy can confirm the identity of "oxygen adduct complexes", with rR being particularly useful for selectively enhancing and detecting of Cu–O and O–O symmetrical vibrational modes.[20] The use of the dioxygen isotope $^{18}O_2$, instead of the more abundant $^{16}O_2$, shifts the vibrational frequencies, providing insights into the O_2 oxidation

state: 1100–1200 cm^{-1} ($\Delta[^{18}O_2] \approx 50\ cm^{-1}$) for superoxide and 750–920 cm^{-1} ($\Delta[^{18}O_2] \approx 50\ cm^{-1}$) for the peroxide.[20,45] Further elucidation can be achieved using X-ray absorption spectroscopy (XAS) and extended X-ray absorption fine structure (EXAFS).[46] XAS enables the determination of formal oxidation states of the "oxygen adduct complexes" *via* a weak pre-edge absorption feature corresponding to the 1s to 3d transition, distinguishing Cu(II): (8979 ± 0.5 eV) from Cu(III): (8981 ± 0.5 eV).[20,47] EXAFS provides an alternative means to obtain structural parameters of "oxygen adduct complexes" like Cu···Cu, Cu–O, and Cu–N distances in both solution and solid, comparable to X-ray crystallography but without its difficulties.[20,46] Although obtaining XRD data is difficult, major "oxygen adduct complexes" depicted in Scheme 7, have been analyzed *via* X-ray diffraction crystallography by specifically designing and optimizing ligand systems (Scheme 8), which will be discussed in the next chapter.

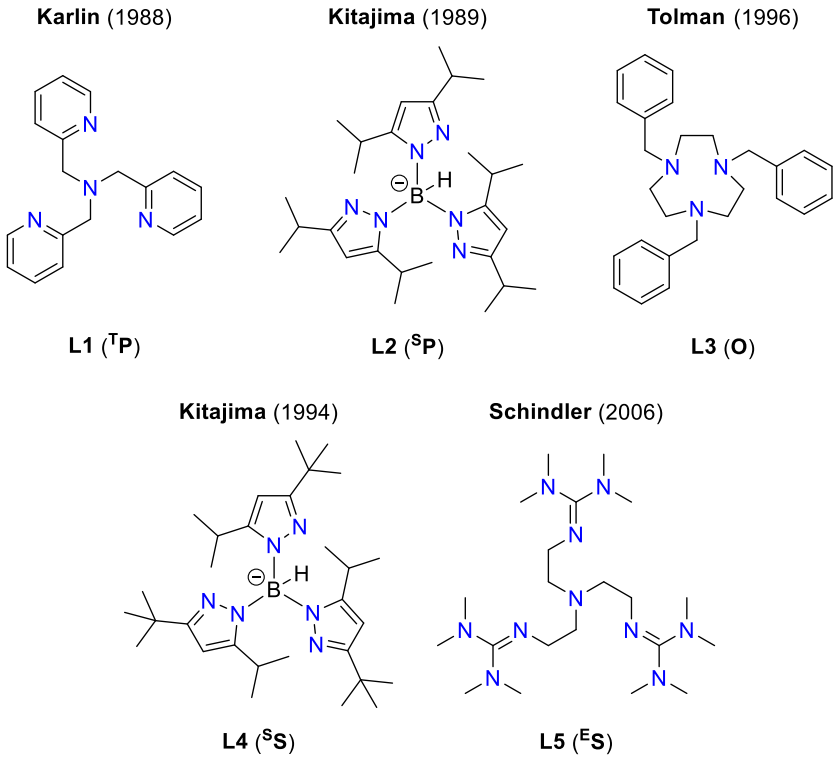

Scheme 8. Ligands used for the initial structural characterization of various "oxygen adduct complexes" from its corresponding copper(I) complexes and dioxygen.[48–53]

1.3.2 Synthetic Copper "Oxygen Adduct Complexes"

In 1988, Karlin and co-workers achieved a milestone by structurally characterizing the first "oxygen adduct complex" with the copper(I) complex of the tetrapodal tridentate ligand tris(2-pyridylmethyl)amine (**L1**, Scheme 8), identifying it as a ^{T}**P** species (Scheme 7).[48]

This pioneering work demonstrated that standard techniques used for inorganic complexes could effectively characterize these thermally sensitive and labile "oxygen adduct complexes",[20] as described above. When the copper(I) complex with **L1** as the ligand reacts with dioxygen at −80 °C in solvents like propionitrile or chloroform, it forms stable purple solutions exhibiting characteristic absorption features typical of ^{T}**P** species, generally observed at ca. 530 nm and a shoulder at ca. 600 nm.[48,20] Although the ^{T}**P** species lack direct biochemical relevance, the copper(I) complex of **L1** can reversibly bind dioxygen by heating under vacuum and rechilling the solution under dioxygen atmosphere (Scheme 9), analogous to the type-3 copper protein hemocyanin,[48,54] which forms a ^{S}**P** species.[24] The accessibility of **L1** and its distinctive spectroscopic features have led to the development of a plethora of derivatives, establishing it as one of the most widely used ligand scaffolds, with several examples to be discussed in the following chapters.[20]

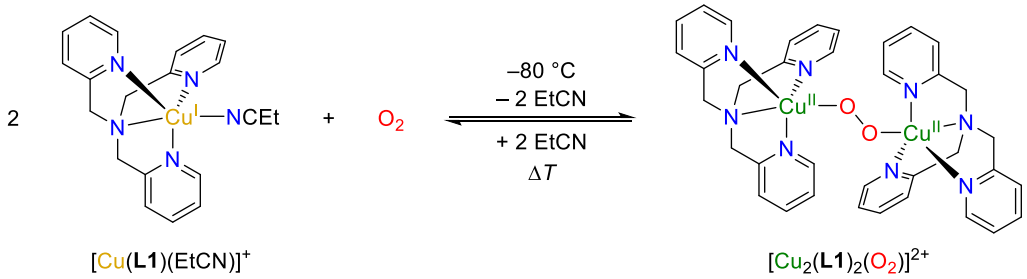

Scheme 9. Reversible dioxygen binding of [Cu(**L1**)(EtCN)]$^{+}$.[48]

One year later, Kitajima and co-workers reported the structural characterization of an ^{S}**P** species using the copper(I) complex of the anionic tripodal tridentate ligand hydrotris(3,5-diisopropylpyrozolyl)borate (**L2**, Scheme 8).[49] The Cu···Cu distance in this ^{S}**P** species is with 3.560 Å significantly shorter than the 4.359 Å reported for the ^{T}**P** species by Karlin and co-workers, but in-line with the later reported Cu···Cu distance of oxy-Hemocyanin (3.5–3.6 Å).[24,48,49] Reacting the copper(I) complex with **L2** as the ligand with dioxygen at −78 °C in acetone forms a relatively stable purple solution that remains stable below 10 °C in non-coordinating solvents.[55] This ^{S}**P** species exhibits absorption features at 349 and 551 nm, distinct from those of the ^{T}**P** species but closely matching the absorption spectra of oxy-hemocyanin found in mollusks (345 and 570 nm).[49] The similarity in absorption and other crystallographic and spectroscopic characteristics to those of oxy-Hemocyanin, strongly implies that the dioxygen binding in oxy-Hemocyanin occurs through a similar mechanism,[20] illustrating how small model complexes can elucidate protein reactivity.

The most recent structurally characterized binuclear copper "oxygen adduct complex" discussed here is the **O** species, reported by Tolman and co-workers in 1996 using the copper(I) complex with the macrocyclic tridentate ligand 1,4,7-tribenzyl-1,4,7-triazacyclononane (**L3**, Scheme 8).[51,52] Compared to the other binuclear ^{T}**P** and ^{S}**P** species, the **O** species features the shortest Cu···Cu distance at 2.287 Å and distinct UV-vis absorption bands at 318 and 430 nm, observed below −70 °C in chloroform.[51,52] This difference compared to the other binuclear copper "oxygen adduct complexes" arises because both copper centers are in a higher oxidation state, being fully reduced by four electrons, which leads to the cleavage of the O–O bond. The resulting oxidizing capacity allows the **O** species to activate C–H bonds, as evidenced by *N*-dealkylation reactions of their respective macrocyclic ligands upon warming the solutions. Additionally, they reported that the copper(I) complex of the isopropyl derivative **L6** exhibits a solvent dependent ^{S}**P**/**O** equilibrium (Scheme 11).[51,52] In chloroform, the ^{S}**P** species is preferred, exhibiting spectroscopic features (UV-vis: 366 and 510 nm) similar to oxy-Hemocyanin, while in tetrahydrofuran, the **O** species is favored.[51,52,56] Generally, polar solvents stabilize the **O** species, whereas non-polar solvents favor the ^{S}**P** species. This trend is likely related to the preferential counterion association with the ^{S}**P** species, reducing its effective charge.[20] While theoretical studies suggest the ^{S}**P** species is preferred in biochemical systems and the **O** species is more enthalpically stable in model complexes,[57] both are nearly isoenergetic. This relationship offers multiple strategies to influence the ^{S}**P**/**O** equilibrium, discussed in the following chapter. Despite being the most recently discovered binuclear copper "oxygen adduct complexes" discussed here, the **O** species is the most prevalent due to the wide variety of bi-, tri-, and tetradentate ligand systems that can facilitate its formation.[20]

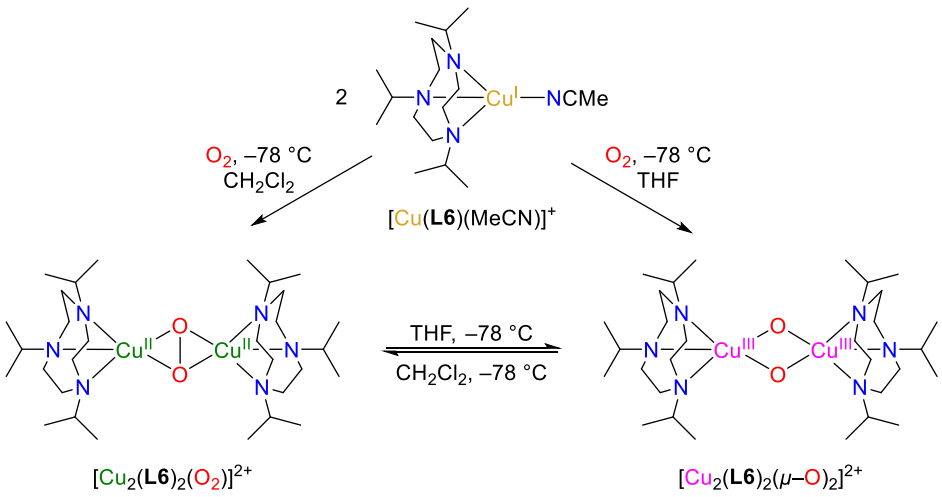

Scheme 10. Influence of solvent effects on ^{S}**P**/**O** equilibrium using [Cu(**L6**)(MeCN)]$^{+}$.[51,52]

Early studies suggested that mononuclear superoxide species are involved in copper proteins,[58] acting as initial copper "oxygen adduct complexes" before forming complexes of higher nuclearity (Scheme 7). The first spectroscopic evidence supporting this in a copper model complex was obtained in 1991.[59] However, due to their high reactivity and tendency to form binuclear species, structural analysis was initially elusive. Consequently, ligands were designed to mitigate the reactivity and facilitate the structural characterization of the superoxide species. In 1994, Kitajima and co-workers reported the first structurally characterized mononuclear copper "oxygen adduct complex" identified as a ^{S}**S** species, using the copper(I) complex of the anionic tripodal tridentate ligand hydrotris(3,5-diisopropylpyrazolyl)borate (**L4**, Scheme 8).[50] Compared to its related ligand **L2**,[49] ligand **L4** introduces increased steric hindrance from substituting one isopropyl with a *tert*-butyl group per arm, thereby shifting the ^{S}**S**/^{S}**P** equilibrium towards the ^{S}**S** species (Scheme 6) and enabling structural characterization.[20,50] To address partial dimerization in solution, the steric hinderance was further increased by substituting the *tert*-butyl with an adamantyl group, allowing for the exclusive detection of the ^{S}**S** species in solution (UV-vis: 452 and 700 nm in DCM at −78 °C).[60]

In 2004, the crystal structure of PHM was reported, revealing an ^{E}**S** species at its active site.[23] This finding contrasts with the ^{S}**S** species identified by Kitajima and co-workers,[50] and provides the first structural evidence that superoxide species are involved in the activation of dioxygen in proteins (Scheme 5B).[23] Spectroscopic evidence of the transient formation of an ^{E}**S** species in copper model complexes was first obtained in 1991, followed by kinetic studies in 1993 using the copper(I) complex of **L1** and dioxygen, which displayed an intense absorption band at 410 nm along with weaker bands around 600 and 750 nm.[59,61] In 1999, Schindler and co-workers investigated copper(I) complex of the aliphatic tris(2-dimethylaminoethyl)amine, exhibiting a more stabilized ^{E}**S** species compared to **L1**, due to increased steric hinderance, although rapid dimerization still occurred.[62] A significant advancement came in 2004 when Schindler and co-workers examined the copper(I) complex of tris(tetramethylguanidino)tren (**L5**, Scheme 8), forming a dark green ^{E}**S** species in solution capable of reversibly binding dioxygen upon heating and rechilling under dioxygen atmosphere.[63] This stabilization of the ^{E}**S** species is attributed to the strong *N*-donor character and increased sterically hinderance of the guanidine groups.[63] In 2006, they achieved the first structural characterization of the ^{E}**S** species using the copper(I) complex with **L5** as the ligand,[53] showing a geometry in-line with that reported for PHM,[23]

demonstrating that the ^{E}**S** species is the primary adduct formed by copper(I) complexes with dioxygen and plays a pivotal role in catalytic oxidation reactions.

1.3.3 Modulation of Copper "Oxygen Adduct Complexes"

As established in the previous chapters, synthetic copper "oxygen adduct complexes" are crucial for understanding the functionality of copper proteins and developing bioinspired copper complexes for selective oxidation reactions. However, as depicted in Scheme 7 and discussed earlier, the formation of these "oxygen adduct complexes" involves sensitive equilibrium reactions. Consequently, minor alterations in the ligand structure significantly influence the type of activated dioxygen species formed, thus affecting their reactivity. These influencing parameters include external factors such as temperature, solvent,[51,52] and the nature of the weakly coordinating counterion,[64] or internal factors, typically related to the characteristics of the first coordination sphere. These include the type of donor atoms, overall charge, denticity, chelate ring size,[65] and electronic and steric effects[66,67] of the ligand,[20] which will be discussed in the following.

Schindler and co-workers investigated how chelate ring size influences dioxygen activation in a series of copper(I) complexes with tripodal ligands, starting from **L1** and gradually increasing the chelate ring size from methyl to ethyl linkers (**L7** – **L9**, Scheme 10).[65] Upon oxygenation of the copper(I) complexes they observed that as the number of six-membered chelate rings increases, first the ^{E}**S** and then the ^{T}**P** species are destabilized (**L7** and **L8**, respectively), while the copper(I) complex containing only six-membered chelate rings (**L9**) showed no reactivity towards dioxygen. Electrochemical studies of the Cu(II)/Cu(I) redox couple support these findings, revealing that complexes with shorter linkers (**L1**, **L7**) have more negative redox potential than those with longer linkers (**L8**, **L9**).This indicates that five-membered chelate rings offer better stabilization for copper(II) compared to six-membered chelate rings and demonstrate the importance of five-membered chelate rings in stabilizing long-lived "oxygen adduct complexes" with tripodal ligands.

Adjusting chelate ring size can also stabilize labile copper(I) complexes or alter the type of "oxygen adduct complex" formed. When synthesizing the tridentate ligand **L10**, where a pyridine group in the tetradentate **L1** is replaced by a phenyl group, the resulting copper(I) complex is labile and rapidly disproportionates into copper(II) and elemental copper, even under anaerobic conditions (Scheme 10).[68,69] Disproportionation is a common challenge when studying dioxygen activation with copper(I) complexes.[70] To stabilize labile copper(I)

complexes, strategies such as adding ancillary ligands like acetonitrile or carbon monoxide,[71] or using bulky anions,[72] have been explored. However, these methods are often ligand-specific and not universally applicable. The stability of the copper(I) complex with ligand **L10** can be enhanced by extending the phenyl linker from a methyl to an ethyl group (**L11**, Scheme 10), promoting η^1-binding of the phenyl moiety to the copper(I) ion, thus stabilizing the complex without hindering its reactivity towards dioxygen, allowing for the formation of an **O** species upon oxygenation.[68] Further increasing the chelate ring size by substituting the remaining methyl with an ether linker results in **L12**, which facilitates η^2-binding of the phenyl moiety to the copper(I) ion, thus stabilizing the copper(I) complex and forming an ^{S}**P** species upon oxygenation (Scheme 10).[73] The alteration in binding mode and the nature of the "oxygen adduct complex" are attributed to steric effects as well as the electron-donating ability of the pyridine nitrogen, both influenced by varying chelate ring sizes. Specifically, the copper(I) complex with **L11** has a stronger donor ability, supporting the higher oxidation state of the **O** species, whereas **L12**, with its lower donor ability, facilitates the formation of the ^{S}**P** species.[68]

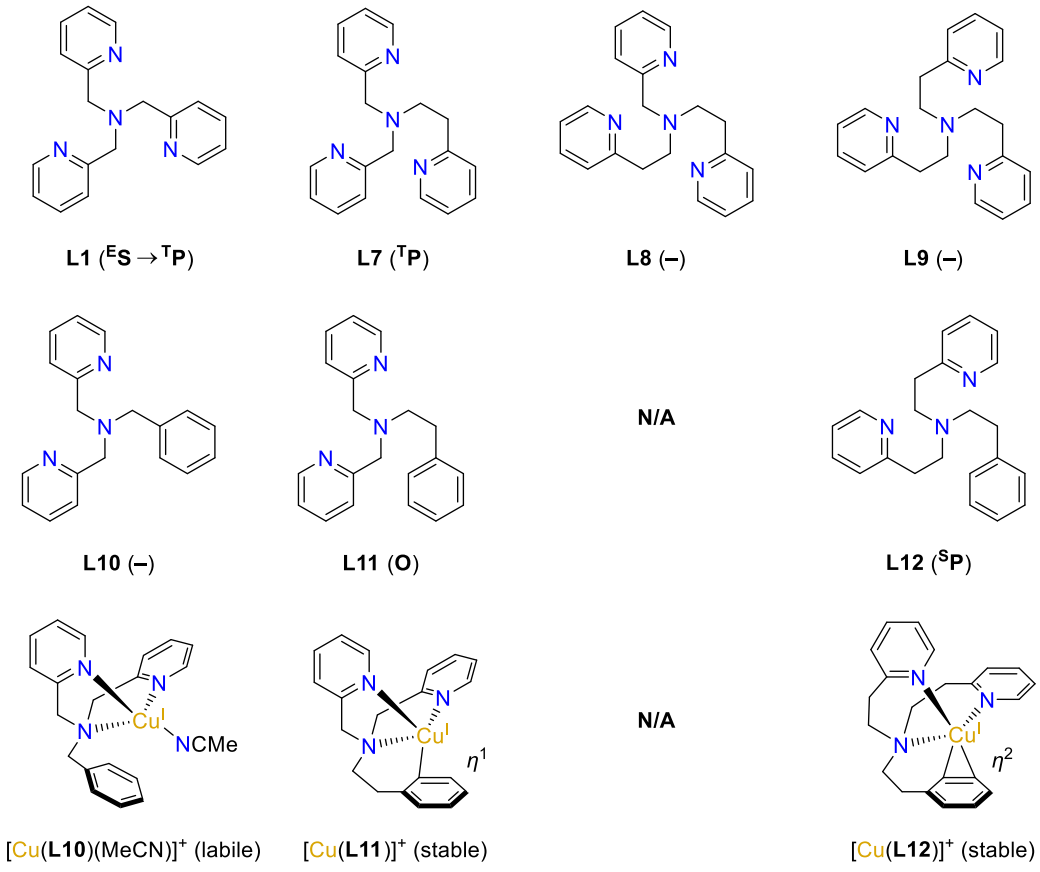

Scheme 11. Influence of chelate ring size on the stability of copper(I) complexes and the copper "oxygen adduct complexes".[48,65,68,73]

To further explore electronic effects on the ^{S}**P**/**O** equilibrium without significantly altering steric demand, Karlin and co-workers investigated tridentate amine copper(I) complexes with different *para*-substituents on pyridyl donor groups (**L13** – **L16**, Scheme 12). Upon oxygenation, they discovered that electron-withdrawing groups, such as chloride (**L13**), favored the exclusive formation of the ^{S}**P** species, while electron-donating groups, like tertiary amines (**L16**), shifted the equilibrium towards the **O** species, due to better stabilization of the copper(III) oxidation state.[66]

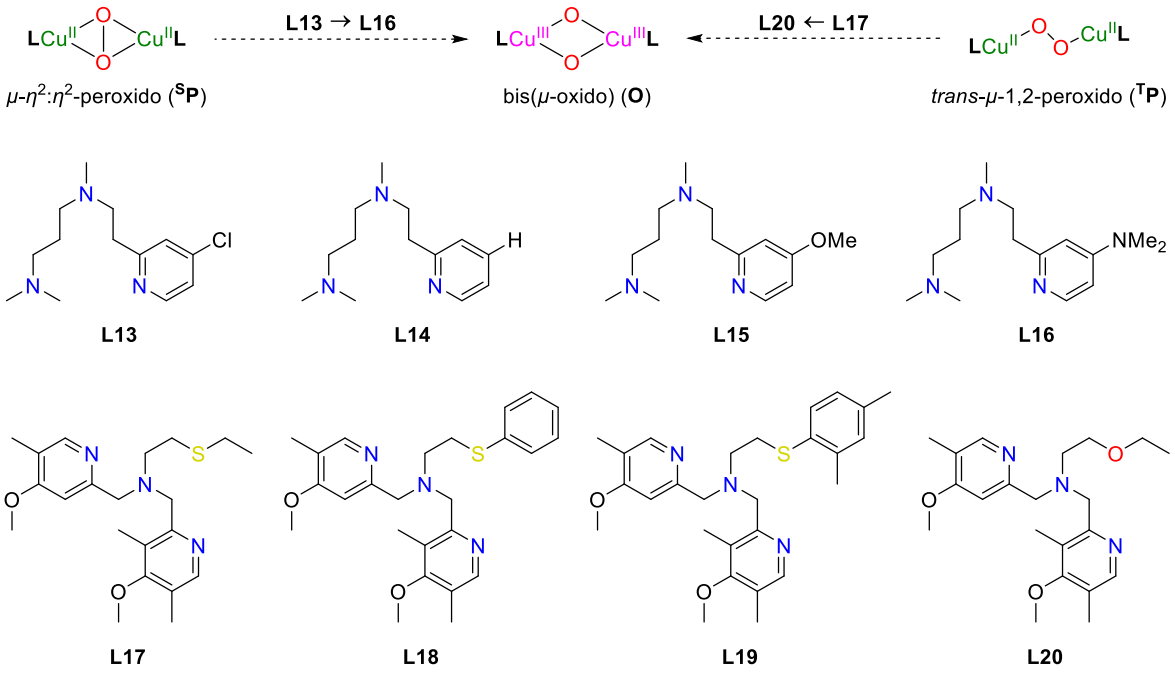

Scheme 12. Influence of electronic and steric effects on the ^{S}**P**/**O** and ^{T}**P**/**O** equilibrium.[66,74]

While isomerization reactions between ^{S}**P**/**O** species are common, examples of isomerization between ^{T}**P**/**O** species are considerably rarer.[75] Karlin and co-workers investigated this equilibrium employing N_3S ligands that incorporate thioether ligation,[74] similar to those found in type-2 copper proteins (Scheme 4). These ligands feature electron-rich 4-methoxy-3,5-dimethylpyridyl donors with ethyl linked thioether moieties, with variations in substituents at the Sulfur atom to adjust the ^{T}**P**/**O** equilibrium (Scheme 12). Oxygenation of the copper(I) complex with an ethyl substituent (**L17**) results exclusively in the formation of the ^{T}**P** species, similar to complexes with tridentate tripodal pyridine ligands like **L1**. Introducing a phenyl substituent to weaken the Cu-S bond (**L18**) initially forms a ^{T}**P** species that subsequently isomerizes to an **O** species. Further weakening of the Cu-S bond by using a bulkier dimethylphenyl residue (**L19**) or a weak-binding ether donor (**L20**) results in the exclusive formation of the **O** species.

The preceding examples demonstrate that the type and reactivity of the copper "oxygen adduct complexes" are influenced by factors related to the array of molecules and ions directly coordinated to the copper ion, known as the first coordination sphere. However, interactions involving functional groups in proximity to the bound dioxygen but not coordinated to the copper center have been less explored (Scheme 13). These second coordination sphere interactions also modulate the properties of metal-oxygen species.[76] Understanding these interactions is crucial for elucidating complex biological mechanisms and allows further tuning of the reactivity of model complexes and will be discussed in the following.

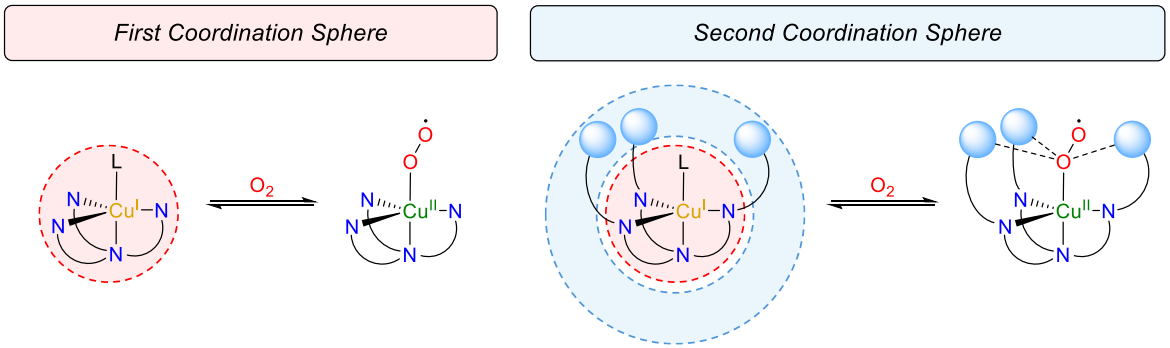

Scheme 13. Comparison between first and second coordination spheres upon oxygenation.

An example demonstrating the role of second coordination sphere interaction in elucidating copper protein mechanisms is the recently proposed reaction pathway for tyrosinase (Scheme 6C), suggesting an initial hydrogen atom abstraction (HAA) from phenolic substrates.[39,40] To validate this mechanism, Karlin and co-workers developed a preorganized synthetic analog using a copper(I) complex with the ligand 2-((bis(3-(dimethylamino)propyl)amino)methyl)-2-^{t}Bu-phenol (**L21**). This ligand incorporates an intramolecular phenolic group in close proximity to the active ^{S}**P** species, analogous to that found in oxy-tyrosinase (Scheme 14).[41] Upon oxygenation of the copper(I) complex, a bis(phenoxyl radical)bis(μ-OH)dicopper(II) intermediate is formed, confirming the occurrence of HAA. This finding is notable because previous studies showed that copper(I) complexes without intramolecular phenolic groups did not react with exogenous monophenol addition.[77] These findings support the HAA mechanism in tyrosinase and demonstrate not only the potential of incorporating functional groups into the ligand backbones to discover novel reactivities but also the advantage of positioning substrates near the active site, which enhances the probability of selective oxidation compared to intermolecular approaches.

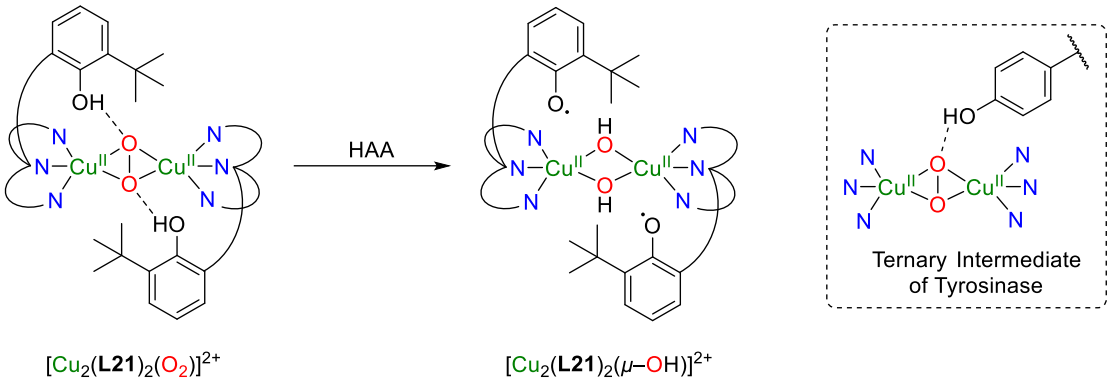

Scheme 14. Reactivity of a preorganized synthetic analog of tyrosinase to investigate HAA and hypothesized ternary intermediate of tyrosinase.[40,41]

Karlin and co-workers also investigated the effects of intramolecular hydrogen bonds on the ^{E}**S** species by examining a series of copper(I) complexes with **L1** derivatives as ligands, which bear various hydrogen bonding moieties at the 6-pyridyl position (Scheme 15).[78,79] Their findings revealed that increasing the number and strength of these substituents systematically shifted the ^{E}**S**/^{T}**P** equilibrium towards the ^{E}**S** species. Additionally, stronger hydrogen bonding significantly increased the electrophilic reactivity of the ^{E}**S** species in HAA. Among the studied copper(I) complexes, the one featuring the bis-pivalamido substituents (**L24**) exhibited the highest reactivity of all the investigated ^{E}**S** species, engaging in reactions with O–H BDEs up to 91.5 kcal mol^{-1} and C–H BDEs up to 79.7 kcal mol^{-1}. These results demonstrate the importance of second coordination sphere interactions in stabilizing and modulating the reactivity of copper "oxygen adduct complexes".

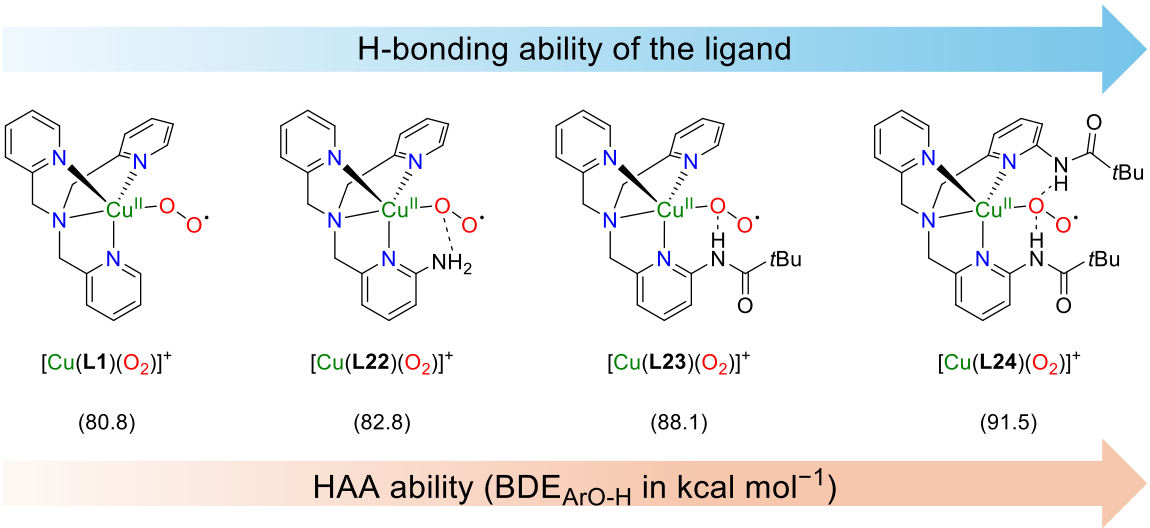

Scheme 15. Ligands based on **L1** with different H-bonding substituents to modulate their HAA reactivity with highest BDE_{ArO-H} from substrates that react with ^{E}**S** species.[30,78,79]

Intramolecular hydrogen bonds can also shift the ^{E}**S**/^{T}**P** equilibrium towards the ^{T}**P** species. Masuda and co-workers demonstrated this by investigating copper(I) complexes with modified **L1** ligands bearing amine substituents at the 6-pyridyl position.[80,81] Upon oxygenation, the resulting ^{T}**P** species exhibited absorption bands that were significantly blue-shifted, compared to classic ^{T}**P** species. Furthermore, the UV-vis absorption intensity decreased as the number of amine substituents at the 6-pyridyl position increased, with the most pronounced effect observed in the trisubstituted ligand tris(6-amino-2-pyridylmethyl)amine (**L25**, Scheme 16). These changes were attributed to the formation of hydrogen bonds between the amine substituents and the bound oxygen in the ^{T}**P** species, restricting their degrees of freedom and altering the LMCT absorption bands. While Masuda and co-workers proposed the existence of these hydrogen bonds, similar spectra were also reported by Karlin and co-workers.[82] The first structurally characterized hydrogen bond stabilized ^{T}**P** species was reported by Szymczak and co-workers, using an **L1**-derived ligand with three 6-phenylamino-2-pyridylmethyl groups at the 6-pyridyl position (**L26**).[83] Here, the monosubstituted amines facilitated hydrogen bonding, and the phenyl groups provided steric protection, enabling crystallization of the hydrogen bond stabilized ^{T}**P** species. The UV-vis spectra aligned with the discussed results, providing further evidence for the role of second coordination sphere interactions, specifically in the form of hydrogen bonds.

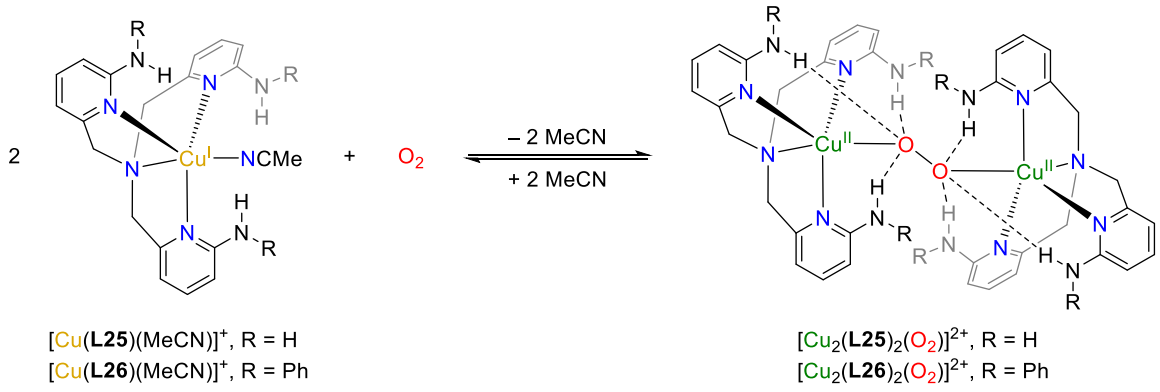

Scheme 16. Formation of hydrogen bond stabilized ^{T}**P** species using amines/amides.[81,83]

A novel example of these second coordination sphere interactions, particularly involving intramolecular hydrogen bonds, was reported by Hong and co-workers. Upon oxygenation of a copper(I) complex with *N*-(2-ethoxyethanol)-bis(2-picolyl)amine (**L27**) as a ligand, the formation of a hydrogen bond stabilized ^{T}**P** species occurred (Scheme 17), similar to the discussed amine derivatives of **L1**. Here, however, the hydrogen donation was facilitated not by amine or amide groups but uniquely by an ethoxyethanol side arm, with the terminal

hydroxy group acting as the hydrogen donor.[84,85] The enhanced solubility provided by the terminal hydroxy group enabled the use of this complex in various processes, such as polymerization reactions and the generation of H_2O_2 in aqueous media, where the hydrogen bond stabilized ^{T}**P** species plays a crucial role in the latter example.[85,86] Although the authors did not specifically investigate the function of the ether moiety of the side arm, its reactivity in **L27** is likely comparable to that in **L20**, potentially acting as a weak binding group that positions the hydroxy group in the proximity of the bound dioxygen, thereby facilitating the formation of the hydrogen bond stabilized ^{T}**P** species.[84,85]

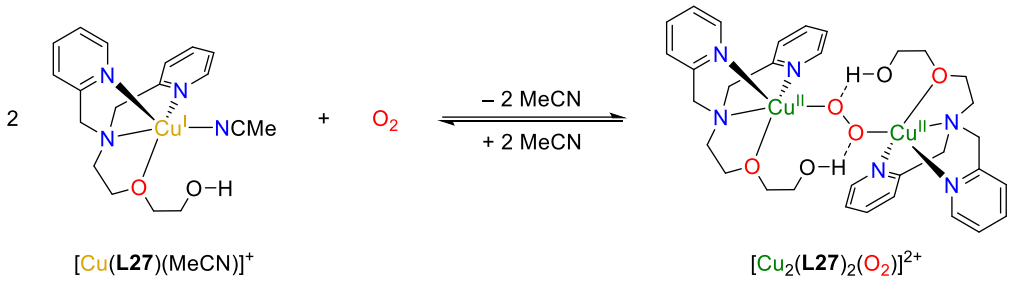

Scheme 17. Formation of hydrogen bond stabilized ^{T}**P** species using alcohols.[85]

In conclusion, the examples discussed emphasize the critical role of both first and second coordination sphere interactions in influencing the nature and reactivity of copper "oxygen adduct complexes". While considerable attention has been given to studies regarding the first coordination sphere, the interactions involving the second coordination sphere remain underexplored. However, examples such as the newly proposed mechanism for tyrosinase and its related model complex offer significant potential for future research. These findings present opportunities to explore a variety of functional groups, thereby enhancing our understanding of natural processes and aiding in the development of novel catalysts for selective oxidation reactions. Additionally, challenges such as the spontaneous disproportionation of copper(I) complexes, which complicate dioxygen activation studies, must be addressed.

2 Research Goals

2.1 Stabilizing Copper(I) Complexes for Studying Dioxygen Activation

As detailed in **Chapter 1.3.3**, certain copper(I) complexes tend to spontaneously disproportionate into copper(II) and elemental copper, making it difficult to study their reactivity towards dioxygen and their possible applications as catalysts for selective oxidation reactions. Although various strategies exist to stabilize labile copper(I) complexes, such as altering the solvent or the steric properties of the anion, these methods are highly ligand-dependent and can influence the reactivity of the copper(I) complex. Consequently, there is significant interest in developing more stabilization techniques applicable to a broader spectrum of copper(I) complexes.

Based on the findings of Itoh and co-workers, which demonstrated that incorporating phenylic side chains can stabilize labile copper(I) complexes (see **Chapter 1.3.3**), this study investigates related olefinic side chains, which have not been explored in this context. The goal of this research was to assess whether integrating olefinic side arms into the ligand structure could suppress disproportionation and how this modification impacts its reactivity towards dioxygen. Initially, a series of ligands should be synthesized (**L28** – **L33**, Scheme 18), to evaluate the effects of isomerism, aromaticity, and linker length. The interactions between the olefinic and aromatic side chains and the copper ion should be examined using nuclear magnetic resonance (NMR) spectra of both the free ligands and their respective copper(I) complexes. Additionally, the reactivity of these complexes towards dioxygen should be investigated utilizing low-temperature stopped-flow UV-vis spectroscopy techniques. The results demonstrated that olefinic side chains can stabilize labile copper(I) complexes while maintaining similar reactivity to non-olefinic counterparts, although the degree of stabilization is influenced by the length and position of the linker. The results were published in the *European Journal of Inorganic Chemistry* (**Chapter 3.1**).

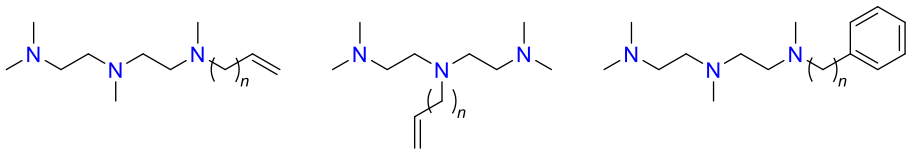

L28, *n* = 1
L31, *n* = 2

L29, *n* = 1
L32, *n* = 2

L30, *n* = 1
L33, *n* = 2

Scheme 18. Ligands with olefinic or aromatic side arms discussed in this work.

2.2 Second Coordination Sphere Interactions in Dioxygen Activation

As discussed in **Chapter 1.3.3**, the formation of various types of copper oxygen adduct complexes is influenced by multiple factors. Most research has focused on the first coordination sphere, examining how subtle changes in the ligand affect oxygen adduct complex formation. This has provided substantial insight into the fundamental interactions within these complexes. However, the role of second coordination sphere interactions remains less explored. Understanding its influence is vital, as it involves additional interactions like hydrogen bonds, which can significantly impact the overall structure and behavior of the "oxygen adduct complex", making the study of these factors crucial for gaining insights into more complex natural and chemical processes.

Most studies on intramolecular hydrogen bonding interactions in this area have utilized additional amine and amide functionalities in the ligand, whereas examples involving interactions with hydroxy functions are limited. Consequently, the goal of this work was to enhance our understanding of second coordination sphere interactions using hydroxy functionalities. Ligand **L27** was employed, whose copper(I) complex can form hydrogen bonds *via* an ethoxyethanol side chain to the activated dioxygen species, resulting in a hydrogen bond stabilized *trans*-μ-1,2-peroxido species. To understand this unique property of the ligand, the reaction should be further investigated using low-temperature stopped-flow UV-vis spectroscopy techniques. Additionally, the significance of the ether moiety as well as the hydrogen donor should be investigated by synthesizing and examining a series of derivatives (**L34** – **L39**, Scheme 19). The findings underscore the importance of the ether moiety, and a revised reaction mechanism for the reaction of the copper(I) complex and dioxygen was elucidated. This mechanism supports the transient formation of a hydrogen bond stabilized *trans*-μ-1,2-peroxido species, which subsequently undergoes a rapid isomerization reaction to a bis(μ-oxido) species. The results were published in the *European Journal of Inorganic Chemistry* (**Chapter 3.2**).

L27, X = O
L34, X = S
L35, X = CH_2

L36, R = OCH_3
L37, R = CH_3
L38, R = NHAc
L39, R = NH_2

Scheme 19. Ligands with ethoxyethanol derived side arms discussed in this work.

3 Published Research Articles

3.1 Stabilizing Copper(I) Complexes by Terminal Olefinic Side Arms and Studying their Reactivity towards Oxidation

This article has been published in

European Journal of Inorganic Chemistry

Alexander Granichny, Christian Würtele, and Siegfried Schindler

Eur. J. Inorg. Chem. **2024**, e202400570

https://doi.org/10.1002/ejic.202400570

Check for updates

EurJIC
European Journal of Inorganic Chemistry

Research Article
doi.org/10.1002/ejic.202400570

Chemistry Europe
European Chemical Societies Publishing

www.eurjic.org

Stabilizing Copper(I) Complexes by Terminal Olefinic Side Arms and Studying Their Reactivity Towards Oxidation

Alexander Granichny,[a] Christian Würtele,[a] and Siegfried Schindler*[a]

Many copper(I) complexes with aliphatic amine ligands have a strong tendency to disproportionate to copper(II) and elemental copper in solution at higher concentrations, making it difficult to isolate them and to study their reactivity. A series of copper(I) complexes with ligands based on tridentate N,N,N′,N″,N″-pentamethldiethylenetriamine (**Me$_5$dien**) were synthesized that included terminal olefinic and aromatic groups. It could be shown that the olefinic side arms stabilized some of the copper(I) complexes. Whether and how strongly the complexes were stabilized depended on the position and length of the olefinic sidearm. Additionally, the reactivity of the copper(I) complexes towards dioxygen was investigated.

Introduction

Selective oxygenation reactions are crucial in biological systems, synthesis, and the chemical industry.[1–5] While oxygenation reactions on an industrial scale usually use rare metal catalysts, apply toxic oxidants, and/or require high-pressure and high-temperature environments, enzymatic oxygenations occur in metal ions-containing catalytic pockets under ambient conditions using dioxygen from air. Biomimetic model complexes have been synthesized to study the underlying mechanisms in nature and find green and sustainable catalysts.[1–3] Especially copper(I) complexes are of particular interest because they can activate dioxygen, forming so-called "oxygen adduct complexes" (Scheme 1), which can oxygenate external substrates such as toluene to benzaldehyde.[6–8]

To observe these "oxygen adduct complexes", it is usually necessary to apply low-temperature stopped-flow techniques due to their short lifetime. The reactivity of a large number of copper(I) complexes towards dioxygen has been investigated and the results are summarized in several review articles.[1–4] However, it is important to point out that most of the time, it is not even possible to detect these reactive species spectroscopically despite the low temperatures. This happens when the consecutive reactions after the formation of the intermediates are much faster and thus do not allow their observation. For example, the copper complex [Cu(**Me$_6$trien**)]$^+$ (**Me$_6$trien** = N,N′-bis[2′(dimethylamino)ethyl]-N,N′-dimethyl-ethane-1,2-diamine, Scheme 2) reacts with dioxygen to the corresponding copper(II) complex without detection of an intermediate.[9] Unfortunately,

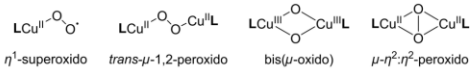

Scheme 1. Selection of "oxygen adduct complexes" (charges are omitted) formed by the reaction of copper(I) with dioxygen.[2]

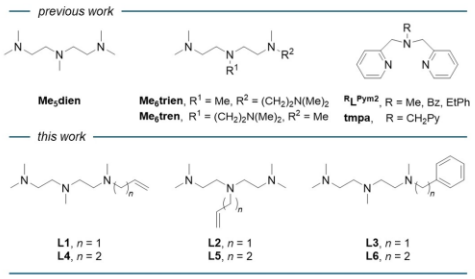

Scheme 2. Ligands for copper(I) complexes discussed in here.[8–10,12,14,20,22–26]

many copper(I) complexes with aliphatic amine ligands have a strong tendency to disproportionate to copper(II) and elemental copper in solution at higher concentrations, making it difficult to isolate them and to study their reactivity.[10,11] However, if complex formation is faster than its reaction with dioxygen, it is possible to investigate this reaction by mixing an inert solution of a copper(I) salt with a dioxygen-saturated ligand solution using stopped-flow techniques.[12] An example is the copper(I) complex with the tridentate ligand N,N,N′,N″,N″-pentamethyldiethylenetriamine (**Me$_5$dien**, Scheme 2), which shows decomposition at higher concentrations.[12] For this system, the copper(I) salt, ligand, and dioxygen were rapidly mixed in a low-temperature stopped-flow setup, generating the copper(I) complex *in situ*, which then reacted with dioxygen. Applying this method, the formation of a bis(μ-oxido)dicopper(III) complex was spectroscopically observed.[12,13] A problem with this procedure is the introduction of acetonitrile derived from the copper(I) salts [Cu(MeCN)$_4$]$^+$. Acetonitrile is a strongly coordinat-

[a] *A. Granichny, C. Würtele, S. Schindler*
Institute of Inorganic and Analytical Chemistry, Justus Liebig University Giessen, Heinrich-Buff-Ring 17, Giessen 35392 Germany
E-mail: siegfried.schindler@anorg.chemie.uni-giessen.de

Supporting information for this article is available on the WWW under https://doi.org/10.1002/ejic.202400570

ing ligand for copper(I), which leads to the stabilization of copper(I) complexes. However, it often leads to the suppression of the reaction with dioxygen.

Some copper(I) complexes are stabilized by sterically demanding anions.[6] The copper(I) complex with the tetradentate tripodal ligand tris(2-dimethylaminoethyl)amine (**Me$_6$tren**, Scheme 2), for example, has a strong tendency for disproportionation but can be stabilized to a large extent by applying tetraphenylborate as an anion.[6] Thus, the complex can be isolated as a colorless crystalline solid. However, kinetic studies were performed as described above by mixing an inert solution of a copper(I) salt with a dioxygen-saturated solution of **Me$_6$tren**.[10,14] At low temperatures, the so-formed copper(I) complex first reacts to a mononuclear η^1-superoxido copper(II) complex before forming a relatively stable *trans*-μ-1,2-peroxido dicopper(II) complex (Scheme 1). This contrasts the copper(I) complex with its isomer **Me$_6$trien** (described above), for which no intermediate could be spectroscopically detected.[9] It is interesting to note at this point that the copper(I) complex of the isomeric ligand **Me$_6$trien** can be obtained by a comproportionation reaction of the copper(II) complex with elemental copper, which was impossible with **Me$_6$tren**.[9,15] Furthermore, it is possible in some cases to achieve stabilization by synthesizing the corresponding copper(I) carbonyl complexes, for example $[Cu(\mathbf{tmpa})(CO)]^+$ (**tmpa** = tris(2-pyridylmethyl)-amine, Scheme 2).[16–18] However, here, the reaction with dioxygen was triggered by photodissociation, and it was determined that the photolabile carbonyl species in solution possessed a tridentate coordination mode to the copper(I) ion with one dangling arm of the tripodal ligand.[18]

Compared to using additional ligands like acetonitrile or carbon monoxide, which are prone to be non-removable and make the copper center sterically inaccessible to associative substitution by dioxygen,[16,18] aromatic ligands like benzene proved to be more hemilabile.[19] Itoh and co-workers showed that incorporating an ethylphenyl arm into $^{R}\mathbf{L}^{Pym2}$ stabilizes the complex compared to its labile methyl or benzyl derivatives (Scheme 2). This is due to a d-π interaction of the copper(I) ion and the phenyl group of the ligand side arm forming a bis(μ-oxido)dicopper(III) complex upon oxygenation.[8,20–22] The absence of a binding mode in the benzyl derivative is due to the shorter linker, which shows that the position of the side arm and the linker length are important to stabilize the complex. Although the incorporation of aromatic groups binding the copper(I) ion is well established by now, the analogous use of olefinic units so far is underexplored. One example of a ligand containing an intramolecular olefinic arm is **L1** (Scheme 2) by Meyerstein and co-workers, whose copper(I) complex showed enhanced stability in aqueous solutions compared to complexes with ligands **Me$_5$dien** and **Me$_6$trien**.[23–25] This prompted us to reinvestigate the copper(I) complex with **L1** to explore its stability in solution and if the allyl function has any implication regarding the reactivity towards dioxygen. In addition, a series of related derivates was synthesized to study the above-mentioned influence of isomerism (**L2**), aromaticity (**L3**), and elongated linker length (**L4**–**L6**, Scheme 2).

Results and Discussion

Synthesis of Ligands L1–L6

The ligands **L1**–**L6** were prepared according to Scheme 3. The synthesis of **L1** has been described in the literature by Meyerstein and co-workers and modified for this work.[23] In contrast to the literature, the reaction of diethylenetriamine (**1**) with allyl bromide did not yield pure monoalkylated (**2**). Instead, a mixture of mono- and dialkylated products was received and purified after subsequent Eschweiler-Clarke methylation to obtain **L1**. The synthesis of the symmetrical ligands **L2** and **L5** started with N,N,N′′,N′′-tetramethyldiethylenetriamine (**3**), which was synthesized from **Me$_6$tren** and *n*-BuLi according to a published procedure.[27] While deprotonation by sodium hydride and subsequent alkylation by allyl bromide was sufficient to obtain **L2** a different approach had to be chosen for **L5** due to the lower reactivity of 4-bromo-1-butene compared to allyl bromide. Hence, potassium iodide is added to exchange the bromide for iodide by a Finkelstein reaction to form a better-leaving group, which can alkylate **3** with potassium carbonate as a base to obtain **L5**. The aromatic ligands **L3** and **L6** were synthesized by reductive amination with benzaldehyde or phenylacetaldehyde and subsequent Eschweiler-Clarke methylation. The synthesis of **L4** starts from **L3** following a benzyl deprotection with palladium on charcoal and hydrogen and subsequent alkylation like for **L5** with potassium iodide, potassium carbonate, and 4-bromo-1-butene.

Synthesis, Characterization, and Dioxygen Reactivity of the Copper(I) Complexes with Ligands L1 and L4

Numerous efforts failed to obtain crystals of the copper(I) complexes with ligands **L1** and **L4** for structural characterization. Therefore, the complexes were characterized by elemental analysis (EA) and nuclear magnetic resonance (NMR) measurements. The synthesis of the copper(I) complex of **L1** was carried out by mixing $[Cu(MeCN)_4]OTf$ and **L1** in acetonitrile before removing the solvent overnight *in vacuo*. While the synthesis of copper(I) complexes in acetonitrile can be a

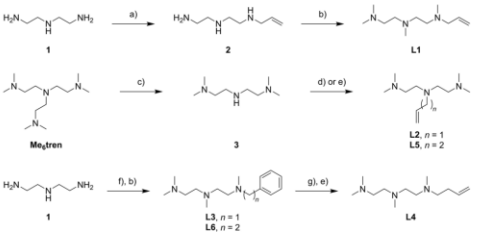

Scheme 3. Synthesis of ligands **L1**–**L6**. a) allyl bromide, EtOH, RT; b) CH_2O, acetic acid, reflux; c) *n*-BuLi, *n*-pentane, 0 °C to RT, d) NaH, allyl bromide, THF, 0 °C to RT (**L2**); e) KI, K_2CO_3, 4-bromo-1-butene, THF, reflux (**L5**); f) $NaBH(OAc)_3$, benzaldehyde (**L3**) or phenylacetaldehyde (**L6**), DCM, RT; g) Pd/C, H_2, MeOH, RT.

Research Article
doi.org/10.1002/ejic.202400570

hindrance, *vide supra*, both EA and NMR spectra showed no presence of acetonitrile coordinating to the complex (Figure 1b). The colorless appearance, the absence of acetonitrile, and the high field shift of the olefinic protons of the copper(I) complex of **L1** compared to the ligand implies that the allylic side arm is coordinated to the copper ion and thus stabilizes it (Figure 1). The overall results show that the copper(I) complex is stabilized by the coordination of the allylic side arm in solid and organic solutions. The corresponding copper(II) complex could be structurally characterized, and, as expected, the allylic side arm is not coordinated with the copper(II) ion. The molecular structure of [Cu(**L1**)(H_2O)(OTf)](OTf) is shown in Figure 2, where the allylic side arm (double bond located between C(1) and C(2)) is pointing outwards away from the copper center. The copper(II) ion is coordinated in a distorted square pyramidal geometry (according to an analysis developed by Addison et al. with $\tau_5 = 0.3$)[28] by three N-donor atoms (N(1), N(2), N(3)) of **L1**, a water molecule (O(1)), and a triflate anion (O(2)).

Reacting a colorless solution of the copper(I) complex [Cu(**L1**)]OTf with dioxygen at −80 °C in acetone in a benchtop experiment first led to a bright yellow color, which then turned rapidly to green and finally to a blue-colored solution. Low-temperature stopped-flow UV-vis measurements revealed the fast formation of a bis(μ-oxido)dicopper(III) complex with an absorbance maximum at 406 nm (Figure 3), in line with previous investigations.[2,12,29] After a few seconds, decomposition of the "oxygen adduct" complex is observed. Extracting the oxygenated solution by basic workup and investigating it with GC-MS revealed that the ligand remains intact, and no intramolecular hydroxylation or demethylation occurred (Figure S34, S35). Furthermore, the reaction under pseudo-first-order conditions is independent of dioxygen concentration. The overall observations are similar to the reaction of [Cu(**Me$_5$dien**)(MeCN)]$^+$ with dioxygen.[12] However, for this complex, we had to perform the reaction *in situ* and could not avoid the presence of additional acetonitrile in the solution.

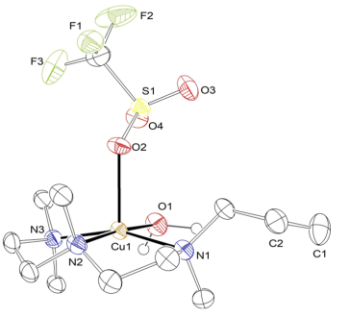

Figure 2. ORTEP Plot of the molecular structure of [Cu(**L1**)(H_2O)(OTf)](OTf). Non-binding anions and carbon-bound hydrogen atoms are omitted for clarity (except H_2O). Ellipsoids are drawn at 50 % probability. Selected Bond Lengths (Å): Cu(1)–N(1): 2.088; Cu(1)–N(2): 2.028; Cu(1)–N(3): 2.087; Cu(1)–O(1): 2.014; Cu(1)–O(2): 2.259; C(1)–C(2): 1.318. Selected bond angles (°): N(1)–Cu(1)–N(2): 85.28; N(1)–Cu(1)–N(3): 158.99; N(2)–Cu(1)–N(3): 85.76; N(1)–Cu(1)–O(1): 94.37; N(1)–Cu(1)–O(2): 99.58; N(2)–Cu(1)–O(1): 174.69; N(2)–Cu(1)–O(2): 93.71; N(3)–Cu(1)–O(1): 92.82; N(3)–Cu(1)–O(2): 99.92; O(1)–Cu(1)–O(2): 91.57.

The mechanism for the formation of the bis(μ-oxido)dicopper(III) complex can be assigned in the same way as reported previously.[12,20,30] According to Scheme 4, the forma-

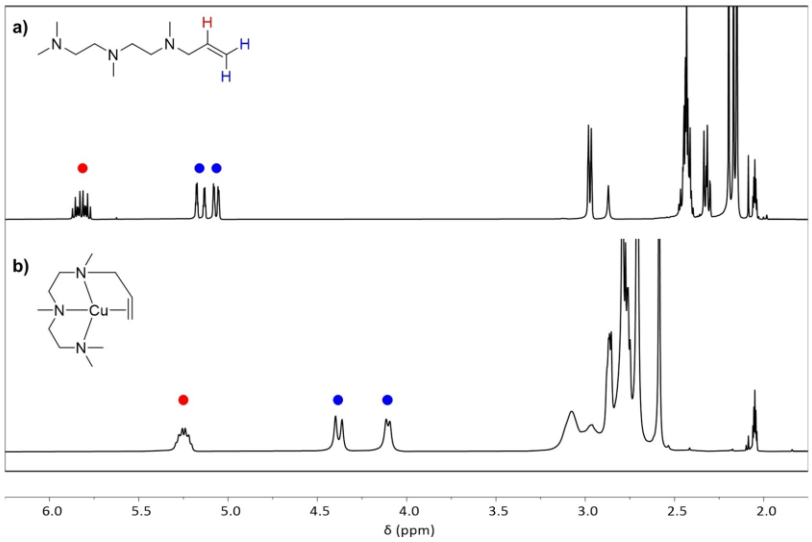

Figure 1. ^{1}H NMR spectra of (a) **L1**, (b) [Cu(**L1**)](OTf) measured in $(CD_3)_2CO$ at room temperature. Charges and anions are omitted for clarity.

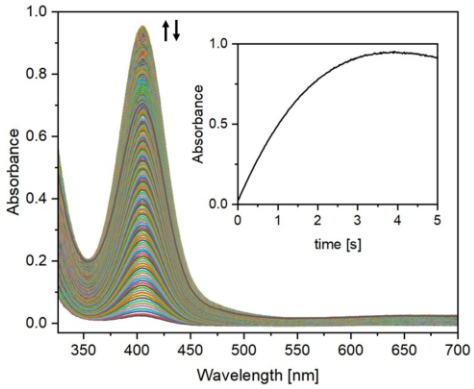

Figure 3. Time-resolved UV-vis spectra of the reaction of [Cu(**L1**)]OTf ($2.5 \cdot 10^{-4}$ mol L^{-1}) with dioxygen ($5.7 \cdot 10^{-3}$ mol L^{-1})[5] in acetone at −80 °C over a period of 5 s. The inset displays the time-dependent change in absorbance at 406 nm.

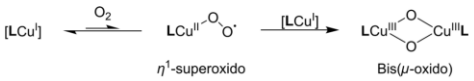

Scheme 4. Proposed mechanism for the formation of the bis(μ-oxido)dicopper(III) complex.

tion of an unstable η^1-superoxido complex in a rapid left-lying preequilibrium is proposed, followed by the reaction with another copper(I) complex to form the observed bis(μ-oxido)dicopper(III) complex.

Thus, we successfully stabilized this copper/dioxygen system by introducing an olefinic group. This conveys that incorporating the allyl sidearm into the ligand scaffold suppressed the disproportionation of the copper(I) complex in solid and solution and did not interfere with the activation of dioxygen. Considering the different reaction conditions, the bis(μ-oxido)dicopper(III) complex with the ligand **L1** lasts for a few seconds longer than with the ligand **Me$_5$dien** before decomposition under the same conditions (Figure S31). Additionally, we observed that the *in situ* reaction with **L1** did not work out. Here, the formation of the copper(I) complex is slower than the reaction of the complex with dioxygen, and only a very small part of the overall reaction could be spectroscopically detected.

Because chelate ring size plays an important role,[31] we investigated the copper(I) complex with ligand **L4**, which differs from **L1** by an elongated olefinic sidearm. As for the copper(I) complex with **L1**, the allylic protons were shifted to high field, and no acetonitrile was found to be coordinated (Figure S21, S22). The difference in linker length caused the copper(I) complex with **L4** as a ligand to become so stable that it did not react with dioxygen anymore (even at room temperature, Figure S32). This is a well-known phenomenon that larger chelate rings can stabilize copper(I) complexes to such an extent that they become less or even unreactive towards dioxygen.[31] Furthermore, it shows that an optimal linker length of the olefinic side arm is crucial for a ligand that can stabilize the copper(I) ion while still being reactive toward dioxygen.

Synthesis, Characterization, and Reactivity Towards Dioxygen of the Copper(I) Complexes with Ligands L2, L3, L5, and L6

After establishing that incorporating an allylic sidearm into the ligand scaffold of **Me$_5$dien** leads to a stable yet reactive copper(I) complex, and its elongated derivative led to an overstabilized and unreactive copper(I) complex; further insights were yet to be obtained. By comparing **L1** with its derivatives, the effect of isomerism (**L2**), aromaticity (**L3**), and elongated linker length (**L5**, **L6**) were studied (Scheme 2). The corresponding copper(I) complexes were synthesized and characterized, and the reactivity with dioxygen was tested. Unfortunately, again crystals of copper(I) as well as of copper(II) complexes with these ligands suitable for structural characterization could not be obtained. Disproportionation was observed for copper(I) complexes with ligands **L2** and **L3**.

The constitutional isomers **L2** and **L5** differ from **L1** and **L4** only by having the olefinic side arm attached to the central instead of the lateral amines. Analogous to the copper(I) complexes of **L1** and **L4** its isomeric complexes with **L2** and **L5** as ligands do not contain a coordinated acetonitrile according to elemental analysis and NMR spectra (Figure S17, S18). However, the copper(I) complex of **L2** showed disproportionation upon isolation, visible by a pale blue appearance (instead of being colorless) and broad signals in the ^{1}H-NMR spectrum (Figure S17). Nevertheless, reactions with the copper(I) complex of **L2** and dioxygen were conducted with stopped-flow measurements at −80 °C in acetone, revealing the formation of a small band at 409 nm resembling a bis(μ-oxido)dicopper(III) complex (Figure S33A), similar to the band appearing for **L1**. The measurements have been repeated under the same conditions with freshly generated copper(I) complex of **L2** in acetone, which showed a much higher absorbance at the same wavelength compared to the isolated complex (Figure S33B). The overall findings showed that the constitutional isomer **L2** cannot stabilize the copper(I) ion, likely due to the position of the allylic group, which is too rigid and not flexible enough to coordinate sufficiently.

Furthermore, the copper(I) complex with the elongated ligand **L5** confirms this. The copper(I) complex is stable in solution and upon isolation. It reacts in benchtop experiments at −80 °C in acetone to a bright, yellow-colored solution before decomposing to a green-colored solution. However, no "oxygen adduct" species was detectable by stopped-flow measurements under the same conditions. Only the formation of the corresponding copper(II) complex is observed by a slow buildup of a shoulder at 359 nm and a broad band at 656 nm over the period of one hour (Figure 4). By comparing the spectra with its corresponding copper(II) complex, it is reasonable that the

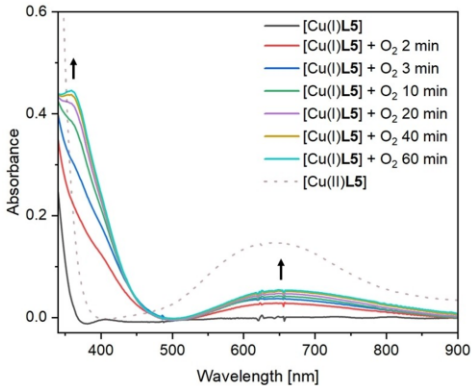

Figure 4. UV-vis spectra of the reaction of [Cu(**L5**)]OTf ($5.0 \cdot 10^{-4}$ mol L^{-1}) with dioxygen gas in acetone at −80 °C over a period of 60 min compared with its corresponding copper(II) complex [Cu(**L5**)(MeCN)$_2$](OTf)$_2$ ($5.0 \cdot 10^{-4}$ mol L^{-1}).

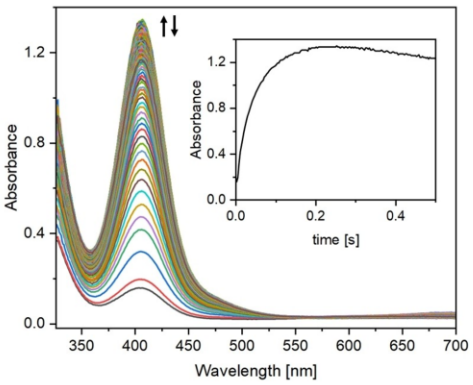

Figure 5. Time-resolved UV-vis spectra of the reaction of [Cu(**L3**)(MeCN)]OTf ($2.5 \cdot 10^{-4}$ mol L^{-1}) with dioxygen ($5.7 \cdot 10^{-3}$ mol L^{-1})[5] in acetone at −80 °C over a period of 0.5 s. The inset displays the time dependent change in absorbance at 406 nm.

broad band shows the formation of copper(II) while the shoulder is likely decomposed ligand.

Following the work by Itoh and co-workers[8] with the ligand $^{R}L^{Pym2}$, aromatic groups were introduced in our ligand system instead of aliphatic olefinic groups, leading to ligands **L3** and **L6**. The synthesis of the copper(I) complex with **L3** as a ligand resulted in a green-colored oil, which turned out to be the mono acetonitrile copper(I) complex through EA and NMR spectra (Figure S19, S20). No shifts in the aromatic region were detected by comparing the ^{1}H and ^{13}C-NMR of **L3** and its corresponding copper(I) complex (Figure S29a, S29b, S30a, S30b). This means that the benzylic side arm is not attached to the copper(I) ion, explaining the reason for the coordinated acetonitrile and, therefore, closely resembles $^{Bz}L^{Pym2}$.[8] The color of the isolated copper(I) complex and a broad band in the 500–700 nm range in the UV-vis spectrum indicated disproportionation, similar to the copper(I) complex with **L2** as a ligand. Stopped-flow measurements with the copper(I) complex of **L3** were conducted at –80 °C in acetone, revealing the formation of a band at 406 nm, indicating a bis(μ-oxido)dicopper(III) complex (Figure 5). While the reactivity of the copper(I) complex with dioxygen is analogous to the copper(I) complexes with **L1** and **L2**, the oxygen adduct starts decaying a magnitude faster. This is likely due to the missing coordination of the benzylic sidearm, which is why the complex is mainly stabilized by the coordinated acetonitrile, making the complex more labile and reactive. Measurements at different dioxygen concentrations under the same conditions showed that the reaction rate was independent of dioxygen concentration. These results are in line with the reactivity of the copper(I) complex of **L1**, and the same mechanism can be proposed (Scheme 4). **L3** compares well with $^{Bz}L^{Pym2}$ because the linker of the additional benzylic side arm is not long enough to bind to the copper(I) center, and therefore the isolated complex coordinated acetonitrile and decomposed partially.[8,20] However, the direct comparison with **L1**, which has the same methyl linker, can coordinate the copper(I) ion, showing that it is likely the rigid nature of the aromatic group that hinders coordination.

The copper(I) complex with **L6** showed no sign of disproportionation, and coordination of acetonitrile was not observed. While the ^{1}H-NMR seemed to suggest that the ethylphenyl side arm was not attached to the copper(I) ion (Figure S29c, S29d), the ^{13}C-NMR clearly showed that two carbon signals of the phenyl group are significantly shifted and broadened (in comparison with the ligand), confirming that the ethylphenyl side arm is coordinated to the copper(I) ion (Figure S30c, S30d). By elongating the linker length from **L3** to **L6**, the phenylic side arm becomes more flexible, coordinates with the copper ion, and stabilizes the complex. In stopped-flow experiments with the copper(I) complex of **L6** the formation of an absorption band at 409 nm again showed the formation of a bis(μ-oxido)dicopper(III) complex (Figure 6). The spectra, as well as the lifetime of the dioxygen adduct complex with **L6** as a ligand, resembles the one with **L1** more than with **L3**, likely because the increased linker length now allows the phenylic side arm to coordinate the copper(I) ion and therefore reacts slower than the corresponding complex with coordinated acetonitrile. This is very similar to the above-discussed results by Itoh and co-workers and their finding that the ligand system $^{R}L^{Pym2}$ with a benzyl side arm is not stable, while its derivative with an ethylphenyl derivative is.[20] Here, the authors could support their findings with molecular structures of the corresponding copper complexes.

Conclusions

In this work, we established with derivatives of **Me$_5$dien** that adding terminal olefinic side arms into a ligands scaffold can

Research Article
doi.org/10.1002/ejic.202400570

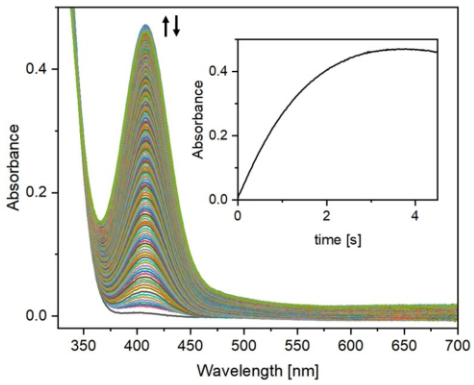

Figure 6. Time-resolved UV-vis spectra of the reaction of [Cu(**L6**)]OTf ($2.5 \cdot 10^{-4}$ mol L^{-1}) with dioxygen ($5.7 \cdot 10^{-3}$ mol L^{-1})[5] in acetone at −80 °C for 4.5 s. The inset displays the time-dependent change in absorbance at 409 nm.

stabilize the corresponding copper(I) complexes upon isolation and in solution in contrast to the non-derivatized ligand. Whether and how strongly the complexes are stabilized highly depends on the position and length of the olefinic sidearm. Generally, sterically hindered positions require a longer linker to bind the copper(I) ion than sterically less hindered positions. However, linkers that are too lengthy over-stabilize the copper(I) complexes, which then become unsusceptible to further reactions with dioxygen. This is not unusual as copper(I) complexes can be pretty stable towards oxidation due to donor atoms and/or the size of the chelate ring or the anion.[31] Furthermore, oxidation of a copper(I) to a copper(II) complex is much more common than observing an intermediate in this process due to the kinetics of this reaction.[32] In addition, we showed that olefinic side arms need shorter linkers to sufficiently bind the copper(I) ions compared to phenylic side arms at the same position, which is probably due to the higher flexibility. Furthermore, the dioxygen activation of the copper(I) complexes was tested. The best result was obtained with the ligand **L1** (reported previously by the Meyerstein group), whose position and length of the allylic side arm allow it to bind the copper(I) ion strongly enough to stabilize it while binding weakly enough to react with dioxygen. According to the mechanism shown in Scheme 4, which had been assigned previously,[20,30] first a η^1-superoxido copper(II) complex forms before reacting to the observed bis(μ-oxido)dicopper(III) complex, confirming that the olefinic side arm does not affect the intermediate formed as it is the same as for **Me_6dien**. The difficulty in spectroscopically observing the η^1-superoxido complex as an intermediate was demonstrated by DFT calculations on related systems.[33] Only recently, England and coworkers obtained and characterized an η^1-superoxido copper(II) complex by using a sterically encumbered tridentate ligand.[34]

All in all, our work demonstrates that incorporating olefinic side arms into a ligand scaffold is a non-invasive way to study the oxygen adduct formation of labile copper(I) complexes. To further elaborate on this methodology, ligands can be equipped with olefinic side arms that form unstable copper(I) complexes to study their dioxygen activation in the future.

Experimental Section

Materials and Methods: Air-sensitive copper(I) complexes were synthesized under inert conditions in a glove box (MBraun, Germany) filled with argon 5.0. Solvents and reagents were used as purchased from common suppliers unless stated otherwise. **Me_6tren**, **3**, and $[Cu(MeCN)_4]OTf$ were prepared according to the literature and stored in the glove box.[27,35] Solvents used to synthesize copper complexes were bought as anhydrous solvents under nitrogen atmosphere, distilled under argon, and stored in the glove box. NMR measurements were performed using a Bruker Avance II 400 MHz, Bruker Avance III 400 MHz HD, Bruker Avance III 600 MHz HD, and Bruker Avance Neo 700 MHz spectrometer. The ^{1}H- and ^{13}C-NMR spectra were calibrated using the residual proton and carbon signals of acetone ($\delta = 2.05$ and $\delta = 29.8$).[36] ESI-MS (HRMS) was measured using a Bruker Daltonica micrOTOF. Elemental analysis was carried out using a Thermo FlashEA-1112 series CHN-analysator. GC-MS measurements were carried out using an Agilent Technologies 5977B mass detector with a 7820 A GC system. UV-vis measurements were carried out using an Agilent 8453 spectrometer. Stopped-Flow UV-vis measurements were performed on a commercial HI-TECH SF61SX2 stopped-flow unit (TgK Scientific, Bratford-on-Avon, UK). The data were processed using Kinetic Studio version 5.02 Beta. The procedure for kinetic measurements was described in detail in previous work.[37] Details of X-Ray crystal structure determination are reported in the Supporting Information. Deposition Number 2376264 (for [Cu(**L1**)(MeCN)](OTf)$_2$) contains the supplementary crystallographic data for this paper. These data are provided free of charge by the joint Cambridge Crystallographic Data Centre and Fachinformationszentrum Karlsruhe Access Structures service.

Preparation of L1: A modified version of the synthesis reported in the literature[23] was used to obtain **L1**. Allyl bromide (7.0 g, 5.0 mL, 0.058 mol) in 20 mL of dry ethanol was added dropwise to a solution of diethylenetriamine (17.9 g, 18.7 mL, 0.175 mol) in 50 mL dry ethanol over the course of 3 h at 0 °C. Then 5 g KOH was added to the reaction mixture, and the colorless precipitate obtained was removed by filtration. The solvent was removed under reduced pressure. The excess amine was removed from the reaction mixture by distillation with a Vigreux column at 91 °C and 15 mbar, while the crude intermediate product was collected above 92 °C (4.80 g). The latter was dissolved in 20 mL acetic acid at 0 °C, then 30 mL formaldehyde (30 wt%) was added. The reaction mixture was refluxed overnight. After cooling to room temperature, the reaction mixture was made basic with aq. NaOH and extracted three times with 50 mL DCM. The combined organic phases were dried over Na_2SO_4, and the solvent was removed under reduced pressure. The crude product was purified by column chromatography (DCM, MeOH 10 : 1 + 1% NEt_3) and a colorless oil (1.39 g, 6.99 mmol, 12%, $R_f = 0.2$) was received. ^{1}H NMR (400 MHz, acetone-d_6): δ [ppm] = 5.87–5.77 (m, 1H, CH=CH_2), 5.19–5.12 (m, 1H, CH=CH_2), 5.09–5.04 (m, 1H, CH=CH_2), 2.99–2.95 (m, 2H, CH_2–CH=CH_2), 2.48–2.39 (m, 6H), 2.34–2.29 (m, 2H), 2.20 (s, 3H, N–(CH_3)), 2.17 (s, 3H, N–(CH_3)), 2.15 (s, 6H, N–(CH_3)$_2$); ^{13}C NMR (101 MHz, acetone-d_6): δ [ppm] = 137.5, 116.9, 61.9, 58.6, 57.1, 57.0, 56.1, 46.1, 43.3, 42.8; HRMS (ESI): *m/z* calcd. for $C_{11}H_{25}N_3$: 200.2121 $[M+H]^+$; found: *m/z* = 200.2120.

Preparation of L2: To a suspension of NaH (0.573 g, 23,3 mmol) in 100 mL dry THF N,N,N'',N''-tetramethldiethylenetriamine (**3**) (3.38 g,

21,2 mmol) was added dropwise over the course of 5 min at 0 °C. After stirring the reaction for 1 h at 0 °C allyl bromide (2.82 g, 2.02 mL, 23.3 mol) was added dropwise over the course of 10 min, and the reaction mixture was allowed to warm to room temperature, at which it was stirred for 19 h. Then 14 mL of deionized water were added, and the reaction was stirred for 10 min before the solvent was removed under reduced pressure. The residue was taken up in 70 mL NaOH (1 mol L^{-1}) and extracted three times with 135 mL DCM. The combined organic phases were dried over Na_2SO_4 and the solvent was removed under reduced pressure. The crude product was purified by column chromatography (DCM, MeOH 10:1 + 2% NEt_3) and a colorless oil (0.328 g, 1.64 mmol, 8%, R_f = 0.34) was received. ^{1}H NMR (400 MHz, acetone-d_6): δ [ppm] = 5.89–5.78 (m, 1H, CH=CH_2), 5.20–5.14 (m, 1H, CH=CH_2), 5.09–5.04 (m, 1H, CH=CH_2), 3.12 (dt, J = 6.3, 1.4 Hz, 2H, CH_2–CH=CH_2), 2.57–2.52 (m, 4H), 2.35–2.30 (m, 4H), 2.15 (s, 12H, N−(CH_3)$_4$); ^{13}C NMR (101 MHz, acetone-d_6): δ [ppm] = 137.7, 116.7, 58.8, 53.2, 46.2; HRMS (ESI): m/z calcd. for $C_{11}H_{25}N_3$: 200.2121 $[M+H]^+$; found m/z = 200.2123.

Preparation of L3: To a solution of diethylenetriamine (1.00 g, 1.04 mL, 9.69 mmol) and benzaldehyde (1.03 g, 0.99 mL, 9.69 mmol) in 30 mL DCM sodium triacetoxyborohydride (3.02 g, 14.5 mmol) was added. After stirring the reaction for 3 h at RT, the reaction was quenched with water, was made basic with aq. NaOH and extracted three times with 30 mL DCM. The combined organic phases were dried over Na_2SO_4, and the solvent was removed under reduced pressure. Without further purification the crude product was dissolved in 4 mL acetic acid at 0 °C and then 4.5 mL formaldehyde (30 wt%) were added. The reaction mixture was refluxed overnight. After cooling to room temperature, the reaction mixture was made basic with aq. NaOH and extracted three times with 30 mL DCM. The combined organic phases were dried over Na_2SO_4 and the solvent was removed under reduced pressure. The crude product was purified by column chromatography (DCM, MeOH 50:1 to 10:1 + 1% NEt_3) and a colorless oil (0.378 g, 1.51 mmol, 15%, R_f = 0.25) was received. ^{1}H NMR (400 MHz, acetone-d_6): δ [ppm] = 7.35–7.27 (m, 4H, Ph), 7.24–7.19 (m, 1H, Ph), 3.50 (s, 2H, CH_2–Ph), 2.54–2.46 (m, 4H), 2.46–2.41 (m, 2H), 2.34–2.30 (m, 2H), 2.19 (s, 3H, N–(CH_3)), 2.17 (s, 3H, N–(CH_3)), 2.14 (s, 6H, N–(CH_3)$_2$); ^{13}C NMR (101 MHz, acetone-d_6): δ [ppm] = 140.7, 129.6, 128.9, 127.6, 63.3, 58.6, 57.1, 57.0, 56.3, 46.1, 43.3, 42.9; HRMS (ESI): m/z calcd. for $C_{15}H_{27}N_3$: 250.2278 $[M+H]^+$; found m/z = 250.2278.

Preparation of L4: To a solution of **L3** (2.21 g, 8.88 mmol) in 200 mL MeOH palladium on carbon (10 wt.%) (0.94 g, 0.89 mmol) was added. The reaction mixture was stirred at room temperature under a hydrogen atmosphere at atmospheric pressure (balloon) for 13 h. The suspension was filtered, and the solvent was removed under reduced pressure to receive the crude intermediate product (0.766 g) as a yellow oil. Without further purification, the crude product and 4-bromo-1-butene (0.71 g, 0.54 mL, 5.29 mmol) were dissolved in 50 mL THF, and KI (0.884 g, 5.29 mmol) and K_2CO_3 (1.33 g, 9.62 mmol) were added. the reaction mixture was refluxed for 40 Then 10 mL deionized water were added, and the reaction was stirred for 10 min before the THF was removed under reduced pressure. The residue was taken up in 20 mL aq. KOH and extracted four times with 40 mL DCM. The combined organic phases were dried over Na_2SO_4, and the solvent was removed under reduced pressure. The crude product was purified by column chromatography (DCM, MeOH 10:1 + 1% NEt_3) and a colorless oil (0.155 g, 0.728 mmol, 8%, R_f = 0.21) was received. ^{1}H NMR (400 MHz, acetone-d_6): δ [ppm] = 5.88–5.77 (m, 1H, CH=CH_2), 5.07–5.00 (m, 1H, CH=CH_2), 4.96–4.91 (m, 1H, CH=CH_2), 2.46–2.38 (m, 8H), 2.35–2.31 (m, 2H), 2.23–2.17 (m, 8H), 2.16 (s, 6H, N–(CH_3)$_2$); ^{13}C NMR (101 MHz, acetone-d_6): δ [ppm] = 138.1, 115.5, 58.6, 58.4, 57.1, 57.0, 56.6, 46.1, 43.3, 42.7, 32.7; HRMS (ESI): m/z calcd. for $C_{12}H_{27}N_3$: 214.2278 $[M+H]^+$; found m/z = 214.2279.

Preparation of L5: To a suspension of KI (1.06 g, 6.39 mmol) and K_2CO_3 (1.60 g, 11.6 mmol) in 50 mL THF, **3** (0.925 g, 1.00 mL, 5.81 mmol) and 4-bromo-1-butene (0.86 g, 0.65 mL, 6.39 mmol) were added and the reaction mixture was kept under reflux for 26 Then 10 mL deionized water were added, and the reaction was stirred for 10 min before the THF was removed under reduced pressure. The residue was taken up in 20 mL aq. KOH and extracted four times with 40 mL DCM. The combined organic phases were dried over Na_2SO_4, and the solvent was removed under reduced pressure. The crude product was purified by column chromatography (DCM, MeOH 10:1 + 1% NEt_3), and a colorless oil (0.219 g, 1.03 mmol, 18%, R_f = 0.21) was received. ^{1}H NMR (400 MHz, acetone-d_6): δ [ppm] = 5.89–5.77 (m, 1H, CH=CH_2), 5.06–5.00 (m, 1H, CH=CH_2), 4.96–4.91 (m, 1H, CH=CH_2), 2.58–2.50 (m, 6H), 2.35–2.29 (m, 4H), 2.22–2.17 (m, 2H), 2.16 (s, 12H, N–(CH_3)$_4$); ^{13}C NMR (101 MHz, acetone-d_6): δ [ppm] = 138.2, 115.5, 58.9, 55.4, 53.6, 46.2, 32.8; HRMS (ESI): m/z calcd. for $C_{12}H_{27}N_3$: 214.2278 $[M+H]^+$; found m/z = 214.2280.

Preparation of L6: To a solution of diethylenetriamine (1.14 g, 1.19 mL, 11.1 mmol) and phenylacetaldehyde (1.34 g, 1.30 mL, 11.1 mmol) in 30 mL DCM sodium triacetoxyborohydride (3.53 g, 16.7 mmol) was added. After stirring the reaction for 6 h at RT the reaction was quenched with water, was made basic with aq. NaOH, and extracted three times with 30 mL DCM. The combined organic phases were dried over Na_2SO_4 and the solvent was removed under reduced pressure. Without further purification the crude product was dissolved in 5 mL acetic acid at 0 °C and then 5.5 mL formaldehyde (37 wt%) were added. The reaction mixture was refluxed overnight. After cooling to room temperature, the reaction mixture was made basic with aq. NaOH and extracted three times with 30 mL DCM. The combined organic phases were dried over Na_2SO_4, and the solvent was removed under reduced pressure. The crude product was purified by column chromatography (DCM, MeOH 20:1 + 1% NEt_3), and an orange oil (0.309 g, 1.17 mmol, 11%, R_f = 0.26) was received. ^{1}H NMR (400 MHz, acetone-d_6): δ [ppm] = 7.29–7.21 (m, 4H, Ph), 7.19–7.13 (m, 1H, Ph), 2.77–2.72 (m, 2H, CH_2–Ph), 2.62–2.57 (m, 2H, CH_2–CH_2–Ph), 2.52–2.47 (m, 2H), 2.47–2.41 (m, 4H), 2.35–2.30 (m, 2H), 2.27 (s, 3H, N–(CH_3)), 2.20 (s, 3H, N–(CH_3)), 2.15 (s, 6H, N–(CH_3)$_2$); ^{13}C NMR (101 MHz, acetone-d_6): δ [ppm] = 141.9, 129.6, 129.0, 126.6, 60.8, 58.6, 57.2, 57.1, 56.5, 46.2, 43.3, 42.9, 34.5; HRMS (ESI): m/z calcd. for $C_{16}H_{29}N_3$: 264.2434 $[M+H]^+$; found m/z = 264.2435.

General procedure for the synthesis of copper(I) complexes: In an argon-filled glovebox, the ligand and copper salt were each dissolved in dry acetonitrile. Then, the copper solution was added dropwise under vigorous stirring to the ligand solution at room temperature. The reaction mixture was stirred for 30 min, and subsequently, the solvent was removed under reduced pressure to obtain the complex without further purification.

[Cu(L1)]OTf: Following the general procedure **L1** (100 mg, 0.502 mmol) and [Cu(MeCN)$_4$]OTf (180 mg, 0.478 mmol) in 6 mL dry acetonitrile were used to obtain the corresponding complex as a colorless solid (194 mg, 0.472 mmol, 99%). ^{1}H NMR (400 MHz, acetone-d_6): δ [ppm] = 5.31–5.18 (m, 1H, CH=CH_2), 4.38 (d, J = 14.5 Hz, 1H CH=CH_2), 4.10 (d, J = 7.9 Hz, 1H, CH=CH_2), 3.18–2.72 (m, 14H), 2.71 (s, 6H, N–(CH_3)$_2$), 2.59 (s, 3H, N–(CH_3)); ^{13}C NMR (101 MHz, acetone-d_6): δ [ppm] = 122.40 (q, J = 322.4 Hz, OTf), 100.9, 79.7, 59.6, 59.2, 58.9, 55.7, 55.2, 48.4, 46.0, 45.8; Elemental analysis calcd. (%) for $C_{12}H_{25}CuF_3N_3O_3S$: C 34.99, H 6.12, N 10.20; found: C 35.28, H 6.06, N 10.02.

[Cu(L2)]OTf: Following the general procedure **L2** (100 mg, 0.502 mmol) and [Cu(MeCN)$_4$]OTf (180 mg, 0.478 mmol) in 6 mL dry acetonitrile were used to obtain the corresponding complex as a pale blue solid (199 mg, 0.472 mmol, 97%). ^{1}H NMR (400 MHz,

acetone-d_6): δ [ppm] = 5.22 (s, 1H, C*H*=CH$_2$), 4.78 (s, 1H, CH=C*H*$_2$), 4.62 (s, 1H, CH=C*H*$_2$), 3.84 (s, 2H, C*H*$_2$–CH=CH$_2$), 3.48–2.46 (m, 20H); ^{13}C NMR (101 MHz, acetone-d_6): δ [ppm] = 122.1 (q, J = 321.4 Hz, OTf), 96.5, 88.2, 59.7, 58.8, 48.8; Elemental analysis calcd. (%) for $C_{12}H_{25}CuF_3N_3O_3S$: C 34.99, H 6.12, N 10.20; found: C 35.22, H 5.98, N 10.27.

[Cu(L3)(MeCN)]OTf: Following the general procedure **L3** (125.3 mg, 0.502 mmol) and [Cu(MeCN)$_4$]OTf (180 mg, 0.478 mmol) in 6 mL dry acetonitrile were used to obtain the corresponding complex as a green oil (248 mg, 0.472 mmol, 98%). ^{1}H NMR (400 MHz, acetone-d_6): δ [ppm] = 7.58–7.54 (m, 2H, Ph), 7.45–7.34 (m, 3H, Ph), 3.87 (s, 2H, C*H*$_2$–Ph), 2.90–2.64 (m, 8H), 2.63 (s, 3H, N–(C*H*$_3$)), 2.59 (s, 6H, N–(C*H*$_3$)$_2$), 2.34 (s, 3H, N–(C*H*$_3$)), 2.24 (s, 3H, MeCN); ^{13}C NMR (101 MHz, acetone-d_6): δ [ppm] = 136.2, 131.3, 129.1, 128.9, 122.5 (q, J = 322.3 Hz, OTf), 117.3 (MeCN), 65.2, 59.8, 57.7, 55.2, 55.0, 48.9, 46.4, 43.3, 1.9 (MeCN); Elemental analysis calcd. (%) for $C_{18}H_{30}CuF_3N_4O_3S$: C 42.98, H 6.01, N 11.14; found: C 43.12, H 5.48, N 11.62.

[Cu(L4)]OTf: Following the general procedure **L4** (53 mg, 0.25 mmol) and [Cu(MeCN)$_4$]OTf (90 mg, 0.24 mmol) in 3 mL dry acetonitrile were used to obtain the corresponding complex as a colorless solid (98 mg, 0.23 mmol, 96%). ^{1}H NMR (700 MHz, acetone-d_6): δ [ppm] = 5.02–4.94 (m, 1H, C*H*=CH$_2$), 4.36 (d, J = 15.3 Hz, 1H, CH=C*H*$_2$), 4.27 (d, J = 8.9 Hz, 1H, CH=C*H*$_2$), 3.05–2.79 (m, 6H), 2.77 (s, 3H, N–(C*H*$_3$)), 2.75–2.67 (m, 6H), 2.64 (s, 3H, N–(C*H*$_3$)), 2.62 (s, 3H, N–(C*H*$_3$)), 2.53–2.47 (m, 1H), 2.32–2.27 (m, 1H), 2.04–1.99 (m, 1H); ^{13}C NMR (176 MHz, acetone-d_6): δ [ppm] = 102.6, 82.5, 59.6, 55.9, 55.6, 55.0, 54.2, 50.6, 48.0, 46.8, 45.0, 31.8; Elemental analysis calcd. (%) for $C_{13}H_{27}CuF_3N_3O_3S$: C 36.66, H 6.39, N 9.86; found: C 36.52, H 6.48, N 9.60.

[Cu(L5)]OTf: Following the general procedure **L5** (53 mg, 0.25 mmol) and [Cu(MeCN)$_4$]OTf (90 mg, 0.24 mmol) in 3 mL dry acetonitrile were used to obtain the corresponding complex as a colorless solid (99 mg, 0.23 mmol, 98%).^{1}H NMR (700 MHz, acetone-d_6): δ [ppm] = 5.57–5.49 (m, 1H, C*H*=CH$_2$), 4.61–4.56 (m, 1H, CH=C*H*$_2$), 4.56–4.53 (m, 1H, CH=C*H*$_2$), 3.09–3.06 (m, 2H), 2.98–2.87 (m, 4H), 2.82–2.69 (m, 4H), 2.66 (s, 12H, (N–(C*H*$_3$)$_2$)$_2$), 2.28 (q, J = 6.3 Hz, 2H); ^{13}C NMR (176 MHz, acetone-d_6): δ [ppm] = 114.3, 88.9, 60.8, 55.9, 51.6, 49.4, 34.8; Elemental analysis calcd. (%) for $C_{13}H_{27}CuF_3N_3O_3S$: C 36.66, H 6.39, N 9.86; found: C 36.68, H 6.41, N 9.97.

[Cu(L6)]OTf: Following the general procedure **L6** (66 mg, 0.25 mmol) and [Cu(MeCN)$_4$]OTf (90 mg, 0.24 mmol) in 3 mL dry acetonitrile were used to obtain the corresponding complex as a colorless solid (113 mg, 0.238 mmol, 99%). ^{1}H NMR (600 MHz, acetone-d_6): δ [ppm] = δ 7.51 (t, J = 7.5 Hz, 2H, Ph), 7.37–7.30 (m, 3H, Ph), 3.18–2.86 (m, 4H, (C*H*$_2$)$_2$=Ph), 2.83–2.08 (m, 20H); ^{13}C NMR (151 MHz, acetone-d_6): δ [ppm] = 129.1, 127.2, 122.8 (broad), 122.5 (q, J = 322.3 Hz, OTf), 117.6 (broad), 59.48, 57.1, 54.9, 54.6, 54.5, 49.2 (broad), 48.5 (broad), 46.0, 45.5, 33.1; Elemental analysis calcd. (%) for $C_{17}H_{29}CuF_3N_3O_3S$: C 42.89, H 6.14, N 8.83; found: C 43.53, H 6.20, N 8.75.

[Cu(L1)(MeCN)](OTf)$_2$: Following the general procedure **L1** (50 mg, 0.25 mmol) and Cu(OTf)$_2$ (91 mg, 0.25 mmol) in 1 mL dry acetonitrile were used to obtain the corresponding complex as a blue solid (160 mg, 0.25 mmol, 99%). Elemental analysis calcd. (%) for $C_{15}H_{28}CuF_6N_4O_6S_2$: C 29.92, H 4.69, N 9.31; found: C 29.72, H 4.72, N 9.19. Slow evaporation of a complex solution in methanol resulted in blue crystals suitable for X-ray structural characterization.

Oxygenation Reaction of [Cu(L1)]OTf: To investigate whether the ligand **L1** is still intact after oxidation of the corresponding copper(I) complex with dioxygen, the copper was extracted, and the organic residue was analyzed. For that, [Cu(L1)]OTf (40 mg, 0.097 mmol) was dissolved in 10 mL acetone, and dioxygen was bubbled through the solution for 5 min at −80 °C. After the solution warmed up to room temperature 20 mL aq. ammonia was added and the solution was extracted three times with 20 mL DCM. The combined organic phases were dried over Na_2SO_4, and the solvent was removed under reduced pressure. The organic residue was analyzed using GC-MS.

Acknowledgements

We gratefully acknowledge the Justus Liebig University Gießen and the German Research Foundation (Deutsche Forschungsgemeinschaft; SS, SCHI 377/20-1) for financial support. Project DEAL enabled and organized open-access funding. Open Access funding enabled and organized by Projekt DEAL.

Conflict of Interests

The authors declare no conflict of interest.

Data Availability Statement

The data that support the findings of this study are available in the supplementary material of this article.

Keywords: Bioinorganic chemistry · Copper · Dioxygen activation · Olefines · Stabilization

[1] E. A. Lewis, W. B. Tolman, *Chem. Rev.* **2004**, *104*, 1047.
[2] L. M. Mirica, X. Ottenwaelder, T. D. P. Stack, *Chem. Rev.* **2004**, *104*, 1013.
[3] C. E. Elwell, N. L. Gagnon, B. D. Neisen, D. Dhar, A. D. Spaeth, G. M. Yee, W. B. Tolman, *Chem. Rev.* **2017**, *117*, 2059.
[4] D. A. Quist, D. E. Diaz, J. J. Liu, K. D. Karlin, *J. Biol. Inorg. Chem.* **2017**, *22*, 253.
[5] H. Sterckx, B. Morel, B. U. W. Maes, *Angew. Chem. Int. Ed.* **2019**, *58*, 7946.
[6] C. Würtele, O. Sander, V. Lutz, T. Waitz, F. Tuczek, S. Schindler, *J. Am. Chem. Soc.* **2009**, *131*, 7544.
[7] C. Noß, R. Göttlich, S. Schindler, *Chem. Eur. J.* **2023**, *29*, e202301142.
[8] H. R. Lucas, L. Li, A. A. N. Sarjeant, M. A. Vance, E. I. Solomon, K. D. Karlin, *J. Am. Chem. Soc.* **2009**, *131*, 3230.
[9] M. Becker, F. W. Heinemann, F. Knoch, W. Donaubauer, G. Liehr, S. Schindler, G. Golub, H. Cohen, D. Meyerstein, *Eur. J. Inorg. Chem.* **2000**, *2000*, 719.
[10] M. Becker, F. W. Heinemann, S. Schindler, *Chem. Eur. J.* **1999**, *5*, 3124.
[11] J. Becker, Y. Y. Zhyhadlo, E. D. Butova, A. A. Fokin, P. R. Schreiner, M. Förster, M. C. Holthausen, P. Specht, S. Schindler, *Chem. Eur. J.* **2018**, *24*, 15543.
[12] J. Astner, M. Weitzer, S. P. Foxon, S. Schindler, F. W. Heinemann, J. Mukherjee, R. Gupta, V. Mahadevan, R. Mukherjee, *Inorg. Chim. Acta* **2008**, *361*, 279.
[13] S. Schindler, *Eur. J. Inorg. Chem.* **2000**, *2000*, 2311.
[14] M. Weitzer, S. Schindler, G. Brehm, S. Schneider, E. Hörmann, B. Jung, S. Kaderli, A. D. Zuberbühler, *Inorg. Chem.* **2003**, *42*, 1800.
[15] a) G. Golub, H. Cohen, D. Meyerstein, *J. Chem. Soc. Chem. Commun.* **1992**, *5* 397; b) G. Golub, H. Cohen, P. Paoletti, A. Bencini, D. Meyerstein, *J. Chem. Soc. Dalton Trans.* **1996**, *10*, 2055.
[16] M. Pasquali, C. Floriani, G. Venturi, A. Gaetani-Manfredotti, A. Chiesi-Villa, *J. Am. Chem. Soc.* **1982**, *104*, 4092.
[17] D. V. Scaltrito, H. C. Fry, B. M. Showalter, D. W. Thompson, H. C. Liang, C. X. Zhang, R. M. Kretzer, E. Kim, J. P. Toscano, K. D. Karlin, et al., *Inorg. Chem.* **2001**, *40*, 4514.

[18] H. C. Fry, H. R. Lucas, A. A. N. Sarjeant, K. D. Karlin, G. J. Meyer, *Inorg. Chem.* **2008**, *47*, 241.
[19] G. J. Karahalis, A. Thangavel, B. Chica, J. Bacsa, R. B. Dyer, C. C. Scarborough, *Inorg. Chem.* **2016**, *55*, 1102.
[20] T. Osako, Y. Ueno, Y. Tachi, S. Itoh, *Inorg. Chem.* **2003**, *42*, 8087.
[21] T. Osako, Y. Tachi, M. Doe, M. Shiro, K. Ohkubo, S. Fukuzumi, S. Itoh, *Chem. Eur. J.* **2004**, *10*, 237.
[22] X. Zhong, C. J. Bouchey, E. Kabir, W. B. Tolman, *J. Inorg. Biochem.* **2021**, *222*, 111498.
[23] N. Navon, G. Golub, H. Cohen, P. Paoletti, B. Valtancoli, A. Bencini, D. Meyerstein, *Inorg. Chem.* **1999**, *38*, 3484.
[24] N. Navon, H. Cohen, P. Paoletti, B. Valtancoli, A. Bencini, D. Meyerstein, *Ind. Eng. Chem. Res.* **2000**, *39*, 3536.
[25] N. Navon, A. Burg, H. Cohen, R. van Eldik, D. Meyerstein, *Eur. J. Inorg. Chem.* **2002**, *2002*, 423.
[26] M. J. Scott, R. H. Holm, *J. Am. Chem. Soc.* **1994**, *116*, 11357.
[27] H. Luitjes, M. Schakel, G. W. Klumpp, *Synth. Commun.* **1994**, *24*, 2257.
[28] A. W. Addison, T. N. Rao, J. Reedijk, J. van Rijn, G. C. Verschoor, *J. Chem. Soc. Dalton Trans.* **1984**, *7*, 1349.
[29] S. Mahapatra, J. A. Halfen, E. C. Wilkinson, G. Pan, X. Wang, V. G. Young, C. J. Cramer, L. Que, W. B. Tolman, *J. Am. Chem. Soc.* **1996**, *118*, 11555.
[30] H.-C. Liang, C. X. Zhang, M. J. Henson, R. D. Sommer, K. R. Hatwell, S. Kaderli, A. D. Zuberbühler, A. L. Rheingold, E. I. Solomon, K. D. Karlin, *J. Am. Chem. Soc.* **2002**, *124*, 4170.
[31] M. Schatz, M. Becker, F. Thaler, F. Hampel, S. Schindler, R. R. Jacobson, Z. Tyeklár, N. N. Murthy, P. Ghosh, Q. Chen, et al., *Inorg. Chem.* **2001**, *40*, 2312.
[32] M. Becker, S. Schindler, R. van Eldik, *Inorg. Chem.* **1994**, *33*, 5370.
[33] A. Hoffmann, M. Wern, T. Hoppe, M. Witte, R. Haase, P. Liebhäuser, J. Glatthaar, S. Herres-Pawlis, S. Schindler, *Eur. J. Inorg. Chem.* **2016**, *2016*, 4744.
[34] S. Debnath, S. Laxmi, O. McCubbin Stepanic, S. Y. Quek, M. van Gastel, S. DeBeer, T. Krämer, J. England, *J. Am. Chem. Soc.* **2024**, *146*, 23704.
[35] a) D. F. Shriver, *Inorganic Syntheses*, Wiley, New York **1979**; b) G. J. P. Britovsek, J. England, A. J. P. White, *Inorg. Chem.* **2005**, *44*, 8125.
[36] G. R. Fulmer, A. J. M. Miller, N. H. Sherden, H. E. Gottlieb, A. Nudelman, B. M. Stoltz, J. E. Bercaw, K. I. Goldberg, *Organometallics* **2010**, *29*, 2176.
[37] M. Weitzer, M. Schatz, F. Hampel, F. W. Heinemann, S. Schindler, *J. Chem. Soc. Dalton Trans.* **2002**, 686.
[38] L. Krause, R. Herbst-Irmer, G. M. Sheldrick, D. Stalke, *J. Appl. Crystallogr.* **2015**, *48*, 3.
[39] G. M. Sheldrick, *Acta Crystallogr. Sect. A: Found. Adv.* **2015**, *71*, 3.
[40] G. M. Sheldrick, *Acta Crystallogr. Sect. C: Struct. Chem.* **2015**, *71*, 3.

Manuscript received: September 2, 2024
Revised manuscript received: September 28, 2024
Accepted manuscript online: October 4, 2024
Version of record online: November 7, 2024

3.2 Mechanistic Studies of Second Coordination Sphere Interactions in the Dioxygen Activation of a Copper(I) Complex with a *N*-(2-Ethoxyethanol)-bis(2-picolyl)amine Ligand

This article has been published in

European Journal of Inorganic Chemistry

Alexander Granichny, Anna Leah Scholl, Christian Würtele, and Siegfried Schindler

Eur. J. Inorg. Chem. **2025**, e202400804

https://doi.org/10.1002/ejic.202400804

Check for updates

EurJIC
European Journal of Inorganic Chemistry

Research Article
doi.org/10.1002/ejic.202400804

Chemistry Europe
European Chemical Societies Publishing

www.eurjic.org

Mechanistic Studies of Second Coordination Sphere Interactions in the Dioxygen Activation of a Copper(I) Complex with a *N*-(2-Ethoxyethanol)-bis(2-picolyl)amine Ligand

Alexander Granichny,[a] Anna Leah Scholl,[a] Christian Würtele,[a] and Siegfried Schindler*[a]

Dedicated to Prof. Rudi van Eldik on the occasion of his 80th Birthday.

While first coordination sphere interactions have been investigated in great detail for the reactivity of copper(I) model complexes with dioxygen, the interactions of the secondary coordination sphere with the bound dioxygen so far remain underexplored. A series of copper(I) complexes with ligands based on *N*-(2-ethoxyethanol)-bis(2-picolyl)amine (**L(O)OH**) were synthesized, and the reactivity towards dioxygen was monitored by low-temperature stopped-flow UV/vis spectroscopy. Various "oxygen adduct complexes" were observed, and the influence of the second coordination sphere interactions was analyzed. If the ether moiety or the hydroxy group in **L(O)OH** is removed/replaced, the formation of a *trans*-μ-1,2-peroxido dicopper(II) complex or a bis(μ-oxido) dicopper(III) complex is observed. Establishing stronger hydrogen bonding while maintaining the ether moiety leads to hydrogen bond stabilized *trans*-μ-1,2-peroxido dicopper(II) complexes. Based on these results, we deduced that the copper(I) complex with **L(O)OH** as ligand reacts with dioxygen first to a hydrogen bond stabilized *trans*-μ-1,2-peroxido dicopper(II) complex, which rapidly converts to a bis(μ-oxido) dicopper(III) complex.

Introduction

Mimicking the active sites of copper-containing enzymes that activate dioxygen under ambient conditions, such as dopamine-β-monooxygenase (DβM) and peptidylglycine-α-monooxygenase (PHM),[1,2] is a major goal in bioinorganic chemistry. It led to the development of many model complexes for copper metalloenzymes.[3] The reaction of copper(I) model complexes with dioxygen provides a diverse range of so-called "oxygen adduct complexes" that are formed *via* various pathways (Scheme 1).[4] To follow the formation of these often unstable "oxygen adduct complexes", low-temperature stopped-flow techniques are applied. In some cases, the structural characterization of such intermediates is possible by using fine-tuned ligand systems that enhance the stability of the "oxygen adduct complexes": e.g., the first molecular structure of a η^1-superoxido copper(II) complex with tris[2-(N-tetramethylguanidyl)ethyl]amine (**TMG$_3$tren**, Scheme 2) as a ligand,[5] and the first structurally characterized *trans*-μ-1,2-peroxido dicopper(II) complex with tris(2-pyridylmethyl)amine (**tmpa**, Scheme 2) as a ligand.[6] While most ligands used to contain only nitrogen donor groups, substituting nitrogen with a sulfur donor atom can lead to the same dioxygen reactivity as

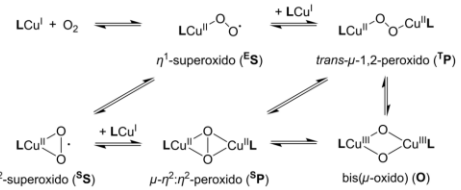

Scheme 1. Typical reaction pathways for copper(I) complexes with dioxygen.[4]

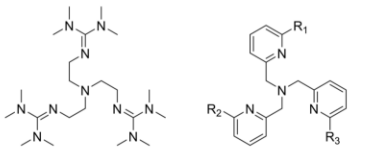

TMG$_3$tren

tmpa, R$_1$ = R$_2$ = R$_3$ = H
L1, R$_1$ = NH$_2$, R$_2$ = R$_3$ = H
L2, R$_1$ = R$_2$ = NH$_2$, R$_3$ = H
L3, R$_1$ = R$_2$ = R$_3$ = NH$_2$
L4, R$_1$ = NHPiv, R$_2$ = R$_3$ = H
L5, R$_1$ = NHBn, R$_2$ = R$_3$ = H
L6, R$_1$ = R$_2$ = R$_3$ = NHPh

Scheme 2. Ligands for copper(I) complexes that are discussed in here.[5,6,12–15]

[a] *A. Granichny, A. L. Scholl, C. Würtele, S. Schindler*
Institute of Inorganic and Analytical Chemistry
Justus Liebig University Giessen
Heinrich-Buff-Ring 17, 35392 Giessen, Germany
E-mail: siegfried.schindler@anorg.chemie.uni-giessen.de

Supporting information for this article is available on the WWW under https://doi.org/10.1002/ejic.202400804

their related nitrogen analogs[7,8] and, therefore, can better represent the active sites of DβM and PHM with sulfur-containing amino acids.[1,2] However, this depends on the residues attached to the sulfur atom, which strengthen or weaken the Cu–S bond, leading to different "oxygen adduct complexes".[9] Aliphatic residues stabilizeed the Cu–S bond, thus forming *trans*-μ-1,2-peroxido dicopper(II) complexes similar to the copper **tmpa** complex.[6] At the same time, sterically bulky electron-withdrawing groups weaken the Cu–S bond, thus forming bis(μ-oxido)dicopper(III) complexes similar to copper complexes with tridentate bispicolylamine ligands.[10]

Substituting the residues affects the dioxygen adduct formation by changing the coordination sphere around the metal ion. On the other hand, other functional groups engage directly with the bound dioxygen through secondary coordination sphere interactions.[11] Masuda and co-workers investigated the effect of incorporating amines in the 6-pyridyl positions of **tmpa** (**L1**–**L4**, Scheme 2) in copper(I) complexes regarding their dioxygen activation.[12,13] The observed *trans*-μ-1,2-peroxido species displayed a sizeable blue shift in their UV/vis spectra. Additionally, the increased number of amine groups led to a decreased absorbance caused by hydrogen bond formation and the resulting restricted movement of the peroxide species.[12,13] Investigations by Karlin and co-workers showed that a copper(I) complex with a **tmpa**-derived ligand with a single 6-phenylamino-2-pyridylmethyl group (**L5**, Scheme 2) led to a similar blue shift in the UV/vis spectrum upon oxidation with dioxygen.[14] Szymczak and co-workers structurally characterized such a hydrogen bond stabilized peroxide species with a **tmpa**-derived ligand with three 6-phenylamino-2-pyridylmethyl groups (**L6**, Scheme 2) whose UV/vis spectra are in line with the discussed ligands above.[15]

The copper complex with *N*-(2-ethoxyethanol)-bis(2-picolyl)amine as a ligand (**L(O)OH**, Scheme 3) was reported previously to also exhibit secondary coordination sphere interactions towards bound dioxygen.[16,17] Copper complexes with this ligand were successfully used in polymerization reactions and the generation of H_2O_2 in water due to its increased solubility caused by the terminal hydroxy group. This hydroxy group plays a significant role in the proposed mechanism for the H_2O_2 generation as it facilitates hydrogen bonds and forms a hydrogen bond stabilized *trans*-μ-1,2-peroxido dicopper(II) complex,[17] analogous to the aforementioned amine derivatives of **tmpa**.[12–15] Similar interactions were discussed with this ligand's copper(II) complex and H_2O_2 derivates.[18] Regarding the unique property to form a hydrogen bond stabilized *trans*-μ-1,2-peroxido dicopper(II) complex with a hydroxy group, we investigated the complex in more detail with low-temperature stopped-flow techniques. Additionally, a series of copper(I) complexes with related ligands shown in Scheme 3 were synthesized and analyzed to explore the role of the ether moiety and the terminal hydrogen donor in the dioxygen activation mechanism.

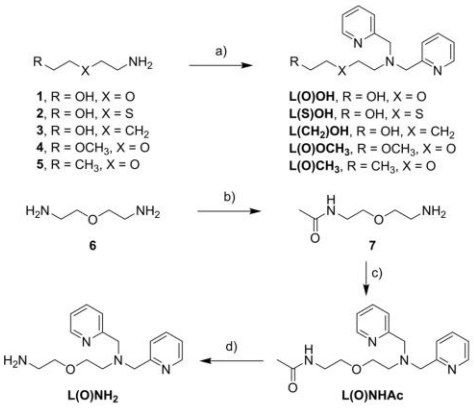

Scheme 3. Ligand syntheses: a) 2-picolyl chloride hydrochloride, potassium carbonate, MeCN, reflux; b) EtOAc, H_2O, reflux; c) pyridine-2-carbaldehyde, $NaBH(OAc)_3$, DCE, RT; d) HCl, reflux.

Results and Discussion

Synthesis of the Ligands

All ligands except for **L(O)NHAc** and **L(O)NH$_2$** were prepared according to the published procedure for **L(O)OH**.[19] According to Scheme 3, amine precursors **1**–**5** react with 2-picolyl chloride hydrochloride and potassium carbonate to the corresponding ligands. The synthesis for **L(O)NHAc** and **L(O)NH$_2$** starts with a modified literature synthesis for the mono-acylation of symmetric diamines by refluxing the diamine **6** in a mixture of ethyl acetate and water.[20] This is followed by reductive amination of the mono-acylated amine **7** with pyridine-2-carbaldehyde and sodium triacetoxyborohydride to receive **L(O)NHAc**. Furthermore, this ligand is refluxed in hydrochloric acid to cleave the acyl-protecting group to obtain **L(O)NH$_2$**.

Synthesis, Characterization, and Dioxygen Reactivity of the Copper(I) Complex of L(O)OH

The synthesis of the copper(I) complex of **L(O)OH** was carried out by mixing $[Cu(MeCN)_4]ClO_4$ and **L(O)OH** in acetonitrile before removing the solvent overnight *in vacuo*. Elemental analysis (EA) confirmed the formation of the monoacetonitrile complex [Cu(**L(O)OH**)(MeCN)]ClO_4. This suggests that the ethoxyethanol side chain is not coordinated, unlike its copper(II) complex, where the ether is weakly coordinated in the axial position of the copper(II) ion.[18,19,21]

Reacting a yellow solution of the copper(I) complex with dioxygen in acetone at −80 °C in a benchtop experiment first led to the formation of a green color, which then rapidly turned into a blue-colored solution. Extracting the oxygenated solution by basic workup and investigating it with GC-MS revealed that the ligand remains intact, and no intramolecular hydroxylation occurred (Figure S20, S21). Low-temperature stopped-flow measurements in acetone revealed the formation of two

Research Article
doi.org/10.1002/ejic.202400804

absorbance maxima at 389 nm and 455 nm and a small band at 680 nm (Figure 1). Notably, the initial copper(I) complex spectrum is unobserved due to the reaction occurring partially during the mixing time of the instrument. First, an increase of the absorbance at 455 nm is observed, followed by an immediate decrease, while simultaneously, there is an increase at 389 nm that again starts to decrease after 1.5 s. This strongly suggests that two distinct "dioxygen adduct" species were formed, with one fully transformed into the other. Based on the literature, the band at 389 nm is most likely caused by the formation of a bis(μ-oxido)dicopper(III) complex similar to the reaction of copper(I) complexes with bispicolylamine derivatives as ligands.[10,22,23] On the other hand, the assignment of the band at 455 nm is less clear, but the region corresponds with hydrogen bond stabilized *trans*-μ-1,2-peroxido dicopper(II) complexes discussed above.[12–15] Although isomerization reactions of *trans*-μ-1,2-peroxido dicopper(II) complexes into bis(μ-oxido)dicopper(III) complexes have been reported previously,[9,24] examples are rather rare. To consolidate the assigned dioxygen adducts, several derivates of the copper(I) complex of **L(O)OH** were synthesized to investigate the importance of the ether function and the terminal hydroxy group.

Synthesis, Characterization, and Dioxygen Reactivity of the Copper(I) Complex of L(S)OH and L(CH_2)OH

To analyze the importance of the ether group for the dioxygen activation, the copper(I) complexes of the two derivatives, **L(S)OH** and **L(CH_2)OH**, were studied. Beginning with **L(S)OH**, which only differs from **L(O)OH** by having a thioether instead of an ether group, we wanted to investigate the implications sulfur would have on the dioxygen activation as a stronger binding partner for the copper(I) ion than oxygen. The corresponding copper(I) complex was synthesized under the same conditions as for **L(O)OH**. Instead of an oil, as for the other copper(I) complexes of the series (Scheme 3), a solid was received, and it was possible to obtain crystals for structural characterization. The molecular structure of the unit cell of [Cu(**L(S)OH**)]ClO_4 is depicted in Figure 2. In contrast to [Cu(**L-(O)OH**)(MeCN)]ClO_4, no acetonitrile was found to be coordinated, which was further confirmed by elemental analysis. The copper(I) ion is coordinated by three N-donor atoms (N(1), N(2), N(3)) of **L(S)OH** and a sulfur atom from the thioether sidearm of a neighboring complex (S(1)#1) in a distorted tetrahedral geometry ($\tau_4 = 0.78$, $\tau_4' = 0.75$).[26,27] This implies that the solid here corresponds to a polynuclear instead of a mononuclear complex.

Reacting a yellow solution of the copper(I) complex in acetone at −80 °C with dioxygen in a benchtop experiment led to a short-lived dark purple color ($t_{1/2}$ ~10 min), turning into a green-colored solution. This shows that the reactivity towards dioxygen differs significantly from the copper(I) complex of **L(O)OH**, which was confirmed by low-temperature stopped-flow UV/vis measurements. They revealed the formation of a typical *trans*-μ-1,2-peroxido dicopper(II) complex with absorbance maxima at 523 and 600 nm (Figure 3), in line with similar copper(I) complexes with N3S thioether ligands reported previously.[8,9,28] While the decomposition of the dioxygen adduct starts immediately, it is still observable after a couple of minutes, in accordance with the benchtop experiments. Extracting the oxygenated solution by basic workup and investigating it with GC-MS revealed that the ligand remains intact, and neither intramolecular hydroxylation nor sulfoxidation occurred (Figure S22, S23). This finding is in accordance with N3S thioether ligands that form *trans*-μ-1,2-peroxido dicopper(II) complexes.[9] The results suggest that while we characterized a polynuclear complex in solid, a mononuclear tetradentate complex is present in solution.

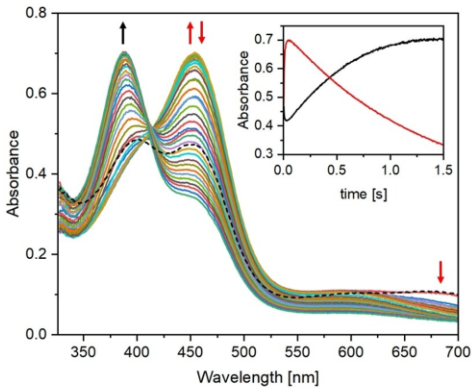

Figure 1. Time-resolved UV/vis spectra of the reaction of [Cu(**L-(O)OH**)(MeCN)]ClO_4 ($2.5 \cdot 10^{-4}$ mol L^{-1}) with dioxygen ($5.7 \cdot 10^{-3}$ mol L^{-1})[25] in acetone at −80 °C throughout 1.5 s. Initial spectra is depicted by the black dashed line. The inset displays the time-dependent change in absorbance at 389 nm (black) and 455 nm (red).

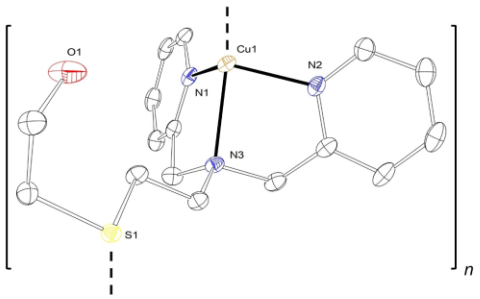

Figure 2. ORTEP Plot of the molecular structure of [Cu(**L(S)OH**)]ClO_4. Non-binding anions, solvent molecules, and carbon-bound hydrogen atoms are omitted for clarity. Ellipsoids are drawn at 50 % probability. Selected Bond Lengths (Å): Cu(1)–N(1): 2.043; Cu(1)–N(2): 2.030; Cu(1)–N(3): 2.228; Cu(1)–S-(1)#1: 2.207. Selected bond angles (°): N(1)–Cu(1)–N(2): 120.67; N(1)–Cu-(1)–N(3): 79.76; N(2)–Cu(1)–N(3): 82.81; N(1)–Cu(1)–S(1)#1: 117.77; N(2)–Cu-(1)–S(1)#1: 116.83; N(3)–Cu(1)–S(1)#1: 129.91. Symmetry transformations used to generate equivalent atoms: #1 -x+y,-x+1,z-1/3.

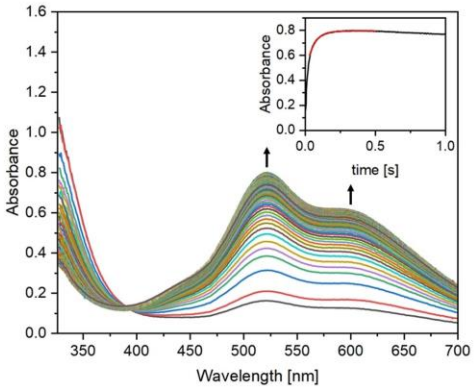

Figure 3. Time-resolved UV/vis spectra of the reaction of [Cu(**L(S)OH**)]ClO_4 ($2.5 \cdot 10^{-4}$ mol L^{-1}) with dioxygen ($5.7 \cdot 10^{-3}$ mol L^{-1})[25] in acetone at −80 °C throughout 1.0 s. The inset displays the time-dependent change in absorbance at 523 nm (experimental fit (black), exponential fit (red)).

The absorbance *vs.* time trace at 523 nm measured under pseudo-first-order conditions can be fitted to a single exponential function, indicating first-order dependency for the complex concentration in the rate law. Furthermore, plotting k_{obs} *vs.* the dioxygen concentration shows a linear dependence in line with first-order dependency regarding the dioxygen concentration in the rate law as well (Figure S15). The intercept indicates that the reaction in the rate-determining step is reversible.[28,29] The mechanism for the formation of the *trans*-μ-1,2-peroxido dicopper(II) complex can be assigned by the overall observations as reported previously.[28] According to Scheme 4, the reversible formation of an unstable η^1-superoxido copper(II) complex is proposed, which is followed by the reaction with another copper(I) complex to form the observed *trans*-μ-1,2-peroxido dicopper(II) complex. Since the formation of the *trans*-μ-1,2-peroxido dicopper(II) is much faster than the formation of the η^1-superoxido copper(II) complex, only the peroxide species is observable.

A temperature-dependent measurement of the reaction allowed the determination of the activation parameters $\Delta H^{\ddagger} = 7.8 \pm 0.4$ kJ mol^{-1} and $\Delta S^{\ddagger} = -133 \pm 2$ J mol^{-1} K^{-1} calculated by an Eyring plot (Figure S16). The strongly negative activation entropy implies an associative pathway, which aligns with our proposed mechanism.

Incorporating a thioether instead of an ether moiety thus led to a drastic change regarding the complex and its dioxygen activation. Due to the higher affinity of sulfur to bind to the copper ion than oxygen a coordinative bond is formed, which results in the formation of a *trans*-μ-1,2-peroxido dicopper(II) complex upon oxygenation (due to being a tetradentate ligand comparable with **tmpa**). For this complex, the terminal hydroxy function probably does not play a role in stabilizing the dioxygen adduct because it points outwards away from the activated dioxygen due to the strongly binding thioether.

While the thioether group forms covalent bonds to copper(I) ions in solid and solution, the effect of the ether group in the ligand system **L(O)OH** was investigated by substituting the oxygen of the ether group with a CH_2 group, thus obtaining the ligand **L(CH_2)OH**. The corresponding copper(I) complex contained a coordinated acetonitrile, as observed for the copper(I) complex of **L(O)OH**. Low-temperature stopped-flow UV/vis measurements in acetone at −80 °C revealed the formation of an absorbance maximum at 387 nm (Figure 4). This band indicates the formation of a bis(μ-oxido)dicopper(III) complex, in line with copper complexes with tridentate bispicolylamine derivatives as ligands.[10,22,23] Under pseudo-first-order conditions, the reaction rate is independent of the dioxygen concentration (Figure S17).

Based on this, and the results reported for similar tripodal ligands bispicolylamine derivatives,[10] the mechanism is proposed as follows: First, the copper(I) complex reacts with dioxygen to an unstable η^1-superoxido complex in a rapid left-lying preequilibrium before reacting with another copper(I) complex to form a bis(μ-oxido)dicopper(III) complex (Scheme 5). Due to the left-lying preequilibrium and the fast consecutive

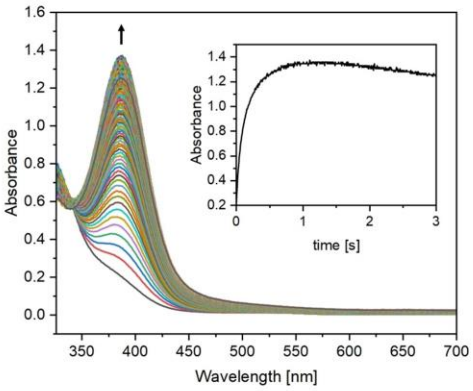

Figure 4. Time-resolved UV/vis spectra of the reaction of [Cu(**L-(CH_2)OH**)(MeCN)]ClO_4 ($2.5 \cdot 10^{-4}$ mol L^{-1}) with dioxygen ($5.7 \cdot 10^{-3}$ mol L^{-1})[25] in acetone at −80 °C throughout 3 s. The inset displays the time-dependent change in absorbance at 387 nm.

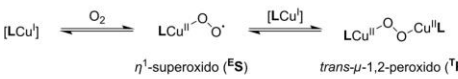

Scheme 4. Proposed mechanism for the formation of the *trans*-μ-1,2-peroxido dicopper(II) complex.

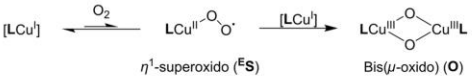

Scheme 5. Proposed mechanism for the formation of the bis(μ-oxido)dicopper(III) complex.

Research Article
doi.org/10.1002/ejic.202400804

reaction, only the formation of the oxido species is observable. Comparing this spectrum with the one of the copper(I) complex of **L(O)OH**, it is reasonable to say that the peak forming at 389 nm in Figure 1 shows the formation of a bis(μ-oxido)dicopper(III) complex.

Both ligands, **L(O)OH** and **L(CH_2)OH**, depict that the ether function is necessary to observe the spectra in Figure 1. While the oxygen of the ether moiety does not coordinate with the copper(I) ion, compared to its sulfur derivative, it plays a role in forming the short-lived species at 455 nm. This became apparent by removing the oxygen atom of the ether group, which led to the sole buildup of the band at around 389 nm, corresponding to a bis(μ-oxido)dicopper(III) complex.

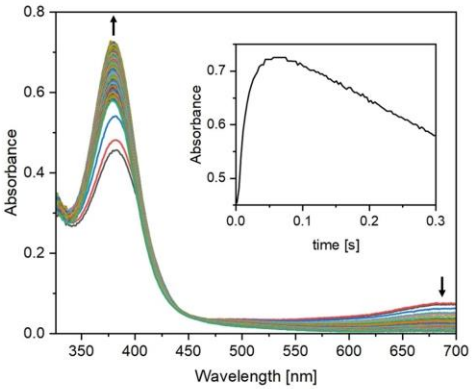

Figure 5. Time-resolved UV/vis spectra of the reaction of [Cu(**L-(O)OCH$_3$**)(MeCN)]ClO_4 ($1.3\cdot10^{-4}$ mol L^{-1}) with dioxygen ($5.7\cdot10^{-3}$ mol L^{-1})[25] in acetone at −80 °C over a period of 0.3 s. The inset displays the time-dependent change in absorbance at 380 nm.

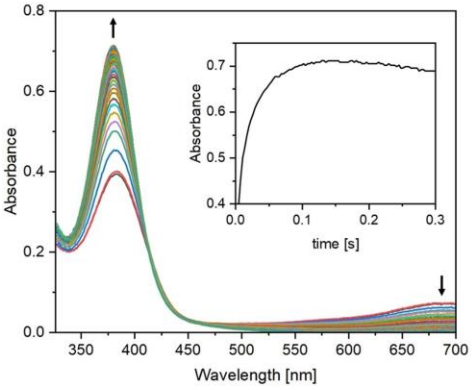

Figure 6. Time-resolved UV/vis spectra of the reaction of [Cu(**L-(O)CH$_3$**)(MeCN)]ClO_4 ($2.5\cdot10^{-4}$ mol L^{-1}) with dioxygen ($5.7\cdot10^{-3}$ mol L^{-1})[25] in acetone at −80 °C over a period of 0.3 s. The inset displays the time-dependent change in absorbance at 380 nm.

Synthesis, Characterization, and Dioxygen Reactivity of the Copper(I) Complexes of L(O)OCH_3 and L(O)CH_3

After establishing that the ether moiety plays a crucial role in the observed spectra in Figure 1, especially the short-lived band at 455 nm, the relevance of the terminal hydroxy group was investigated. For that, the two ligands with a methylated hydroxy group (**L(O)OCH$_3$**) and terminal alkane group (**L(O)CH$_3$**) were applied. Similar to the copper(I) complex of **L(O)OH**, copper(I) complexes with both ligands coordinate an additional acetonitrile molecule as a ligand. Performing stopped-flow UV/vis measurements in acetone at −80 °C for the reaction of the copper(I) complexes with both ligands and dioxygen showed the development of absorption bands at 380 nm (Figure 5 and 6). These results align with the formation of bis(μ-oxido)dicopper(III) complexes.[10,22,23] While exhibiting the same spectral features, both complexes differ in their lifetime of these intermediates.

The copper(I) complex with the ligand **L(O)OCH$_3$** decomposed quickly after the initial formation, thus making follow-up measurements impossible. The copper(I) complex with the ligand **L(O)CH$_3$** is slightly more stable. Due to its longer lifetime, dioxygen-dependent measurements were possible. Under pseudo-first-order conditions, the reaction rate is independent of the dioxygen concentration (Figure S18), which is in line with the results described above. While the oxidation of the copper(I) complexes with both ligands can be assumed to follow the same reaction mechanism as for the complex with **L(CH_2)OH** (Scheme 5), the intermediate complex decomposes much faster, demonstrating that altering the terminal hydroxy group has a negative impact on its stability.

These results reveal that altering or removing the hydroxy function while maintaining the ether group results in the same "dioxygen adduct" complexes as for the non-ether-containing copper complex with **L(CH_2)OH** as a ligand. Therefore, the copper(I) complexes of **L(CH_2)OH**, **L(O)OCH$_3$**, and **L(O)CH$_3$** react in the same way as similar tridentate bispipicolylamine ligands forming bis(μ-oxido)dicopper(III) complexes. Hence, for forming the short-lived band at 455 nm in Figure 1, both the ether functionality and a terminal hydroxy group must be present.

Synthesis, Characterization, and Dioxygen Reactivity of the Copper(I) Complexes of L(O)NHAc and L(O)NH_2

After demonstrating that both ether and the terminal hydroxy group were necessary for the formation of an absorbance maximum at 455 nm in Figure 1, which presumably corresponds to a hydrogen bond stabilized *trans*-μ-1,2-peroxido dicopper(II) complex, we tried to enhance the formation of this "oxygen adduct complex" to confirm the formation of this species. To accomplish this, we incorporated an amide (**L-(O)NHAc**) or a primary amine (**L(O)NH_2**) function at the terminal position of the ligand, whose hydrogen donor ability is more potent than that of the hydroxy group. Therefore, both ligands should be able to form hydrogen bond stabilized *trans*-μ-1,2-peroxido dicopper(II) complexes, similar to the above-discussed

complexes, where amines were incorporated in ligand backbones.[12–15] The syntheses of both copper(I) complexes resulted in mono acetonitrile coordinated complexes similar to all copper(I) complexes in this work except for the complex with ligand **L(S)OH**. Stopped-flow UV/vis measurements of the reaction of the copper(I) complex with the amide ligand **L(O)NHAc** and dioxygen in acetone at −80 °C showed the formation of a band at 380 nm and a small band and shoulder at 488 and 616 nm respectively (Figure 7). Similar to the reactivity of the initial copper(I) complex of **L(O)OH** and dioxygen (Figure 1), first, the band at 488 nm and the shoulder at 616 nm developed before fully interconverting into the band at 380 nm. The location of the first band and shoulder corresponds well to the reactivity of the above-discussed copper(I) complexes with **tmpa** derivatives containing one additional N-donor function. In contrast, the second band corresponds to the reactivity of the copper(I) complexes of **L(CH_2)OH**, **L(O)OCH_3**, and **L(O)CH_3**. Therefore, we conclude that in the reaction of copper(I) complex with the amide ligand **L(O)NHAc** and dioxygen, we observe the fast formation of a hydrogen bond stabilized *trans*-μ-1,2-peroxido dicopper(II), which rapidly turns into a bis(μ-oxido)dicopper(III) complex. The considerably smaller appearance of the band of the hydrogen bond stabilized *trans*-μ-1,2-peroxido dicopper(II) complex compared to the band bis(μ-oxido)dicopper(III) complex in Figure 7 in contrast to Figure 1, where both are at equal size, is in line with stronger hydrogen bond interactions, as discussed above.[12,13] Unfortunately, the fast buildup time of both species made no follow-up measurements possible.

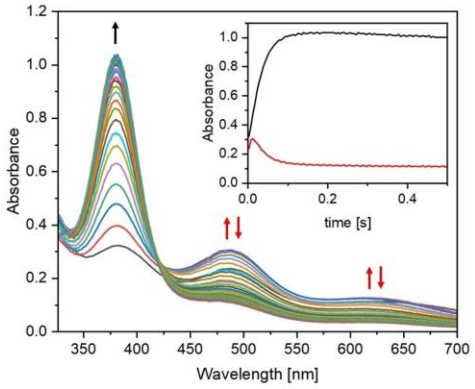

Figure 7. Time-resolved UV/Vis spectra of the reaction of [Cu(**L-(O)NHAc**)(MeCN)]ClO_4 ($2.5 \cdot 10^{-4}$ mol L^{-1}) with dioxygen ($5.7 \cdot 10^{-3}$ mol L^{-1})[25] in acetone at −80 °C over a period of 0.5 s. The inset displays the time-dependent change in absorbance at 380 nm (black) and 488 nm (red).

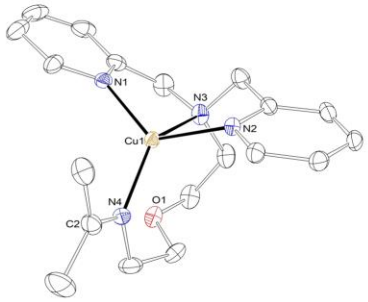

Figure 8. ORTEP Plot of the molecular structure of [Cu(**L(O)NC(CH_3)$_2$**)]ClO_4. Non-binding anions and carbon-bound hydrogen atoms are omitted for clarity. Ellipsoids are drawn at 50% probability. Selected Bond Lengths (Å): Cu(1)–N(1): 1.998; Cu(1)–N(2): 2.055; Cu(1)–N(3): 2.306; Cu(1)–N(4): 2.005; N(4)–C(2): 1.284. Selected bond angles (°): N(1)–Cu(1)–N(2): 125.25; N(1)–Cu-(1)–N(3): 79.36; N(1)–Cu(1)–N(4): 123.14; N(2)–Cu(1)–N(3): 80.62; N(2)–Cu-(1)–N(4): 107.35; N(3)–Cu(1)–N(4): 133.68.

Furthermore, we investigated the copper(I) complex with the primary amine ligand **L(O)NH_2**, for which we could grow single crystals from acetone and diethyl ether for structural characterization. Instead of the copper(I) complex with a primary amine function, we received single crystals of its imine derivative, as depicted in Figure 8. The copper(I) ion is coordinated by four N-donor atoms (N(1), N(2), N(3), N(4)) of **L(O)NHC(CH_3)$_2$** (imine double bond located between N(4) and C(2)) in a distorted tetrahedral geometry ($\tau_4 = 0.72$, $\tau_4' = 0.69$).[26,27] While the equilibrium of imine condensation reactions favors the side of the primary amine and ketone and usually requires dehydrating agents, it is reasonable that the reaction was slowly enforced by the presence of the copper(I) ion. This reaction presumably occurred over days and, therefore, should not play a role in freshly synthesized acetone solutions for the mechanistic studies.

Benchtop experiments of yellow copper(I) complex solutions with dioxygen in acetone at −80 °C and 20 °C led to no color change. Only when the oxidized solution stood overnight at room temperature did a color change from yellow to a green-colored solution occur, corresponding to its copper(II) form. To determine whether only the slow decomposition of a copper(I) to a copper(II) complex took place or whether traces of a "dioxygen adduct complex" were formed, we carried out stopped-flow UV/vis measurements in acetone at −80 °C. The sole formation of a small band at 487 nm was observed (the decrease of the band at 354 nm corresponds to the decrease of copper(I) complex, Figure 9). The fast buildup of the absorbance at 487 nm is followed by an immediate decrease of the absorbance, but rather slowly over several minutes, in line with the observation that the copper(I) species reacted overnight to the corresponding copper(II) complex. The location of the band aligns perfectly with the immediate absorbance of the copper(I) complex with **L(O)NHAc** as a ligand with dioxygen and thus is in line with the copper(I) complexes with **tmpa** derivatives that contain one additional amine function.[12–14] The magnitude of the absorbance in Figure 9 is the same as in Figure 7, which shows that the aforementioned imine condensation does not play a significant role. Still, the measurements were repeated in a 10 : 1 mixture of THF and acetonitrile, which showed the same behavior (Figure S19). Due to the fast buildup time and low absorbance, no follow-up measurements were performed. All in all, the inclusion of an amide or primary amine function shows

Research Article
doi.org/10.1002/ejic.202400804

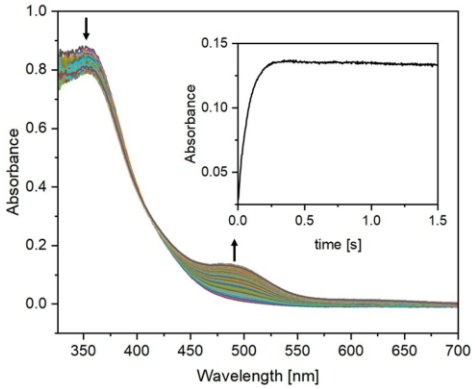

Figure 9. Time-resolved UV/vis spectra of the reaction of [Cu(**L-(NH$_2$)OH**)(MeCN)]ClO$_4$ ($2.5 \cdot 10^{-4}$ mol L^{-1}) with dioxygen ($5.7 \cdot 10^{-3}$ mol L^{-1})[25] in acetone at −80 °C over a period of 1.5 s. The inset displays the time-dependent change in absorbance at 487 nm.

Table 1. Spectral data of copper(I) complexes in its reaction with dioxygen and its observed "oxygen adduct complexes" in acetone at −80 °C.

Complex[a]	Max$_1$ [nm]	Max$_2$ [nm]	Dioxygen-Adduct
[Cu(**L(O)OH**)(MeCN)]$^+$	389	455	^{T}**P**[b] to **O**
[Cu(**L(S)OH**)]$^+$	523	600	^{T}**P**
[Cu(**L(CH$_2$)OH**)(MeCN)]$^+$	387	–	**O**
[Cu(**L(O)OCH$_3$**)(MeCN)]$^+$	380	–	**O**
[Cu(**L(O)CH$_3$**)(MeCN)]$^+$	380	–	**O**
[Cu(**L(O)NHAc**)(MeCN)]$^+$	380	488	^{T}**P**[b] to **O**
[Cu(**L(O)NH$_2$**)(MeCN)]$^+$	–	487	^{T}**P**[b]

[a] Perchlorate anions are omitted for clarity. [b] Second coordination sphere interactions *via* hydrogen bonds.

that a stronger hydrogen bond donor can lead to similar spectra as for the copper(I) complex with **L(O)OH** as a ligand.

Conclusions

In this work, it was demonstrated that in the reaction of the copper(I) complex with **L(O)OH** as a ligand and dioxygen under low-temperature stopped-flow conditions, two distinct "oxygen adduct species" were observed. Investigating copper(I) complexes with derivatives of this ligand by systematically changing functional groups revealed that both the ether moiety and the terminal hydrogen donor were crucial for observing both short-lived "oxygen adduct species". Removing either the ether moiety or the hydroxy group led to the sole formation of bis(μ-oxido)dicopper(III) complexes. In contrast, the incorporation of stronger hydrogen-bonding donors led to similar spectra as for the copper(I) complex of **L(O)OH** or the sole formation of a hydrogen bond stabilized *trans*-μ-1,2-peroxido dicopper(II) complex (Table 1). Based on these results, a reaction mechanism for the reaction of the copper(I) complex of **L(O)OH** and dioxygen is proposed, where after the initial formation of a η^1-superoxido copper(II) complex, first a hydrogen bond stabilized *trans*-μ-1,2-peroxido dicopper(II) complex is formed, as reported previously, which rapidly reacts to a bis(μ-oxido)dicopper(III) complex (Scheme 6). The overall results provide new insights into secondary coordination sphere interactions of the ethoxyethanol sidearm, which can be used in future applications of copper "oxygen adduct complexes" for catalytic reactions.

Experimental Section

Materials and Methods: Synthesis of air-sensitive copper(I) complexes was carried out under inert conditions in a glove box (MBraun) filled with argon 5.0. Solvents and reagents were used as purchased from common suppliers unless stated otherwise. [Cu(MeCN)$_4$]ClO$_4$ was prepared according to the literature and stored in the glove box.[30] Solvents used for the synthesis of copper complexes were bought as anhydrous solvents under nitrogen atmosphere, distilled under argon, and stored in the glove box. NMR measurements were performed using a Bruker Avance II 400 MHz, Bruker Avance III 400 MHz HD spectrometer. The ^{1}H- and ^{13}C-NMR spectra were calibrated using the residual proton and carbon signals of chloroform ($\delta = 7.26$ and $\delta = 77.2$) and acetone ($\delta = 2.05$ and $\delta = 29.8$).[31] ESI-MS (HRMS) was measured using a Bruker Daltonica micrOTOF. Elemental analysis was carried out using a Thermo FlashEA-1112 series CHN-analysator. GC-MS measurements were carried out using an Agilent Technologies 5977B mass detector with a 7820 A GC system. UV/vis measurements were carried out using an Agilent 8453 spectrometer. Stopped-Flow UV/vis measurements were carried out on a commercial HI-TECH SF61SX2 stopped-flow unit (TgK Scientific, Bratford-on-Avon, UK). The data was processed using Kinetic Studio version 5.02 Beta. The

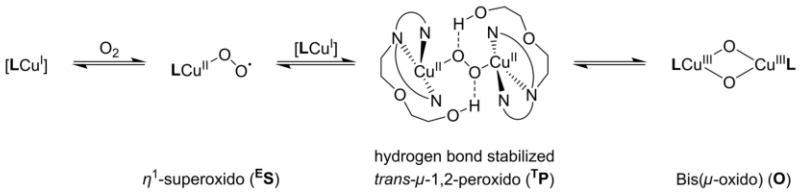

Scheme 6. Proposed mechanism for the reaction of [Cu(**L(O)OH**)(MeCN)]ClO$_4$ and dioxygen in acetone.

procedure for kinetic measurements was described in detail in previous work.[32] Details of X-Ray crystal structure determination are reported in the Supporting Information. Deposition Numbers 2405535 (for [Cu(**L(S)OH**)]ClO_4) and 2405536 (for [Cu(**L-(O)NHC(CH_3)$_2$)]ClO_4) contain the supplementary crystallographic data for this paper. These data are provided free of charge by the joint Cambridge Crystallographic Data Centre and Fachinformationszentrum Karlsruhe Access Structures service.

General procedure for the synthesis of the ligands: A modified version of the literature known synthesis of **L(O)OH** was used as the general procedure.[19] Under argon atmosphere a suspension of amine precursor, 2-picolylchloride hydrochloride, and potassium carbonate in 50 mL dry acetonitrile was refluxed for four days. The reaction mixture is filtrated, and the solvent was removed under reduced pressure. The crude product was dissolved in 30 mL DCM, washed three times with 30 mL saturated sodium bicarbonate, and dried over sodium sulfate. The solvent was removed under reduced pressure and the crude product was purified by column chromatography over silica using a gradient of ethyl acetate and methanol.

L(O)OH: Following the general procedure 2-(2-aminoethoxy)ethanol (0.50 g, 0.47 mL, 4.8 mmol), 2-picolylchloride hydrochloride (1.56 g, 9.51 mol), and potassium carbonate (6.57 g, 47.6 mmol) were used to obtain the corresponding ligand as a brown oil (0.87 g, 3.0 mmol, 64 %). ^{1}H NMR (400 MHz, $CDCl_3$): δ [ppm] = 8.53–8.50 (m, 2H), 7.65 (td, J = 7.6, 1.8 Hz, 2H), 7.54 (d, J = 7.8 Hz, 2H), 7.18–7.13 (m, 2H), 3.95 (s, 4H), 3.72–3.68 (m, 2H), 3.64 (t, J = 5.0 Hz, 2H), 3.53–3.50 (m, 2H), 2.83 (t, J = 5.0 Hz, 2H); ^{13}C NMR (101 MHz, $CDCl_3$): δ [ppm] = 159.5, 149.0, 136.7, 123.4, 122.2, 72.7, 68.9, 61.8, 60.7, 53.1; HRMS (ESI): m/z calcd. for $C_{16}H_{21}N_3O_2$: 310.1526 $[M+Na]^+$; found: m/z = 310.1526. This data is in accordance with the literature.[21]

L(S)OH: Following the general procedure 2-[(2-aminoethyl)thio]ethanol (0.64 g, 0.57 mL, 4.8 mmol), 2-picolylchloride hydrochloride (1.56 g, 9.51 mol), and potassium carbonate (6.57 g, 47.6 mmol) were used to obtain the corresponding ligand as a brown oil (1.37 g, 4.51 mmol, 85 %). ^{1}H NMR (400 MHz, $CDCl_3$): δ [ppm] = 8.53–8.49 (m, 2H), 7.65 (td, J = 7.7, 1.8 Hz, 2H), 7.52 (d, J = 7.8 Hz, 2H), 7.18–7.12 (m, 2H), 3.85 (s, 4H), 3.70 (t, J = 5.9 Hz, 2H), 2.84–2.78 (m, 2H), 2.77–2.71 (m, 2H), 2.65 (t, J = 5.9 Hz, 2H); ^{13}C NMR (101 MHz, $CDCl_3$): δ [ppm] = 159.2, 149.1, 136.7, 123.4, 122.3, 61.1, 60.2, 53.9, 35.3, 29.1; HRMS (ESI): m/z calcd. for $C_{16}H_{21}N_3OS$: 326.1297 $[M+Na]^+$; found: m/z = 326.1297.

L(CH_2)OH: Following the general procedure 5-Amino-1-pentanol (0.50 g, 4.8 mmol), 2-picolylchloride hydrochloride (1.56 g, 9.51 mol), and potassium carbonate (6.70 g, 48,5 mmol) were used to obtain the corresponding ligand as a yellow oil (0.76 g, 2.7 mmol, 55 %). ^{1}H NMR (400 MHz, acetone-d_6): δ [ppm] = 8.48–8.46 (m, 2H), 7.73 (td, J = 7.6, 1.8 Hz, 2H), 7.60 (d, J = 7.8 Hz, 2H), 7.22–7.17 (m, 2H), 3.78 (s, 4H), 3.50 (t, J = 6.4 Hz, 2H), 2.54–2.50 (m, 2H), 1.62–1.54 (m, 2H), 1.49–1.41 (m, 2H), 1.40–1.31 (m, 2H); ^{13}C NMR (101 MHz, acetone-d_6): δ [ppm] = 161.2, 149.65, 137.0, 123.5, 122.7, 62.3, 61.2, 55.0, 33.6, 27.8, 24.3; HRMS (ESI): m/z calcd. for $C_{17}H_{23}N_3O$: 286.1914 $[M+H]^+$; found: m/z = 286.1914.

L(O)OCH_3: Following the general procedure (2-(2-Methoxyethoxy)ethanamine (0.50 g, 0.52 mL, 4.2 mmol), 2-picolylchloride hydrochloride (1.38 g, 8.39 mol), and potassium carbonate (5.80 g, 42.0 mmol) were used to obtain the corresponding ligand as a yellow oil (0.55 g, 1.83 mmol, 44 %). ^{1}H NMR (400 MHz, acetone-d_6): δ [ppm] = 8.49–8.46 (m, 2H), 7.72 (td, J = 7.6, 1.8 Hz, 2H), 7.64 (d, J = 7.8 Hz, 2H), 7.22–7.17 (m, 2H), 3.87 (s, 4H), 3.61 (t, J = 5.9 Hz, 2H), 3.53–3.49 (m, 2), 3.47–3.44 (m, 2H), 3.27 (s, 3H), 2.76 (t, J = 5.9 Hz, 2H); ^{13}C NMR (101 MHz, acetone-d_6): δ [ppm] = 161.1, 149.7, 137.0, 123.5, 122.7, 72.7, 71.0, 70.4, 61.6, 58.8, 54.5; HRMS (ESI): m/z calcd. for $C_{17}H_{23}N_3O_2$: 324.1682 $[M+Na]^+$; found: m/z = 324.1681.

L(O)CH_3: Following the general procedure 2-Aminoethylpropylether (0.50 g, 0.59 mL, 4.8 mmol), 2-picolylchloride hydrochloride (1.59 g, 9.69 mol), and potassium carbonate (6.70 g, 48.5 mmol) were used to obtain the corresponding ligand as a yellow oil (0.72 g, 2.51 mmol, 52 %). ^{1}H NMR (400 MHz, acetone-d_6): δ [ppm] = 8.49–8.45 (m, 2H), 7.73 (td, J = 7.6, 1.8 Hz, 2H), 7.64 (d, J = 7.8 Hz, 2H), 7.22–7.17 (m, 2H), 3.87 (s, 4H), 3.56 (t, J = 5.8 Hz, 2H), 3.32 (t, J = 6.5 Hz, 2H), 2.76 (t, J = 5.8 Hz, 2H), 1.57–1.47 (m, 2H), 0.88 (t, J = 7.4 Hz, 3H); ^{13}C NMR (101 MHz, acetone-d_6): δ [ppm] = 161.2, 149.7, 137.0, 123.5, 122.7, 73.2, 70.1, 61.6, 54.5, 23.7, 11.0; HRMS (ESI): m/z calcd. for $C_{17}H_{23}N_3O$: 308.1733 $[M+Na]^+$; found: m/z = 308.1733.

L(O)NHAc: The first step follows a literature known synthesis for the mono-acylation of symmetric diamines.[20] To a solution of the diamine **6** (1.04 g, 1.06 mL, 10.0 mmol) in ethyl acetate (0.88 g, 0.99 mL, 10 mmol) 0.5 mL deionized water was added and the reaction mixture was refluxed for 21 h. The solvent was removed under reduced pressure and 1.55 g yellow oil was received. Without further purification the crude product was dissolved in 50 mL dry DCE and pyridine-2-carbaldehyde (2.14 g, 1.90 mL, 20.0 mmol) and sodium triacetoxyborohydride (6.36 g, 30.0 mmol) were added. After stirring the reaction for 3 h at RT the reaction was quenched with water, was made basic with aq. KOH, and extracted three times with 50 mL DCM. The combined organic phases were dried over Na_2SO_4 and the solvent was removed under reduced pressure. The crude product was purified by column chromatography (DCM, MeOH 20 : 1) and a yellow oil (9.97 g, 2.97 mmol, 30 %) was received. ^{1}H NMR (400 MHz, acetone-d_6): δ [ppm] = 8.50–8.47 (m, 2H), 7.74 (td, J = 7.6, 1.8 Hz, 2H), 7.63 (d, J = 7.8 Hz, 2H), 7.23–7.19 (m, 2H), 3.89 (s, 4H), 3.59 (t, J = 5.6 Hz, 2H), 3.42 (t, J = 5.6 Hz, 2H), 3.30 (q, J = 5.6 Hz, 2H), 2.88 (s, 1H), 2.77 (t, J = 5.6 Hz, 2H), 1.85 (s, 3H); ^{13}C NMR (101 MHz, acetone-d_6): 169.9, 161.1, 149.7, 137.1, 123.6, 122.7, 70.4, 69.9, 61.5, 54.1, 39.8, 22.9; HRMS (ESI): m/z calcd. for $C_{18}H_{24}N_4O_2$: 357.1791 $[M+Na]^+$; found: m/z = 351.1790.

L(O)NH_2: The acyl deprotection was performed by refluxing **L(O)NHAc** (1.43 g, 4.36 mmol) in 50 mL 5 molar HCl for 20 h. After cooling to room temperature, the reaction mixture was made basic with aq. KOH and extracted four times with 50 mL DCM. The combined organic phases were dried over Na_2SO_4 and the solvent was removed under reduced pressure. The crude product was purified by Kugelrohr distillation to obtain the ligand as a yellow oil (0.54 g, 1.9 mmol, 44 %). ^{1}H NMR (400 MHz, acetone-d_6): δ [ppm] = 8.49–8.45 (m, 2H), 7.72 (td, J = 7.6, 1.8 Hz, 2H), 7.64 (d, J = 7.8 Hz, 2H), 7.21–7.17 (m, 2H), 3.87 (s, 4H), 3.63–3.56 (m, 4H), 3.33 (t, J = 6.1 Hz, 2H), 2.95 (s, 2H), 2.75 (t, J = 5.8 Hz, 2H); ^{13}C NMR (101 MHz, acetone-d_6): δ [ppm] = 161.2, 149.6, 137.0, 123.5, 122.6, 72.1, 70.4, 61.6, 54.5, 52.1; HRMS (ESI): m/z calcd. for $C_{16}H_{22}N_4O$: 287.1867 $[M+H]^+$; found: m/z = 287.1869.

***Caution!** Perchlorate salts are potentially explosive and should be handled with great care.*

General procedure for the synthesis of copper(I) complexes: In an argon filled glovebox ligand and copper salt were each dissolved in dry acetonitrile. Then the copper solution was added dropwise under vigorous stirring to the ligand solution at room temperature. The reaction mixture was stirred for 30 min and subsequently the solvent was removed under reduced pressure to obtain the complex without further purification.

[Cu(L(O)OH)(MeCN)][ClO_4]: Following the general procedure Ligand **L(O)OH** (83.0 mg, 0.289 mmol) and [Cu(MeCN)$_4$](ClO_4) (90.0 mg, 0.275 mmol) in 6 mL dry acetonitrile were used to obtain the corresponding complex as a yellow oil (145.9 mg, 0.297 mmol).

Elemental analysis calcd. (%) for $C_{18}H_{24}ClCuN_4O_6$: C 44.00, H 4.92, N 11.40; found: C 44.91, H 4.91, N 11.61.

[Cu(L(S)OH)](ClO$_4$): Following the general procedure Ligand **L(S)OH** (87.6 mg, 0.289 mmol) and [Cu(MeCN)$_4$](ClO$_4$) (90.0 mg, 0.275 mmol) in 6 mL dry acetonitrile were used to obtain the corresponding complex as a yellow solid (137.4 mg, 0.295 mmol). Elemental analysis calcd. (%) for $C_{16}H_{21}ClCuN_3O_5S$: C 41.20, H 4.54, N 9.01; found: C 42.31, H 4.47, N 9.50. Yellow single crystals suitable for X-ray structural characterization were received by dissolving small amounts in acetone and slow ether diffusion over a week at room temperature.

[Cu(L(CH$_2$)OH(MeCN))](ClO$_4$): Following the general procedure Ligand **L(CH$_2$)OH** (82.4 mg, 0.289 mmol) and [Cu(MeCN)$_4$](ClO$_4$) (90.0 mg, 0.275 mmol) in 6 mL dry acetonitrile were used to obtain the corresponding complex as a yellow oil (142.2 mg, 0.291 mmol). Elemental analysis calcd. (%) for $C_{19}H_{26}ClCuN_4O_5$: C 46.63, H 5.35, N 11.45; found: C 46.99, H 5.40, N 12.06.

[Cu(L(O)OCH$_3$)(MeCN)](ClO$_4$): Following the general procedure Ligand **L(O)OCH$_3$** (87.0 mg, 0.289 mmol) and [Cu(MeCN)$_4$](ClO$_4$) (90.0 mg, 0.275 mmol) in 6 mL dry acetonitrile were used to obtain the corresponding complex as a yellow oil (144.6 mg, 0.286 mmol). Elemental analysis calcd. (%) for $C_{19}H_{26}ClCuN_4O_6$: C 45.15, H 5.19, N 11.09; found: C 45.71, H 5.33, N 11.20.

[Cu(L(O)CH$_3$)(MeCN)](ClO$_4$): Following the general procedure Ligand **L(O)CH$_3$** (82.4 mg, 0.289 mmol) and [Cu(MeCN)$_4$](ClO$_4$) (90.0 mg, 0.275 mmol) in 6 mL dry acetonitrile were used to obtain the corresponding complex as a yellow oil (134.9 mg, 0.276 mmol). Elemental analysis calcd. (%) for $C_{19}H_{26}ClCuN_4O_5$: C 46.63, H 5.35, N 11.45; found: C 47.16, H 5.39, N 11.50.

[Cu(L(O)NHAc)(MeCN)](ClO$_4$): Following the general procedure Ligand **L(O)NHAc** (94.9 mg, 0.289 mmol) and [Cu(MeCN)$_4$](ClO$_4$) (90.0 mg, 0.275 mmol) in 6 mL dry acetonitrile were used to obtain the corresponding complex as a dark orange oil (157.0 mg, 0.295 mmol). Elemental analysis calcd. (%) for $C_{20}H_{27}ClCuN_5O_6$: C 45.12, H 5.11, N 13.15; found: C 45.36, H 5.08, N 13.00.

[Cu(L(O)NH$_2$)(MeCN)](ClO$_4$): Following the general procedure Ligand **L(O)NH$_2$** (82.7 mg, 0.289 mmol) and [Cu(MeCN)$_4$](ClO$_4$) (90.0 mg, 0.275 mmol) in 6 mL dry acetonitrile were used to obtain the corresponding complex as a dark orange oil (138.5 mg, 0.282 mmol). Elemental analysis calcd. (%) for $C_{18}H_{25}ClCuN_5O_5$: C 44.08, H 5.14, N 14.28; found: C 44.14, H 5.09, N 13.48.

[Cu(L(O)NC(CH$_3$)$_2$)](ClO$_4$): Yellow single crystals suitable for X-ray structural characterization were received by dissolving small amounts of [Cu(**L(O)NH$_2$**)(MeCN)](ClO$_4$) in acetone and slow ether diffusion over several days at room temperature.

Oxygenation Reaction of [Cu(L(O)OH)(MeCN)](ClO$_4$) and [Cu(L(S)OH)](ClO$_4$): To investigate whether the ligands **L(O)OH** and **L(S)OH** are still intact after oxidation of the corresponding copper(I) complexes with dioxygen, the copper was extracted and the organic residue was analyzed. For that about 40 mg of the corresponding copper(I) complex was dissolved in 5 mL acetone and dioxygen was bubbled through the solution for 5 min at −80 °C. After the solution warmed up to room temperature aq. ammonia (20 mL) was added and the solution was extracted three times with 20 mL DCM. The combined organic phases were dried over Na_2SO_4 and the solvent was removed under reduced pressure. The organic residue was analyzed using GC-MS.

Acknowledgements

We gratefully acknowledge support by the Justus Liebig University Gießen and the German Research Foundation (Deutsche Forschungsgemeinschaft) for financial support (SS, SCHI 377/20-1). Open Access funding enabled and organized by Project DEAL. Open Access funding enabled and organized by Projekt DEAL.

Conflict of Interests

The authors declare no conflict of interest.

Data Availability Statement

The data that support the findings of this study are available from the corresponding author upon reasonable request.

Keywords: Bioinorganic chemistry · Copper · Dioxygen activation · Hydrogen bonding · Second coordination sphere interactions

[1] S. T. Prigge, B. A. Eipper, R. E. Mains, L. M. Amzel, *Science (New York, N. Y.)* **2004**, *304*, 864.
[2] T. V. Vendelboe, P. Harris, Y. Zhao, T. S. Walter, K. Harlos, K. El Omari, H. E. M. Christensen, *Sci. Adv.* **2016**, *2*, e1500980.
[3] a) D. A. Quist, D. E. Diaz, J. J. Liu, K. D. Karlin, *J. Biol. Inorg. Chem.* **2017**, *22*, 253; b) C. E. Elwell, N. L. Gagnon, B. D. Neisen, D. Dhar, A. D. Spaeth, G. M. Yee, W. B. Tolman, *Chem. Rev.* **2017**, *117*, 2059.
[4] L. M. Mirica, X. Ottenwaelder, T. D. P. Stack, *Chem. Rev.* **2004**, *104*, 1013.
[5] C. Würtele, E. Gaoutchenova, K. Harms, M. C. Holthausen, J. Sundermeyer, S. Schindler, *Angew. Chem. Int. Ed.* **2006**, *45*, 3867.
[6] R. R. Jacobson, Z. Tyeklar, A. Farooq, K. D. Karlin, S. Liu, J. Zubieta, *J. Am. Chem. Soc.* **1988**, *110*, 3690.
[7] M. Bhadra, W. J. Transue, H. Lim, R. E. Cowley, J. Y. C. Lee, M. A. Siegler, P. Josephs, G. Henkel, M. Lerch, S. Schindler, et al., *J. Am. Chem. Soc.* **2021**, *143*, 3707.
[8] L. Q. Hatcher, D.-H. Lee, M. A. Vance, A. E. Milligan, R. Sarangi, K. O. Hodgson, B. Hedman, E. I. Solomon, K. D. Karlin, *Inorg. Chem.* **2006**, *45*, 10055.
[9] S. Kim, J. W. Ginsbach, A. I. Billah, M. A. Siegler, C. D. Moore, E. I. Solomon, K. D. Karlin, *J. Am. Chem. Soc.* **2014**, *136*, 8063.
[10] T. Osako, Y. Ueno, Y. Tachi, S. Itoh, *Inorg. Chem.* **2003**, *42*, 8087.
[11] a) R. L. Shook, A. S. Borovik, *Inorg. Chem.* **2010**, *49*, 3646; b) M. Bhadra, J. Y. C. Lee, R. E. Cowley, S. Kim, M. A. Siegler, E. I. Solomon, K. D. Karlin, *J. Am. Chem. Soc.* **2018**, *140*, 9042.
[12] S. Yamaguchi, A. Wada, Y. Funahashi, S. Nagatomo, T. Kitagawa, K. Jitsukawa, H. Masuda, *Eur. J. Inorg. Chem.* **2003**, *2003*, 4378.
[13] A. Wada, Y. Honda, S. Yamaguchi, S. Nagatomo, T. Kitagawa, K. Jitsukawa, H. Masuda, *Inorg. Chem.* **2004**, *43*, 5725.
[14] S. Kim, C. Saracini, M. A. Siegler, N. Drichko, K. D. Karlin, *Inorg. Chem.* **2012**, *51*, 12603.
[15] E. W. Dahl, H. T. Dong, N. K. Szymczak, *Chem. Commun.* **2018**, *54*, 892.
[16] F. Tao, Q. Wang, *RSC Adv.* **2015**, *5*, 46007.
[17] H. Oh, S. Choi, J. Y. Kim, H. S. Ahn, S. Hong, *Chem. Commun.* **2019**, *55*, 12659.
[18] H. Oh, W.-M. Ching, J. Kim, W.-Z. Lee, S. Hong, *Inorg. Chem.* **2019**, *58*, 12964.
[19] Y. Mikata, T. Fujimoto, Y. Sugai, S. Yano, *Eur. J. Inorg. Chem.* **2007**, *2007*, 1143.
[20] W. Tang, S. Fang, *Tetrahedron Lett.* **2008**, *49*, 6003.
[21] S. I. Kirin, C. M. Happel, S. Hrubanova, T. Weyhermuller, C. Klein, N. Metzler-Nolte, *Dalton Trans.* **2004**, *8*, 1201.

[22] H. R. Lucas, L. Li, A. A. N. Sarjeant, M. A. Vance, E. I. Solomon, K. D. Karlin, *J. Am. Chem. Soc.* **2009**, *131*, 3230.
[23] X. Zhong, C. J. Bouchey, E. Kabir, W. B. Tolman, *J. Inorg. Biochem.* **2021**, *222*, 111498.
[24] a) P. K. Wick, K. D. Karlin, M. Suzuki, A. D. Zuberbühler, *Micron* **2004**, *35*, 137; b) M. Costas, X. Ribas, A. Poater, J. M. López Valbuena, R. Xifra, A. Company, M. Duran, M. Solà, A. Llobet, M. Corbella, et al., *Inorg. Chem.* **2006**, *45*, 3569; c) M. T. Kieber-Emmons, J. W. Ginsbach, P. K. Wick, H. R. Lucas, M. E. Helton, B. Lucchese, M. Suzuki, A. D. Zuberbühler, K. D. Karlin, E. I. Solomon, *Angew. Chem. Int. Ed.* **2014**, *53*, 4935; d) L. Siebe, C. Butenuth, A. Stammler, H. Bögge, S. Walleck, T. Glaser, *Inorg. Chem.* **2024**, *63*, 2627.
[25] H. Sterckx, B. Morel, B. U. W. Maes, *Angew. Chem. Int. Ed.* **2019**, *58*, 7946.
[26] L. Yang, D. R. Powell, R. P. Houser, *Dalton Trans.* **2007**, *9*, 955.
[27] A. Okuniewski, D. Rosiak, J. Chojnacki, B. Becker, *Polyhedron* **2015**, *90*, 47.
[28] T. Rotärmel, P. Specht, J. Becker, A. Neuba, S. Schindler, *Eur. J. Inorg. Chem.* **2023**, *26*, e202200626.
[29] a) K. D. Karlin, S. Kaderli, A. D. Zuberbühler, *Acc. Chem. Res.* **1997**, *30*, 139; b) C. X. Zhang, S. Kaderli, M. Costas, E.-I. Kim, Y.-M. Neuhold, K. D. Karlin, A. D. Zuberbühler, *Inorg. Chem.* **2003**, *42*, 1807; c) M. Weitzer, S. Schindler, G. Brehm, S. Schneider, E. Hörmann, B. Jung, S. Kaderli, A. D. Zuberbühler, *Inorg. Chem.* **2003**, *42*, 1800; d) M. Lerch, M. Weitzer, T.-D. J. Stumpf, L. Laurini, A. Hoffmann, J. Becker, A. Miska, R. Göttlich, S. Herres-Pawlis, S. Schindler, *Eur. J. Inorg. Chem.* **2020**, *2020*, 3143.
[30] D. F. Shriver, *Inorganic Syntheses*, Wiley, **1979**.
[31] G. R. Fulmer, A. J. M. Miller, N. H. Sherden, H. E. Gottlieb, A. Nudelman, B. M. Stoltz, J. E. Bercaw, K. I. Goldberg, *Organometallics* **2010**, *29*, 2176.
[32] M. Weitzer, M. Schatz, F. Hampel, F. W. Heinemann, S. Schindler, *J. Chem. Soc. Dalton Trans.* **2002**, 686.
[33] L. Krause, R. Herbst-Irmer, G. M. Sheldrick, D. Stalke, *J. Appl. Crystallogr.* **2015**, *48*, 3.
[34] G. M. Sheldrick, *Acta Crystallogr., Sect. A: Found. Adv.* **2015**, *71*, 3.
[35] G. M. Sheldrick, *Acta Crystallogr. Sect. C* **2015**, *71*, 3.

Manuscript received: December 4, 2024
Revised manuscript received: January 15, 2025
Accepted manuscript online: January 15, 2025
Version of record online: ■■, ■■

4 References

[1] *Katalytische Oxidationsreaktionen als Schlüsseltechnologie*. *Positionspapier*, DECHEMA Gesellschaft für Chemische Technik und Biotechnologie e.V, Frankfurt am Main, **2015**.

[2] F. Cavani, J. H. Teles, *ChemSusChem* **2009**, *2*, 508.

[3] D. A. Quist, D. E. Diaz, J. J. Liu, K. D. Karlin, *J. Biol. Inorg. Chem.* **2017**, *22*, 253.

[4] H. Sterckx, B. Morel, B. U. W. Maes, *Angew. Chem. Int. Ed.* **2019**, *58*, 7946.

[5] W. T. Borden, R. Hoffmann, T. Stuyver, B. Chen, *J. Am. Chem. Soc.* **2017**, *139*, 9010.

[6] J. Smidt, W. Hafner, R. Jira, J. Sedlmeier, R. Sieber, R. Rüttinger, H. Kojer, *Angew. Chem.* **1959**, *71*, 176.

[7] J. A. Keith, P. M. Henry, *Angew. Chem. Int. Ed.* **2009**, *48*, 9038.

[8] M. Economidou, N. Mistry, K. M. P. Wheelhouse, D. M. Lindsay, *Org. Process Res. Dev.* **2023**, *27*, 1585.

[9] R. Horn, R. Schlögl, *Catal. Lett.* **2015**, *145*, 23.

[10] *KATALYSE. Eine interdisziplinäre Schlüsseltechnologie zur nachhaltigen Wirtschaftsentwicklung*. *Roadmap der deutschen Katalyseforschung*, DECHEMA Gesellschaft für Chemische Technik und Biotechnologie e.V, Frankfurt am Main, **2023**.

[11] N. J. Gunsalus, A. Koppaka, S. H. Park, S. M. Bischof, B. G. Hashiguchi, R. A. Periana, *Chem. Rev.* **2017**, *117*, 8521.

[12] a) A. Riaz, G. Zahedi, J. J. Klemeš, *J. Cleaner Prod.* **2013**, *57*, 19; b) B. Wang, S. Albarracín-Suazo, Y. Pagán-Torres, E. Nikolla, *Catal. Today* **2017**, *285*, 147.

[13] M. J. Da Silva, *Fuel Process. Technol.* **2016**, *145*, 42.

[14] G. A. Olah, *Angew. Chem. Int. Ed.* **2005**, *44*, 2636.

[15] F. J. Tucci, A. C. Rosenzweig, *Chem. Rev.* **2024**, *124*, 1288.

[16] a) H. Fujisaki, T. Ishizuka, H. Kotani, Y. Shiota, K. Yoshizawa, T. Kojima, *Nature* **2023**, *616*, 476; b) H. Takahashi, K. Wada, K. Tanaka, K. Fujikawa, Y. Hitomi, T. Endo, M. Kodera, *Bull. Chem. Soc. Jpn.* **2022**, *95*, 1148.

[17] I. A. Koval, P. Gamez, C. Belle, K. Selmeczi, J. Reedijk, *Chem. Soc. Rev.* **2006**, *35*, 814.

[18] a) S. A. K. WILSON, *Brain* **1912**, *34*, 295; b) A. Członkowska, T. Litwin, P. Dusek, P. Ferenci, S. Lutsenko, V. Medici, J. K. Rybakowski, K. H. Weiss, M. L. Schilsky, *Nat. Rev. Dis. Primers* **2018**, *4*, 21; c) J. H. Menkes, M. Alter, G. K. Steigleder, D. R.

Weakley, J. H. Sung, *Pediatrics* **1962**, *29*, 764; d) Z. Tümer, L. B. Møller, *Eur. J. Hum. Genet.* **2010**, *18*, 511.

[19] W. Kaim, J. Rall, *Angew. Chem. Int. Ed. Engl.* **1996**, *35*, 43.

[20] L. M. Mirica, X. Ottenwaelder, T. D. P. Stack, *Chem. Rev.* **2004**, *104*, 1013.

[21] E. I. Solomon, U. M. Sundaram, T. E. Machonkin, *Chem. Rev.* **1996**, *96*, 2563.

[22] P. M. Colman, H. C. Freeman, J. M. Guss, M. Murata, V. A. Norris, J. A. M. Ramshaw, M. P. Venkatappa, *Nature* **1978**, *272*, 319.

[23] S. T. Prigge, B. A. Eipper, R. E. Mains, L. M. Amzel, *Science* **2004**, *304*, 864.

[24] A. Volbeda, W. G. Hol, *J. Mol. Biol.* **1989**, *209*, 249.

[25] J. A. Guckert, M. D. Lowery, E. I. Solomon, *J. Am. Chem. Soc.* **1995**, *117*, 2817.

[26] K. I. Tishchenko, E. K. Beloglazkina, A. G. Mazhuga, N. V. Zyk, *Rev. J. Chem.* **2016**, *6*, 49.

[27] H. B. Gray, B. G. Malmström, R. J. Williams, *J. Biol. Inorg. Chem.* **2000**, *5*, 551.

[28] I. S. MacPherson, M. E. P. Murphy, *Cell. Mol. Life Sci.* **2007**, *64*, 2887.

[29] a) J. A. Tainer, E. D. Getzoff, K. M. Beem, J. S. Richardson, D. C. Richardson, *J. Mol. Biol.* **1982**, *160*, 181; b) J. A. Tainer, E. D. Getzoff, J. S. Richardson, D. C. Richardson, *Nature* **1983**, *306*, 284.

[30] C. Belle, J. de Tovar, R. Leblay, Y. Wang, L. Wojcik, A. Thibon-Pourret, M. Reglier, A. J. Simaan, N. Le Poul, *Chem. Sci.* **2024**.

[31] P. Wu, F. Fan, J. Song, W. Peng, J. Liu, C. Li, Z. Cao, B. Wang, *J. Am. Chem. Soc.* **2019**, *141*, 19776.

[32] T. V. Vendelboe, P. Harris, Y. Zhao, T. S. Walter, K. Harlos, K. El Omari, H. E. M. Christensen, *Sci. Adv.* **2016**, *2*, e1500980.

[33] R. E. Cowley, L. Tian, E. I. Solomon, *Proc. Natl. Acad. Sci. U. S. A.* **2016**, *113*, 12035.

[34] T. Klabunde, C. Eicken, J. C. Sacchettini, B. Krebs, *Nat. Struct. Biol.* **1998**, *5*, 1084.

[35] Y. Matoba, T. Kumagai, A. Yamamoto, H. Yoshitsu, M. Sugiyama, *J. Biol. Chem.* **2006**, *281*, 8981.

[36] E. I. Solomon, D. E. Heppner, E. M. Johnston, J. W. Ginsbach, J. Cirera, M. Qayyum, M. T. Kieber-Emmons, C. H. Kjaergaard, R. G. Hadt, L. Tian, *Chem. Rev.* **2014**, *114*, 3659.

[37] a) L. Vámos-Vigyázó, *Crit. Rev. Food Sci. Nutr.* **1981**, *15*, 49; b) Vincent J. Hearing, Katsuhiko Tsukamoto, *FASEB J.* **1991**, *5*, 2902.

[38] N. Fujieda, K. Umakoshi, Y. Ochi, Y. Nishikawa, S. Yanagisawa, M. Kubo, G. Kurisu, S. Itoh, *Angew. Chem. Int. Ed.* **2020**, *59*, 13385.

[39] I. Kipouros, A. Stańczak, J. W. Ginsbach, P. C. Andrikopoulos, L. Rulíšek, E. I. Solomon, *Proc. Natl. Acad. Sci. U. S. A.* **2022**, *119*, e2205619119.

[40] I. Kipouros, A. Stańczak, E. M. Dunietz, J. W. Ginsbach, M. Srnec, L. Rulíšek, E. I. Solomon, *J. Am. Chem. Soc.* **2023**, *145*, 22866.

[41] S. Panda, H. Phan, E. M. Dunietz, M. T. Brueggemeyer, P. K. Hota, M. A. Siegler, A. Jose, M. Bhadra, E. I. Solomon, K. D. Karlin, *J. Am. Chem. Soc.* **2024**.

[42] R. Trammell, K. Rajabimoghadam, I. Garcia-Bosch, *Chem. Rev.* **2019**, *119*, 2954.

[43] L. Q. Hatcher, K. D. Karlin, *J. Biol. Inorg. Chem.* **2004**, *9*, 669.

[44] M. Weitzer, M. Schatz, F. Hampel, F. W. Heinemann, S. Schindler, *J. Chem. Soc., Dalton Trans.* **2002**, 686.

[45] K. Nakamoto (Hrsg.) *Infrared and Raman spectra of inorganic and coordination compounds*, *Part B*, Wiley, Hoboken, N.J., **2009**.

[46] R. M. Roat-Malone, *Bioinorganic Chemistry: A Short Course, 2nd Edition*, John Wiley & Sons, **2007**.

[47] a) L. S. Kau, D. J. Spira-Solomon, J. E. Penner-Hahn, K. O. Hodgson, E. I. Solomon, *J. Am. Chem. Soc.* **1987**, *109*, 6433; b) J. L. DuBois, P. Mukherjee, T. D. P. Stack, B. Hedman, E. I. Solomon, K. O. Hodgson, *J. Am. Chem. Soc.* **2000**, *122*, 5775.

[48] R. R. Jacobson, Z. Tyeklar, A. Farooq, K. D. Karlin, S. Liu, J. Zubieta, *J. Am. Chem. Soc.* **1988**, *110*, 3690.

[49] N. Kitajima, K. Fujisawa, Y. Morooka, K. Toriumi, *J. Am. Chem. Soc.* **1989**, *111*, 8975.

[50] K. Fujisawa, M. Tanaka, Y. Moro-oka, N. Kitajima, *J. Am. Chem. Soc.* **1994**, *116*, 12079.

[51] J. A. Halfen, S. Mahapatra, E. C. Wilkinson, S. Kaderli, V. G. Young, L. Que, A. D. Zuberbühler, W. B. Tolman, *Science* **1996**, *271*, 1397.

[52] S. Mahapatra, J. A. Halfen, E. C. Wilkinson, G. Pan, X. Wang, V. G. Young, C. J. Cramer, L. Que, W. B. Tolman, *J. Am. Chem. Soc.* **1996**, *118*, 11555.

[53] C. Würtele, E. Gaoutchenova, K. Harms, M. C. Holthausen, J. Sundermeyer, S. Schindler, *Angew. Chem. Int. Ed.* **2006**, *45*, 3867.

[54] Z. Tyeklar, R. R. Jacobson, N. Wei, N. N. Murthy, J. Zubieta, K. D. Karlin, *J. Am. Chem. Soc.* **1993**, *115*, 2677.

[55] N. Kitajima, K. Fujisawa, C. Fujimoto, Y. Morooka, S. Hashimoto, T. Kitagawa, K. Toriumi, K. Tatsumi, A. Nakamura, *J. Am. Chem. Soc.* **1992**, *114*, 1277.

[56] S. Mahapatra, J. A. Halfen, E. C. Wilkinson, L. Que, W. B. Tolman, *J. Am. Chem. Soc.* **1994**, *116*, 9785.

[57] a) P. E. M. Siegbahn, *J. Biol. Inorg. Chem.* **2003**, *8*, 577; b) M. Flock, K. Pierloot, *J. Phys. Chem. A* **1999**, *103*, 95.

[58] a) S. O. Pember, K. A. Johnson, J. J. Villafranca, S. J. Benkovic, *Biochemistry* **1989**, *28*, 2124; b) D. M. Dooley, M. A. McGuirl, D. E. Brown, P. N. Turowski, W. S. McIntire, P. F. Knowles, *Nature* **1991**, *349*, 262.

[59] K. D. Karlin, N. Wei, B. Jung, S. Kaderli, A. D. Zuberbuehler, *J. Am. Chem. Soc.* **1991**, *113*, 5868.

[60] P. Chen, D. E. Root, C. Campochiaro, K. Fujisawa, E. I. Solomon, *J. Am. Chem. Soc.* **2003**, *125*, 466.

[61] K. D. Karlin, N. Wei, B. Jung, S. Kaderli, P. Niklaus, A. D. Zuberbuehler, *J. Am. Chem. Soc.* **1993**, *115*, 9506.

[62] a) M. Becker, F. W. Heinemann, S. Schindler, *Chem. Eur. J.* **1999**, *5*, 3124; b) M. Weitzer, S. Schindler, G. Brehm, S. Schneider, E. Hörmann, B. Jung, S. Kaderli, A. D. Zuberbühler, *Inorg. Chem.* **2003**, *42*, 1800.

[63] M. Schatz, V. Raab, S. P. Foxon, G. Brehm, S. Schneider, M. Reiher, M. C. Holthausen, J. Sundermeyer, S. Schindler, *Angew. Chem. Int. Ed.* **2004**, *43*, 4360.

[64] X. Ottenwaelder, D. J. Rudd, M. C. Corbett, K. O. Hodgson, B. Hedman, T. D. P. Stack, *J. Am. Chem. Soc.* **2006**, *128*, 9268.

[65] M. Schatz, M. Becker, F. Thaler, F. Hampel, S. Schindler, R. R. Jacobson, Z. Tyeklár, N. N. Murthy, P. Ghosh, Q. Chen et al., *Inorg. Chem.* **2001**, *40*, 2312.

[66] L. Q. Hatcher, M. A. Vance, A. A. Narducci Sarjeant, E. I. Solomon, K. D. Karlin, *Inorg. Chem.* **2006**, *45*, 3004.

[67] T. D. P. Stack, *Dalton Trans.* **2003**, 1881.

[68] T. Osako, Y. Ueno, Y. Tachi, S. Itoh, *Inorg. Chem.* **2003**, *42*, 8087.

[69] R. R. Jacobson, Z. Tyeklár, K. D. Karlin, *Inorg. Chim. Acta* **1991**, *181*, 111.

[70] a) J. Astner, M. Weitzer, S. P. Foxon, S. Schindler, F. W. Heinemann, J. Mukherjee, R. Gupta, V. Mahadevan, R. Mukherjee, *Inorg. Chim. Acta* **2008**, *361*, 279; b) J. Becker, Y. Y. Zhyhadlo, E. D. Butova, A. A. Fokin, P. R. Schreiner, M. Förster, M. C. Holthausen, P. Specht, S. Schindler, *Chem. Eur. J.* **2018**, *24*, 15543.

[71] a) M. Pasquali, C. Floriani, G. Venturi, A. Gaetani-Manfredotti, A. Chiesi-Villa, *J. Am. Chem. Soc.* **1982**, *104*, 4092; b) D. V. Scaltrito, H. C. Fry, B. M. Showalter, D. W. Thompson, H. C. Liang, C. X. Zhang, R. M. Kretzer, E. Kim, J. P. Toscano, K. D. Karlin et al., *Inorg. Chem.* **2001**, *40*, 4514; c) H. C. Fry, H. R. Lucas, A. A. N. Sarjeant, K. D. Karlin, G. J. Meyer, *Inorg. Chem.* **2008**, *47*, 241.

[72] C. Würtele, O. Sander, V. Lutz, T. Waitz, F. Tuczek, S. Schindler, *J. Am. Chem. Soc.* **2009**, *131*, 7544.

[73] T. Osako, Y. Tachi, M. Taki, S. Fukuzumi, S. Itoh, *Inorg. Chem.* **2001**, *40*, 6604.

[74] S. Kim, J. W. Ginsbach, A. I. Billah, M. A. Siegler, C. D. Moore, E. I. Solomon, K. D. Karlin, *J. Am. Chem. Soc.* **2014**, *136*, 8063.

[75] a) P. K. Wick, K. D. Karlin, M. Suzuki, A. D. Zuberbühler, *Micron* **2004**, *35*, 137; b) M. T. Kieber-Emmons, J. W. Ginsbach, P. K. Wick, H. R. Lucas, M. E. Helton, B. Lucchese, M. Suzuki, A. D. Zuberbühler, K. D. Karlin, E. I. Solomon, *Angew. Chem. Int. Ed.* **2014**, *53*, 4935; c) L. Siebe, C. Butenuth, A. Stammler, H. Bögge, S. Walleck, T. Glaser, *Inorg. Chem.* **2024**, *63*, 2627.

[76] a) R. L. Shook, A. S. Borovik, *Inorg. Chem.* **2010**, *49*, 3646; b) D. L. Ross, A. J. Jasniewski, J. W. Ziller, E. L. Bominaar, M. P. Hendrich, A. S. Borovik, *J. Am. Chem. Soc.* **2024**, *146*, 500.

[77] a) H.-C. Liang, C. X. Zhang, M. J. Henson, R. D. Sommer, K. R. Hatwell, S. Kaderli, A. D. Zuberbühler, A. L. Rheingold, E. I. Solomon, K. D. Karlin, *J. Am. Chem. Soc.* **2002**, *124*, 4170; b) G. Y. Park, M. F. Qayyum, J. Woertink, K. O. Hodgson, B. Hedman, A. A. Narducci Sarjeant, E. I. Solomon, K. D. Karlin, *J. Am. Chem. Soc.* **2012**, *134*, 8513.

[78] M. Bhadra, J. Y. C. Lee, R. E. Cowley, S. Kim, M. A. Siegler, E. I. Solomon, K. D. Karlin, *J. Am. Chem. Soc.* **2018**, *140*, 9042.

[79] D. E. Diaz, D. A. Quist, A. E. Herzog, A. W. Schaefer, I. Kipouros, M. Bhadra, E. I. Solomon, K. D. Karlin, *Angew. Chem. Int. Ed.* **2019**, *58*, 17572.

[80] S. Yamaguchi, A. Wada, Y. Funahashi, S. Nagatomo, T. Kitagawa, K. Jitsukawa, H. Masuda, *Eur. J. Inorg. Chem.* **2003**, *2003*, 4378.

[81] A. Wada, Y. Honda, S. Yamaguchi, S. Nagatomo, T. Kitagawa, K. Jitsukawa, H. Masuda, *Inorg. Chem.* **2004**, *43*, 5725.

[82] S. Kim, C. Saracini, M. A. Siegler, N. Drichko, K. D. Karlin, *Inorg. Chem.* **2012**, *51*, 12603.

[83] E. W. Dahl, H. T. Dong, N. K. Szymczak, *Chem. Commun.* **2018**, *54*, 892.

[84] H. Oh, W.-M. Ching, J. Kim, W.-Z. Lee, S. Hong, *Inorg. Chem.* **2019**, *58*, 12964.

[85] H. Oh, S. Choi, J. Y. Kim, H. S. Ahn, S. Hong, *Chem. Commun.* **2019**, *55*, 12659.

[86] F. Tao, Q. Wang, *RSC Adv.* **2015**, *5*, 46007.